

THE CATALYTIC REDUCTION OF NITRIC OXIDE WITH AMMONIA

by

John William Walker

A Thesis Submitted to the Faculty
of Graduate Studies and Research
in Partial Fulfillment for the
Degree of Master of Engineering
in the Department of Chemical Engineering
of McGill University in Montreal

March 19, 1974

THE CATALYTIC REDUCTION OF NITRIC OXIDE WITH AMMONIA

ABSTRACT

The reduction of nitric oxide with ammonia was studied over two series of copper-nickel catalysts supported on silica. Activities of Raney alloy catalysts are low; the temperature had to be raised to 350°C to achieve significant conversion at a space velocity of 500 hr^{-1} . Activities of nitrate-based mixed-oxide catalysts are much higher; these are active enough to justify further investigation with a view towards possible commercialization. High conversions were observed at 150°C and a space velocity of 3000 hr^{-1} over these catalysts.

The experimental data demonstrate that alloy composition is an important variable and that alloy formation is an important technique to prepare catalysts for nitrogen oxide reduction.

by John William Walker

Department of Chemical Engineering

McGill University

March 19, 1974

M. Eng.

La réduction catalytique de l'oxide nitrique par l'ammoniac

Résumé

La réduction d'oxide nitrique par l'ammoniac a été étudiée en utilisant deux groupes de catalyseurs de cuivre et de nickel sur un support de silice. A cause de la basse activité catalysante des alliages de Raney, la température a dû être augmentée jusqu'à 350°C pour atteindre une conversion significative à une vitesse spaciales de 500 par heure. L'activité des catalyseurs à base de nitrate est assez haute pour justifier une enquête plus approfondie en vue d'un développement commercial possible. En utilisant ces catalyseurs, de hautes conversions ont été observées à 150°C et à une vitesse spaciales de 3000 par heure.

Les données expérimentales montre que la composition de l'alliage est une variable importante et que la formation de l'alliage est une technique essentielle dans la préparation des catalyseurs pour la réduction de l'oxide nitrique.

par John William Walker
Département de Génie Chimique
Université McGill
Le 19 mars, 1974

ACKNOWLEDGMENTS

The author would like to take this opportunity to thank all those who helped make this thesis possible.

Prof. O.M. Fuller and Dr. N.E. Cooke of the Department of Chemical Engineering at McGill University initiated and supervised this project.

Financial support was provided by a National Health Grant from the Department of National Health and Welfare and the Quebec Ministry of Social Affairs.

My wife, Debbie Walker, helped and encouraged me throughout the project.

Prof. E.J. Farkas and D. Reay evaluated the initial research proposal. C. Coady, A. Dresner, L. Mok, and P. Oberoi assisted with the experimental work. W.R. Grace & Company supplied the copper-nickel-aluminum alloys for the preparation of the Raney alloy catalysts. Mr. A.M. Jamieson of Molson Industries Limited advised on the chromatographic separation of argon, oxygen, and nitrogen. Prof. R.B. Anderson of McMaster University suggested the leaching procedure used on the Raney alloy catalysts.

FOREWORD

This thesis was written in partial fulfillment of the requirements of the Master of Engineering Degree at McGill University. It is based on research undertaken by the author under the supervision of Prof. O.M. Fuller and Dr. N.E. Cooke at the Department of Chemical Engineering. Financial support was provided by a National Health Grant.

The reduction of nitric oxide with ammonia has been studied by other investigators. However, none has measured the activities of Raney catalysts for this reaction, although Raney metals have proven active for other reactions. Neither have alloy catalysts been tested for nitric oxide reduction with ammonia. Since alloy formation is a powerful technique in the preparation of active catalysts, its investigation was undertaken in conjunction with the Raney procedure. A second set of mixed-oxide metal catalysts were also tested. Activity measurements on both series of catalysts demonstrated the importance of metal composition to activity and selectivity.

In the course of the investigation, capillary flowmeters were constructed to meter the reactants. The friction factors for laminar compressible flow in small diameter capillaries can significantly exceed the friction factors predicted by standard correlations for incompressible laminar flow.

TABLE OF CONTENTS

	Page
Abstract	ii
Acknowledgments	iv
Foreword	v
List of Figures	viii
List of Tables	x
I. Introduction	1
II. Copper-Nickel Alloy Catalysts	4
III. Microreactor Construction and Operation	13
IV. Flow Control System	17
V. Chemical Analyses	28
VI. Catalyst Support	42
VII. Preparation of Raney Alloy Catalysts	49
VIII. Activity of Raney Catalysts	69
IX. Nitrate-Based Mixed-Oxide Catalysts	92
X. Discussion of Apparatus and Procedures	106
XI. Discussion of Catalyst Activities	112
Appendices	
A. Capillary Flowmeters	125
B. Chromatographic Analysis	147
C. Preparation of Silica Support for Raney Metals	154
D. Properties of Cabosil Fumed Silicon Dioxide and Ludox Colloidal Silica	156

Appendices

E. Preparation of Active Raney Alloys	157
F. Preparation of Nitrate-Based Mixed-Oxide Catalysts	167
G. Definition of Conversions	169
H. Calculation of Raney Catalyst Bed Weights	171
Bibliography	174

LIST OF FIGURES

Figure	Title	Page
1	Hardness, Electrical Conductivity, and Thermal Conductivity of Copper-Nickel Alloys	6
2	Activity of Copper-Nickel Alloy Films for Hydrogenation of Benzene	7
3	Activity of Copper-Nickel Alloy Films for Hydrogenation of Ethylene	7
4	Activity of Raney Manganese-Nickel Alloys for Hydrogenation of Heptene-1	9
5	Catalytic Microreactor	14
6	Reactant Supply System	18
7	Apparent Friction Factor Versus Reynolds Number	21
8	Apparent Friction Factor Versus Reynolds Number for Small Capillaries	23
9	Predicted and Actual Flow Rates for Flowmeter No. H-1-B	26
10	Stability of Ludox HS-40	46
11	Formation of Active Raney Metal	52
12	Dependence of Specific Surface Area on Extent of Leaching of Raney Nickel	55
13	Aluminum Removal and Specific Surface Area of Raney Copper-Nickel Alloy Catalysts	57
14	Magnetic Susceptibilities and Activities of Raney Copper-Nickel Alloy Catalysts	58
15	Phase Diagram of Slowly Cooled Copper-Nickel-Aluminum Alloys	62
16	Aluminum Leached from Copper-Nickel-Aluminum Alloys	66

Figure	Title	Page
17	Activity of Silica Support for Reduction of Nitric Oxide with Ammonia	81
18	Reactor Outlet Gas Composition over Catalyst R-Cu375	83
19	Activity of Raney Alloy Catalysts for Reduction of Nitric Oxide with Ammonia at 350°C and 500 hr ⁻¹ Space Velocity	86
20	Effect of Space Velocity on Nitric Oxide Destruction over Catalyst R-Cu-A	88
21	Surface Areas of Copper-Nickel Alloy Catalysts	94
22	Conversion over Catalyst G-Cu250	98
23	Activity of Nitrate-Based Catalysts for Reduction of Nitric Oxide with Ammonia at 200°C and 3000 hr ⁻¹ Space Velocity	100
24	Effect of Metal Composition on Product Distribution Ratio for Nitric Oxide Reduction over Nitrate-Based Catalysts	101
25	Effect of Exit Mach Number on Downstream Temperature for Ideal, Adiabatic Flow	128
26	Exit Pressure Losses for Laminar and Turbulent Incompressible Flow	131
27	Capillary Flowmeter Construction	145
28	Chromatograph Sampling System	148
29	Typical Chromatograms of Reactor Inlet and Outlet Gases.	151
30	Apparatus to Leach Raney Metal Alloys	158

LIST OF TABLES

Table	Title	Page
1	Flowmeters for Raney Catalyst Tests	25
2	Composition of Starting Alloys	60
3	Phase Composition of Starting Alloys	63
4	Effect of Catalyst Pellet Size on Conversion	73
5	Effect of Temperature and Space Velocity on Conversion over Commercial Raney Copper Catalyst #C1	78
6	Effect of Temperature and Space Velocity on Conversion over Silica Support	80
7	Effect of Alloy Composition on Conversion over Raney Copper-Nickel Alloy Catalysts	84
8	Activities of Raney Copper-Nickel Alloy Catalysts	87
9	Ammonia Decomposition over Raney Copper-Nickel Alloy Catalysts	90
10	Composition of Nitrate-Based Mixed-Oxide Catalysts	95
11	Effect of Composition on Conversion over Nitrate-Based Mixed-Oxide Catalysts	99
12	Activities of Nitrate-Based Mixed-Oxide Catalysts	103
13	Effect of Temperature on Ammonia Decomposition over Nitrate-Based Catalyst #N-Mix	104
14	Comparison of Catalyst Activities for Reduction of Nitrogen Oxides with Ammonia	104
15	Product Distribution Ratio for Reduction of Nitric Oxide with Ammonia	120
16	Entrance and Exit Loss Coefficients in Incompressible Flow	130

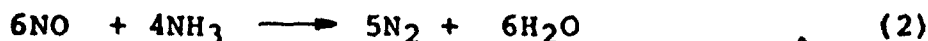
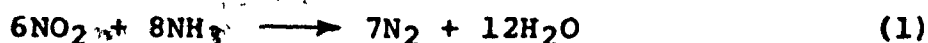
Table	Title	Page
17	Dimensions of Test Capillaries	130
18	Preliminary Capillary Test Data	133
19	Preliminary Capillary Test Data	137
20	Design of Capillary Flowmeter No. H-1-B	141
21	Summary of Flowmeter Designs	142
22	Design Parameters for Capillary Flowmeters Used for the Raney Catalyst Tests	146
23	Chromatograph Operational Variables	150
24	Adsorbent Bed Characteristics	153
25	Properties of Cabosil Fumed Silicon Dioxide Grade M-7	156
26	Properties of Ludox Colloidal Silica Type HS-40	156
27	Reactivities of Copper-Nickel-Aluminum Alloys Towards Alkali Solution	163
28	Gel Times of Ludox Suspensions of 5% Raney Metals	165
29	Calculations of Raney Metal Catalyst Bed Weights	173

Section I: Introduction

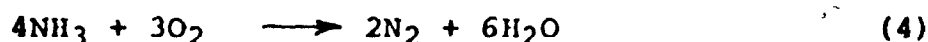
In the manufacture of nitric acid, nitrogen dioxide is absorbed by water to form nitric acid and nitric oxide in the final absorption tower. The nitric oxide then reacts with oxygen to form more nitrogen dioxide and the cycle is repeated. At low concentrations of nitrogen oxides, the rate of absorption falls and complete removal by absorption is impossible. The tail gas usually contains about 0.3% oxides of nitrogen, 3% oxygen, and 97% nitrogen. To avoid the detrimental health effects of nitrogen oxides, the ground level concentrations must be kept low by venting the gas through a tall stack.

Processes based on catalytic decomposition, on adsorption, and on absorption have been proposed for nitrogen oxide removal (6,8,20,91). With the exception of adsorption on molecular sieves, none of the sorption processes appear commercially feasible. However, catalytic reduction is a promising method of emission control. Non-selective processes, such as the reduction of the tail gas with natural gas, are not entirely satisfactory; the catalysts are expensive, generally have a short life, and the oxygen reacts preferentially with the fuel. For economic reasons, the usual practice is to recover the power to pay for the fuel used in burning the oxygen.

Ammonia can reduce both nitric oxide and nitrogen dioxide to water and either nitrogen or nitrous oxide.



It can also reduce oxygen with formation of nitrogen and water.



Since the concentration of oxygen is approximately ten times that of the nitrogen oxides, a selective catalyst to promote the reactions with nitrogen oxides rather than with oxygen is desired.

The selective reaction can be promoted; so catalytic reduction with ammonia is a promising method. Anderson, Green, and Steele (6) investigated catalysts and fuels for both the selective and non-selective reduction of nitrogen oxides with ammonia. Effective catalysts include platinum, palladium, ruthenium, cobalt, and nickel. Supported platinum is superior to all others in completeness of nitrogen oxide removal.

The noble metal catalysts are not suitable for industrial applications because they are easily poisoned by sulfur and because the presence of nitrogen dioxide results in a loss of activity. Non-noble metals and metal oxide catalysts have also been tested by other investigators, but none possesses both the high activity and resistance to poisoning required in a commercial catalyst.

Cooke, Fuller, and Pitblado (20) completed a preliminary study of the selective reduction of nitrogen oxides with ammonia at the Department of Chemical Engineering of McGill University

under a grant from the Quebec Department of Health as Project Number 604-7-695. A series of commercial catalysts was tested, including vanadium oxide and platinum catalysts which were claimed to be active for the reaction. The reactor feed was 0.8% nitric oxide, 0.8% ammonia, 4.4% oxygen, and 94% argon. Reactant and product compositions were measured on a chromatograph. Results confirm that copper, platinum, and vanadium oxide are among the catalysts active for the selective reaction. However, extensive testing was hampered by difficulties in the chromatographic analysis.

The present investigation is a continuation of this preliminary work. The overall objective is to define a selective process to reduce nitrogen oxides with ammonia. A preferred catalyst must be selected and tested to provide sufficient information to predict its useful life and design a prototype reactor.

As part of the overall objectives, the preparation and testing of specific catalysts are being studied with emphasis on non-noble metal catalysts whose activities for the reduction of nitrogen oxides with ammonia have not yet been measured.

The objectives of the work reported in this thesis are more limited. Two series of non-noble metal catalysts were prepared by a novel method for this reaction and their activities for the reduction of nitric oxide with ammonia were measured. Oxygen and nitrogen dioxide were not present in the reaction mixture because of limitations of the chemical analyses.

Section II: Copper-Nickel Alloy Catalysts

Cooke, Fuller, and Pitblado (20) surveyed catalysts active for the reduction of nitrogen oxides with ammonia. Both noble and non-noble metals and some metal oxides are active. The study of metal catalysts was continued in this investigation. The activity of a supported metal catalyst depends mainly on bulk chemical composition, surface chemical composition, total amount of metal present, surface area of metal present, and metal crystallite size and structure. The presence of impurities or adsorbed species on the surface, surface defects, and oxidation state of the metal on the surface are also important. Each of these factors can affect the number and type of sites available for adsorption and chemical reaction.

With the exceptions of bulk chemical composition and metal loading, these variables are difficult to measure and control. Chemical composition of the metal particle surface may differ considerably from that in the bulk phase (15,39,78,79,80,92). Metal crystallite size, specific surface area, oxidation state, and presence of adsorbed species on the surface require relatively sophisticated equipment to measure. Even then firm conclusions are often difficult to reach.

The most important factor is the nature of the metal present in the bulk metal phase. One possible investigation would be comparison of the reaction rates over a series of metal

catalysts, such as copper, nickel, iron, vanadium, and manganese. A more interesting and sometimes more fruitful approach is the formation of metal alloy catalysts.

Alloying metals is used as a method to alter bulk chemical composition, physical characteristics, and electronic structure of metal catalysts. Figure 1 shows mechanical and electronic properties of annealed copper-nickel alloys (94). Alloy catalytic activities can drastically differ from the starting metals. The following three examples illustrate the dependence of activity on composition for three different reactions.

Van der Plank and Sachtler (92) measured the activity of copper-nickel alloy films for hydrogenation of benzene at 150°C. Their results in Figure 2 show that nickel is more active than copper. Alloy activities are close to that of copper, except when the concentration of nickel becomes very large. These results have been interpreted by proposing a miscibility gap in the copper-nickel system and diffusion of the copper-rich phase to the surface.

Campbell and Emmett (16) observed a different effect for initial reaction rates in the hydrogenation of ethylene on copper-nickel films. Their results in Figure 3 show a wide variation of catalytic activity with alloy composition; some alloys are fifteen times more active than nickel. A satisfactory theory has not yet been proposed to account for these data.

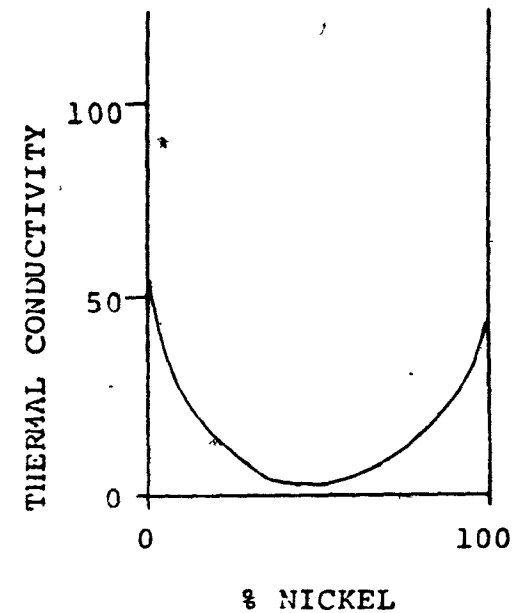
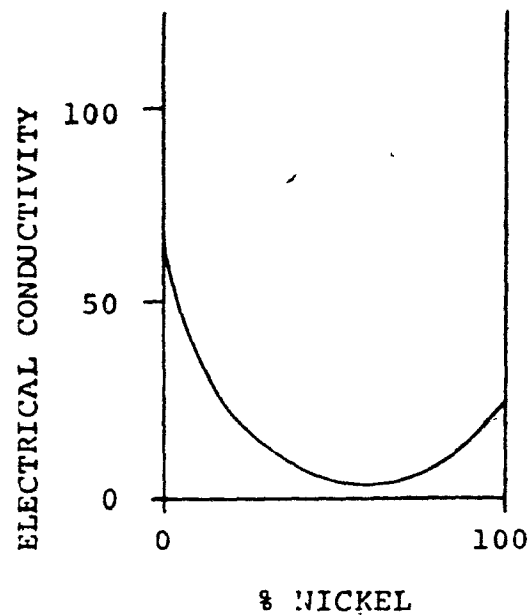
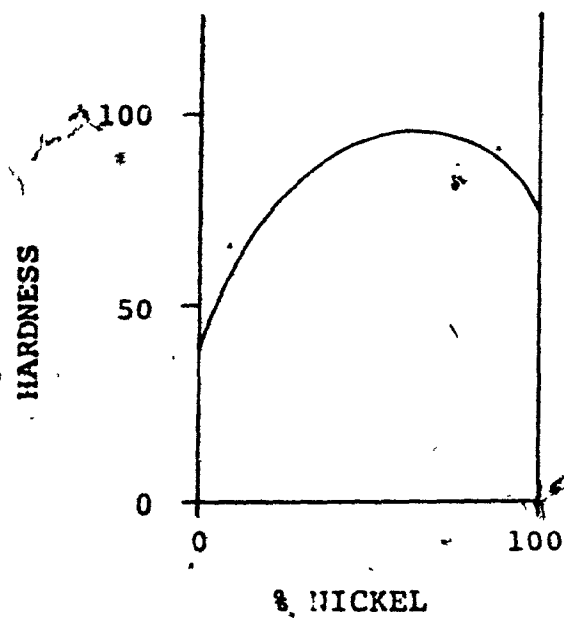


FIGURE 1: HARDNESS, ELECTRICAL CONDUCTIVITY, AND THERMAL CONDUCTIVITY OF COPPER-NICKEL ALLOYS (94)

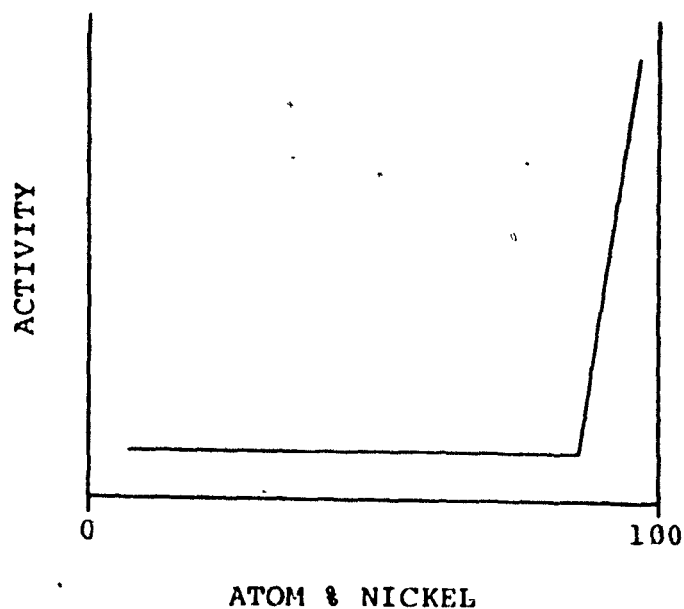


FIGURE 2: ACTIVITY OF COPPER-NICKEL ALLOY FILMS
FOR HYDROGENATION OF BENZENE (92)

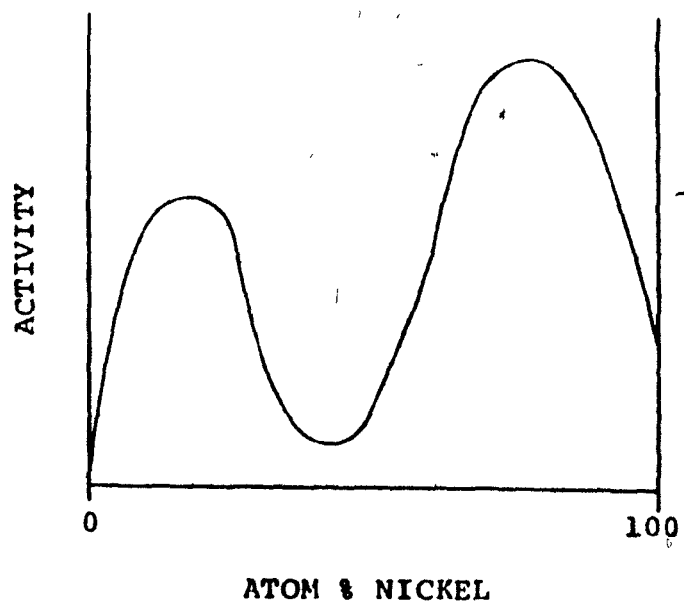


FIGURE 3: ACTIVITY OF COPPER-NICKEL ALLOY FILMS
FOR HYDROGENATION OF ETHYLENE (16)

Petrov et al. (68) measured the activity of Raney manganese-nickel alloys for the hydrogenation of heptene-1. Their results in Figure 4 show a definite effect of alloy composition. Petrov correlated this activity variation with the content of the NiAl_3 phase in the starting alloy.

Active alloy catalysts have been reported for many reactions. Several theories have been proposed to interpret the experimental data (16,18,27,39,80,83,84,92). Some are based on filling vacant d-orbitals of one of the alloy components. Others are based on chemisorption of active species. However, there is no theory that could be used successfully to predict general alloy activities.

The overall reaction rate observed over a catalyst in the absence of mass transfer limitations depends on the number and nature of the active sites, the rates of adsorption of reactants and desorption of products, the strengths of sorption of the reactants and products, surface diffusion between sorption sites, the mechanism of the reaction, and the inherent reaction rate at an active site. Since the number of pure metals which are active catalysts is small, the possibilities for independent variation of these processes are limited. Moreover, it is unlikely that a pure metal will possess the optimum characteristics for a given reaction. Alloying removes this restriction; in some cases, electronic and physical structures can be varied continuously by alloy formation.

Metal alloying was the method used to prepare the catalysts tested in this work. Copper and nickel were used as the base

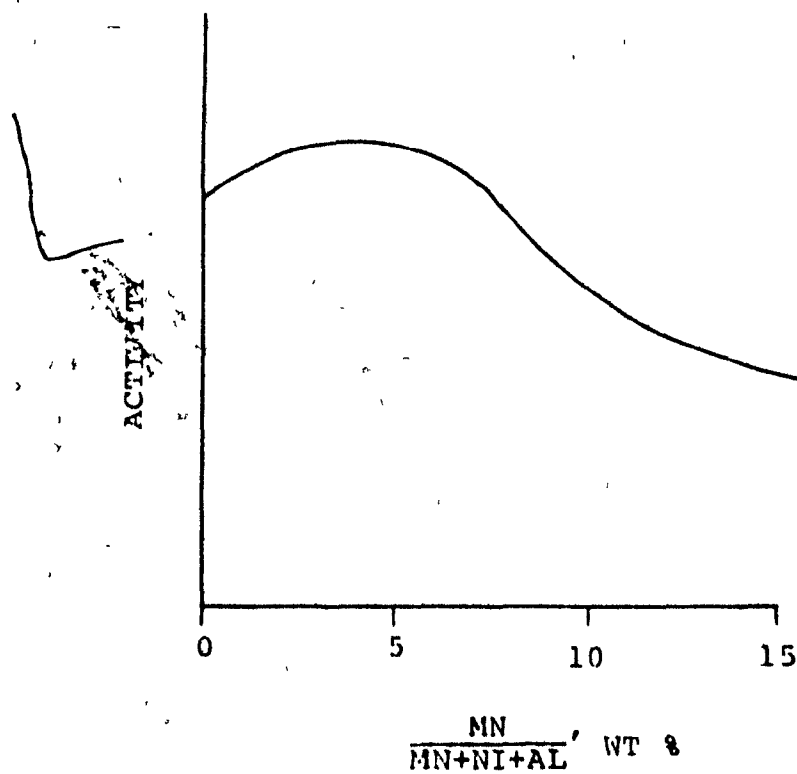


FIGURE 4: ACTIVITY OF RANEY MANGANESE-NICKEL ALLOYS
FOR HYDROGENATION OF HEPTENE-1 (68)

metals since they have both been proven active for the selective and non-selective reduction of nitrogen oxides. Copper-nickel alloy catalysts have also given valuable activity results in a number of other reactions (18,27,83). The copper-nickel system is attractive for several other reasons. The lattice spacings of these two metals are close, so this variable should not be significant. The electronic structure should change as the alloys are formed. The single 4s electron from copper will fill the partially vacant 3d band of the nickel.

The preparation method was chosen to result in a large metal surface area, a small crystallite size, and a known bulk oxidation state. Copper-nickel alloy catalysts can be prepared by grinding a copper-nickel alloy, by impregnating a catalyst support with copper and nickel salts either simultaneously or successively, by ion exchange on molecular sieves, by co-precipitation, by the Raney method, or by gelling the metal salts in a colloidal suspension.

For this investigation the Raney method was used because it has produced catalysts active for many other reactions, but has not yet been tested for the reduction of nitrogen oxides with ammonia.

The Raney method is used to produce catalysts for many industrial processes. Raney nickel, the most common of the Raney metals, is active for hydrogenation, reductive amidation, saturation of olefinic bonds, reduction of aldehydes to alcohols, and other reactions. Raney copper, although less commonly used,

is often more selective than Raney nickel. Other commercial Raney metals available include Raney cobalt and chromium-promoted Raney nickel. Raney molybdenum-nickel, copper-nickel, cobalt-nickel, iron-nickel, iron, and manganese have been used in laboratory investigations.

Copper, nickel, and three copper-nickel alloy catalysts were prepared by the Raney method, dispersed on an inert substrate, and ground to a suitable particle size. One other catalyst was prepared by simultaneously dispersing Raney copper and Raney nickel on the support. These catalysts were conditioned and tested in a fixed bed microreactor. The extent of reduction of nitric oxide with ammonia by Reactions (2) and (3) was measured at a fixed temperature and space velocity.

The experiments were designed to test the following three research hypotheses.

- (A) The Raney method can be used to prepare copper-nickel alloy catalysts which are active for the reduction of nitric oxide with ammonia.
- (B) The preparation method used, and in particular, the bulk oxidation state of the metal, will affect catalyst activities.
- (C) The activity of a mechanical mixture of Raney copper and Raney nickel will differ from the activity of a Raney copper-nickel alloy of the same overall composition.

The first hypothesis was tested by comparing the activities of the Raney catalysts to the activities of known catalysts for

the reaction. Testing of the second hypothesis was based primarily upon comparison of the activities of oxidized and unoxidized catalysts. The third hypothesis suggests that there is a difference in the reaction mechanism on copper, nickel, and alloy catalyst sites. No difference in activity between the alloy and the mechanical mixture would suggest no interaction between the copper sites and the nickel sites. A higher activity for the mechanical mixture would suggest a gas-phase intermediate. Otherwise the reaction on a particle of Raney nickel could not affect the reaction on a spatially separated particle of Raney copper. A higher activity for the alloy would suggest active copper-nickel alloy sites or surface diffusion from a copper site to an adjacent nickel one.

Although the preparation and testing of the Raney metals formed the core of the work reported in this thesis, another series of copper-nickel catalysts was prepared by gelling the metal nitrates in a colloidal dispersion. Comparison of the Raney catalysts to the nitrate-based catalysts yields an evaluation of the suitability of the Raney method to prepare catalysts for the reduction of nitrogen oxides with ammonia. The dependence of activities of the nitrate-based catalysts on composition is another indication of the usefulness of alloy catalysts.

Section III: Microreactor Construction and Operation

Catalyst activities for the reduction of nitric oxide with ammonia were measured by passing the gaseous reactants over a stationary catalyst bed inside the 6 cc microreactor shown in Figure 5.

The reactor was an 11 cm length of $\frac{1}{2}$ in type 316 stainless steel tubing containing a fine screen to hold the catalyst bed in place. The reactants flow downward through the catalyst bed and out the exit to the chromatograph sampling valves.

The reactor dimensions and construction were chosen to match the rest of the experimental system. The relatively small reactor volume of 6 cc did not require excessive gas flow rates even at high space velocities, thus helping to limit consumption of reactants. Large flow rates would also have resulted in excessive pressure drops in other parts of the system, especially in the chromatograph sampling valves.

The same reactor volume could have been constructed from smaller diameter pipe, such as $\frac{1}{4}$ in. However, this would have necessitated grinding the catalyst pellets much smaller and would have resulted in large pressure drops through the bed. Pressure drops were estimated from Equation 5-163 in the Handbook of Chemical Engineering (67) and the constraint that the pellet size be at least thirty times smaller than the reactor inside diameter to eliminate radial concentration

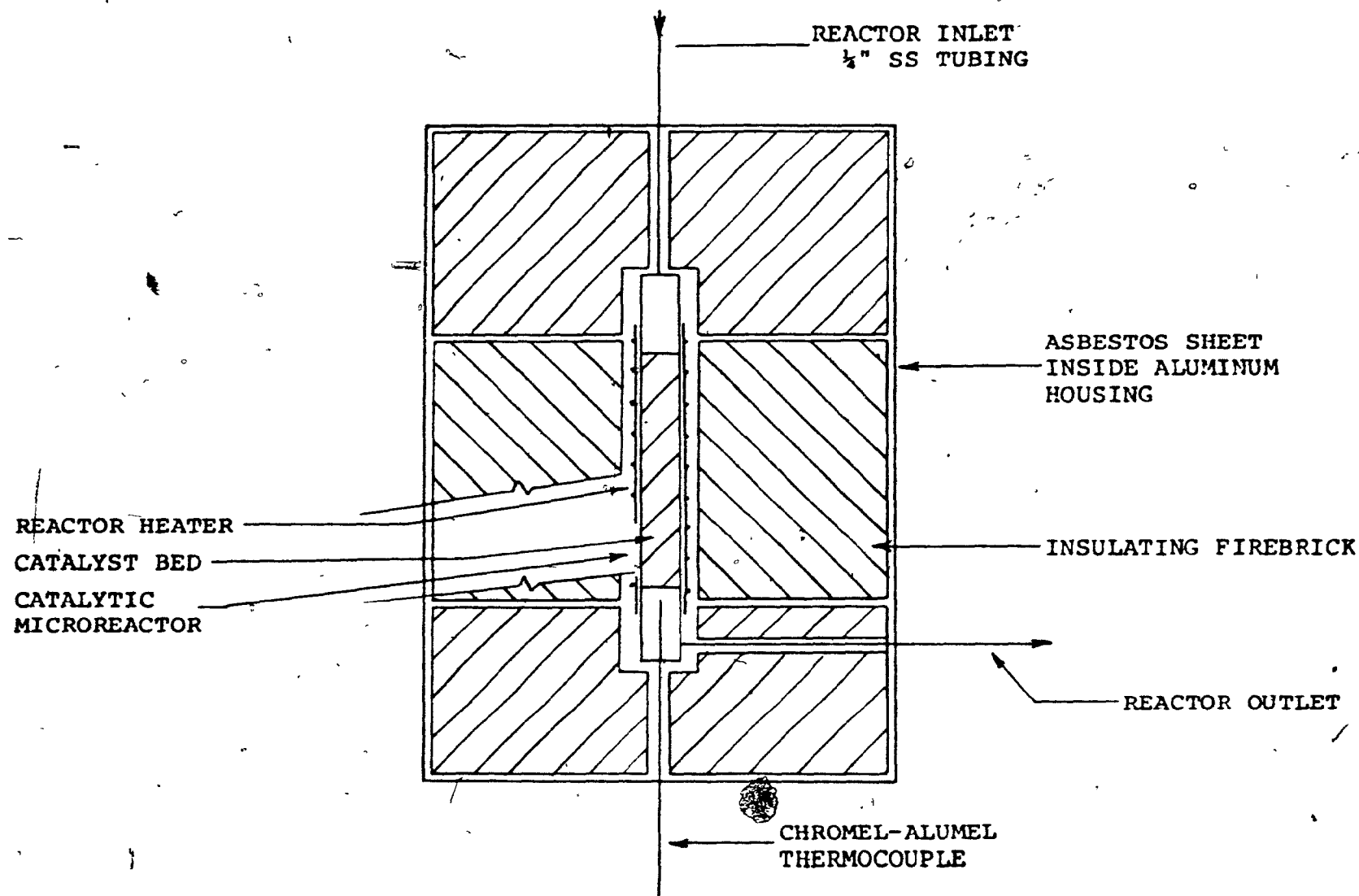


FIGURE 5: CATALYTIC MICROREACTOR

gradients. The resulting calculations showed that for a fixed mass flow rate, the pressure drop varied inversely as the fourth power of the reactor diameter and would become excessive at low reactor diameters.

The reactor was inert to both nitrogen oxides and to ammonia. No evidence of corrosion was found after a year of operation.

The reactor was leaktight compared to the gas flow rates through it. In leak tests, average leak flow rates were less than 0.003 cc/min at a pressure difference of ten psi. This is negligible in comparison to typical reactant flow rates of 100 cc/min at less than one psi pressure difference.

The reactor was electrically heated by nichrome wire wound around an alundum refractory core. Reactor and heater were insulated by a ceramic brick housing inside a metal casing. The heater was controlled by a temperature controller whose sensing element was a chromel-alumel thermocouple located in the gas stream immediately below the catalyst bed.

The temperature control loop was first tested by measuring the response of the controller to known millivolt signals while the thermocouple was disconnected. Then the thermocouple was reconnected to the controller and placed inside a muffle furnace at a known temperature. Both tests verified that the temperature indication and control were accurate within two centigrade degrees.

The reactor could be operated up to 400°C. Above this temperature, seizing of the stainless steel mating surfaces made leaktight assembly and disassembly difficult. Even above 300°C care had to be taken to prevent seizing. An anti-seize compound was used on the outside surfaces, but not on the inner ones since it might have catalytic effects.

An integral part of the reactor design was consideration of the catalyst pellet sizes which would reduce radial concentration gradients and the corresponding mass transfer limitations. These factors will be considered in more detail in later sections.

Section IV: Flow Control System

The microreactor was supplied with a steady stream of reactant gas whose normal composition was 0.3% nitric oxide and 0.6% ammonia in argon. Typical flow rates ranged from 10 to 2000 cc/min of mixture. The flow system designed to suit these requirements is shown in Figure 6. Other flow rates and gas compositions could be supplied by varying the relative flow rates between the three streams, by changing the capillary flowmeters, or by changing the concentrations of the gases in the supply cylinders.

The three gas cylinders contained argon, 1.2% nitric oxide in argon, and 1.2% ammonia in argon. The gases flowed from their supply cylinders through double-stage pressure regulators into flowmeters and then into two union crosses where they were well mixed before reaching the reactor. The downstream pressure was measured at one of the crosses.

The metering effect was achieved by allowing the gas to expand through a narrow glass capillary, typically about 0.1 mm in inside diameter and 20 cm long. Once the meter was calibrated the mass flow rate could be calculated from the upstream and downstream pressures. The dual function of flow control and measurement was achieved in one unit of equipment, thereby minimizing corrosion and leak problems that can prove especially troublesome when handling nitrogen oxides and ammonia.

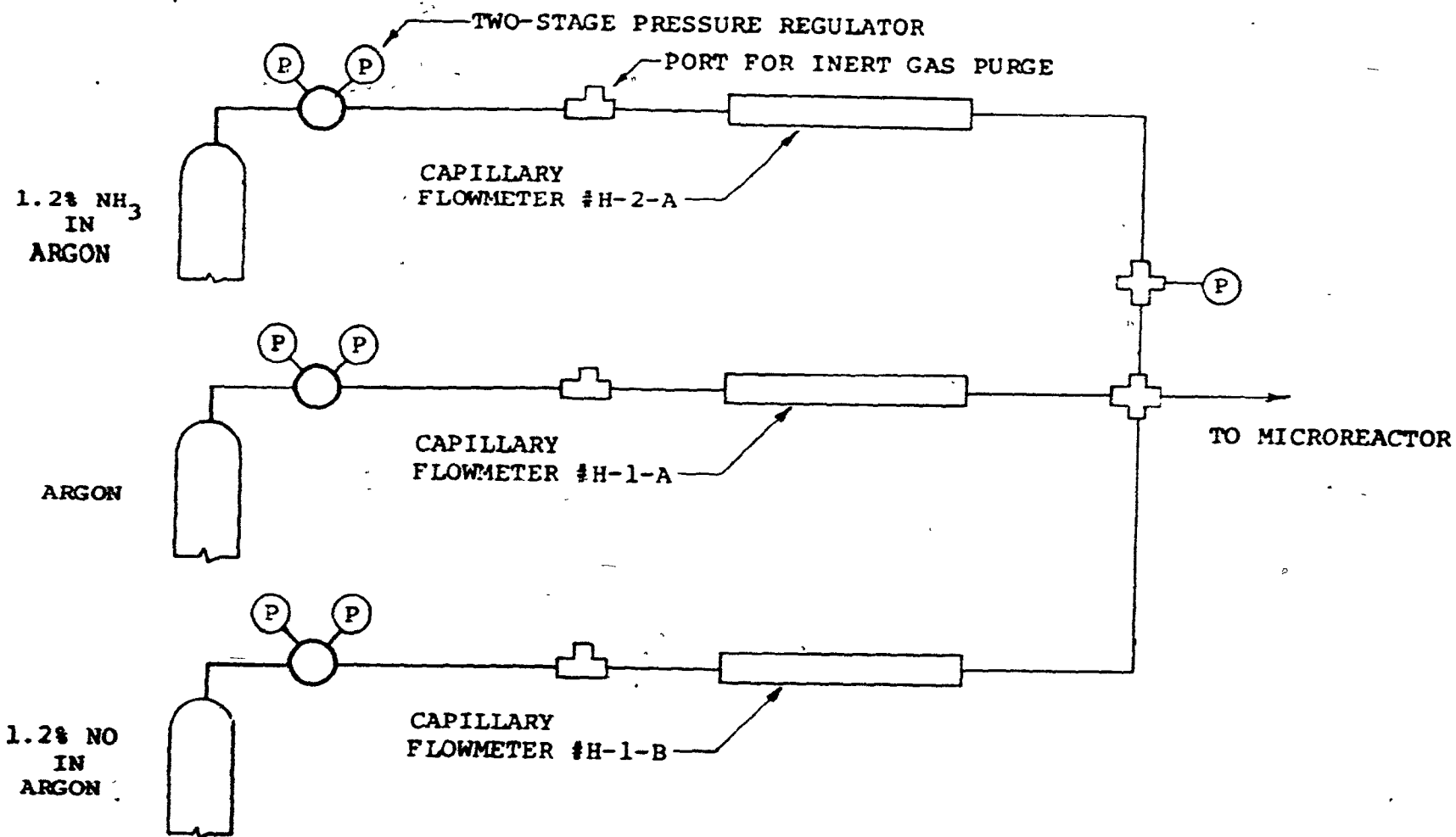


FIGURE 6: REACTANT SUPPLY SYSTEM

All tubes and fittings were constructed of type 316 stainless steel to resist corrosion by the nitrogen oxides and ammonia; the non-metal components were also inert. This system was simple, inexpensive, rugged, and leaktight.

Details of the mathematical modelling, design, construction, and calibration of the capillary flowmeters are presented in Appendix A. The results are summarized here.

The following equation for isothermal, compressible, ideal gas flow in a long pipe was used to correlate the preliminary flow data and size the flowmeters,

$$Q^2 = \frac{\pi^2}{16} \frac{RTg_c}{M} \frac{P_1^2 - P_2^2}{P_0^2} \frac{1}{1 + \frac{4.61}{4fL/D} K \log_{10}(P_1/P_2)} \frac{D^4}{4fL/D} \quad (5)$$

where Q is the volumetric flow rate in cc/sec, reduced to the reference pressure, P_0 , of one atmosphere absolute

R is the universal gas constant (8.314×10^7 g cm/gmole $^{\circ}\text{K}$)

M is the molecular weight of the gas (40 g/gmole for argon)

T is the gas temperature in $^{\circ}\text{K}$

g_c is the gravitational constant (981 cm/sec²)

P_1 is the inlet pressure in atm abs

P_2 is the outlet pressure in atm abs

L is the length of the capillary in cm

D is the internal diameter of the capillary in cm

f is the apparent friction factor

K is the kinetic energy factor (1.07 for turbulent flow and 2.00 for laminar flow).

This equation does not account for end effects, the L/D ratio, non-isothermal flow and other non-idealities which are discussed in Appendix A. These can usually be neglected at low Mach numbers.

The applicability of this equation was determined by measuring argon flow rates and the corresponding inlet and outlet pressures for two capillaries with a high length-to-diameter ratio. Results are given in Tables 18 and 19 of Appendix A. A computer program was written to analyze these data and calculate the friction factors and Reynolds numbers. Equation 5 can be used without restriction to model the flow only if the apparent friction factor data points from different flowmeters and different downstream pressures fall on one curve.

Data for meter number 1 are plotted in Figure 7. Reference to the original data points in Table 18 will show that the discharge pressure has a negligible effect on the apparent friction factor when it is less than 10 psig. When the discharge pressure is above 10 psig, the flow rate is less than that predicted by Equation 5 and the corresponding apparent friction factors are higher. For example, Figure 7 shows that at a Reynolds number of 88, the apparent friction factor for discharge to atmospheric pressure is 0.26, while that for discharge to 46 psig is 0.29.

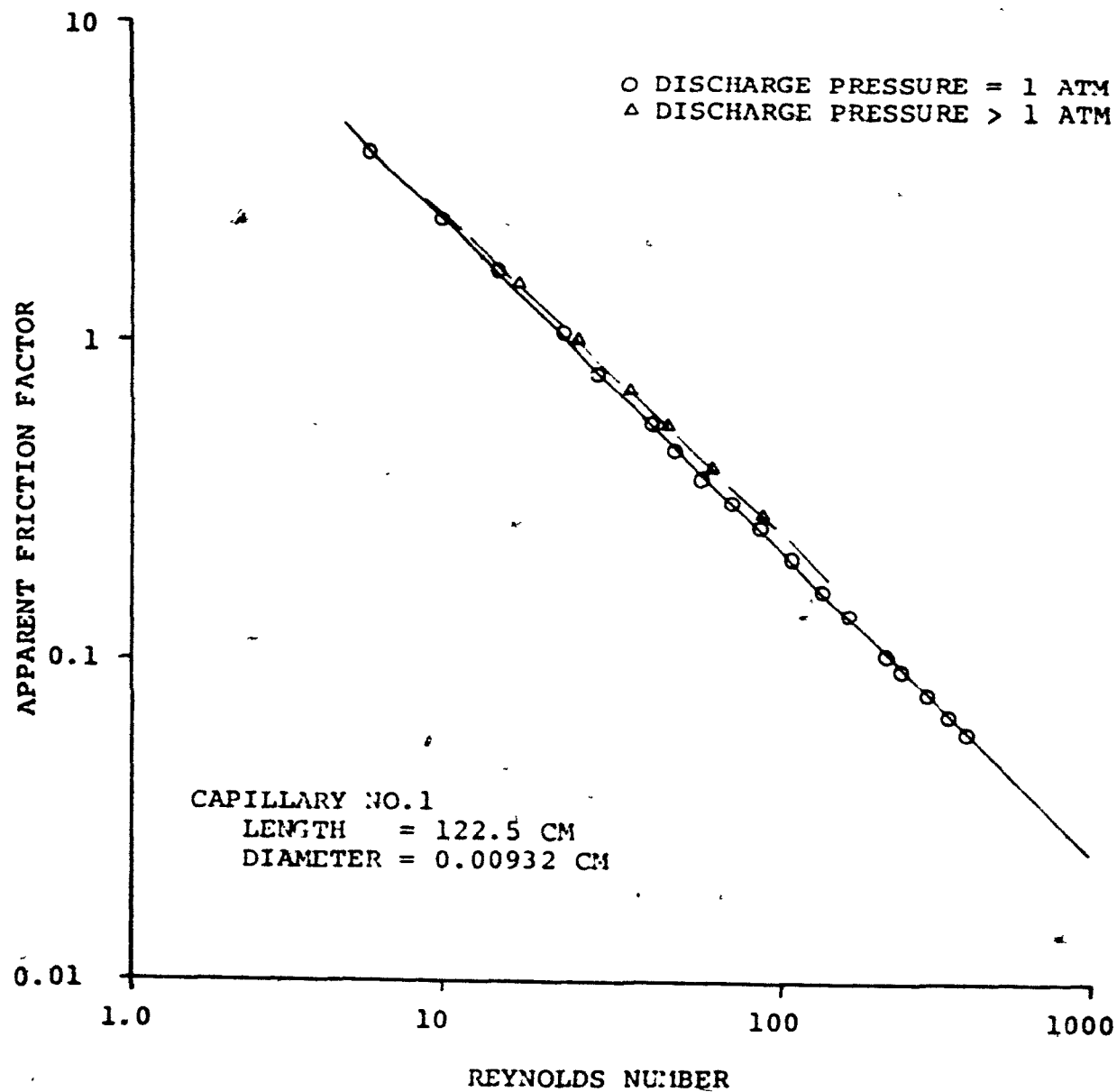


FIGURE 7: APPARENT FRICTION FACTOR VERSUS REYNOLDS NUMBER

This difference of 10% in the friction factors corresponds to a 5% difference in the flow rates.

The effect of capillary diameter is shown in Figure 8, where the apparent friction factor is plotted as a function of the Reynolds number for discharge to atmospheric pressure through two capillaries. Note that the apparent friction factor is approximately 25% less in the larger diameter capillary.

These two sets of data demonstrate that the apparent friction factor is strongly dependent on the tube diameter and slightly dependent on downstream pressure. The reasons for this deviation from the behaviour predicted by the model described by Equation 5 are discussed in greater detail in Appendix A. These limitations must be kept in mind when applying Equation 5 to the design of capillary flowmeters.

Another computer program was then written to use this preliminary flow data with Equation 5 to design flowmeters for catalyst testing. The apparent friction factor was assumed to have the following dependence on the Reynolds number,

$$f = 23/Re \quad Re < 2300 \quad (6)$$

$$f = 0.01 \quad Re > 2300 \quad (7)$$

Flow rates for different capillary dimensions and pressure drops were computed. Mach numbers, end effects, and temperature effects were also calculated.

Capillaries of different dimensions could be used to deliver the same gas flow rates. Usually lengths of about 20 cm

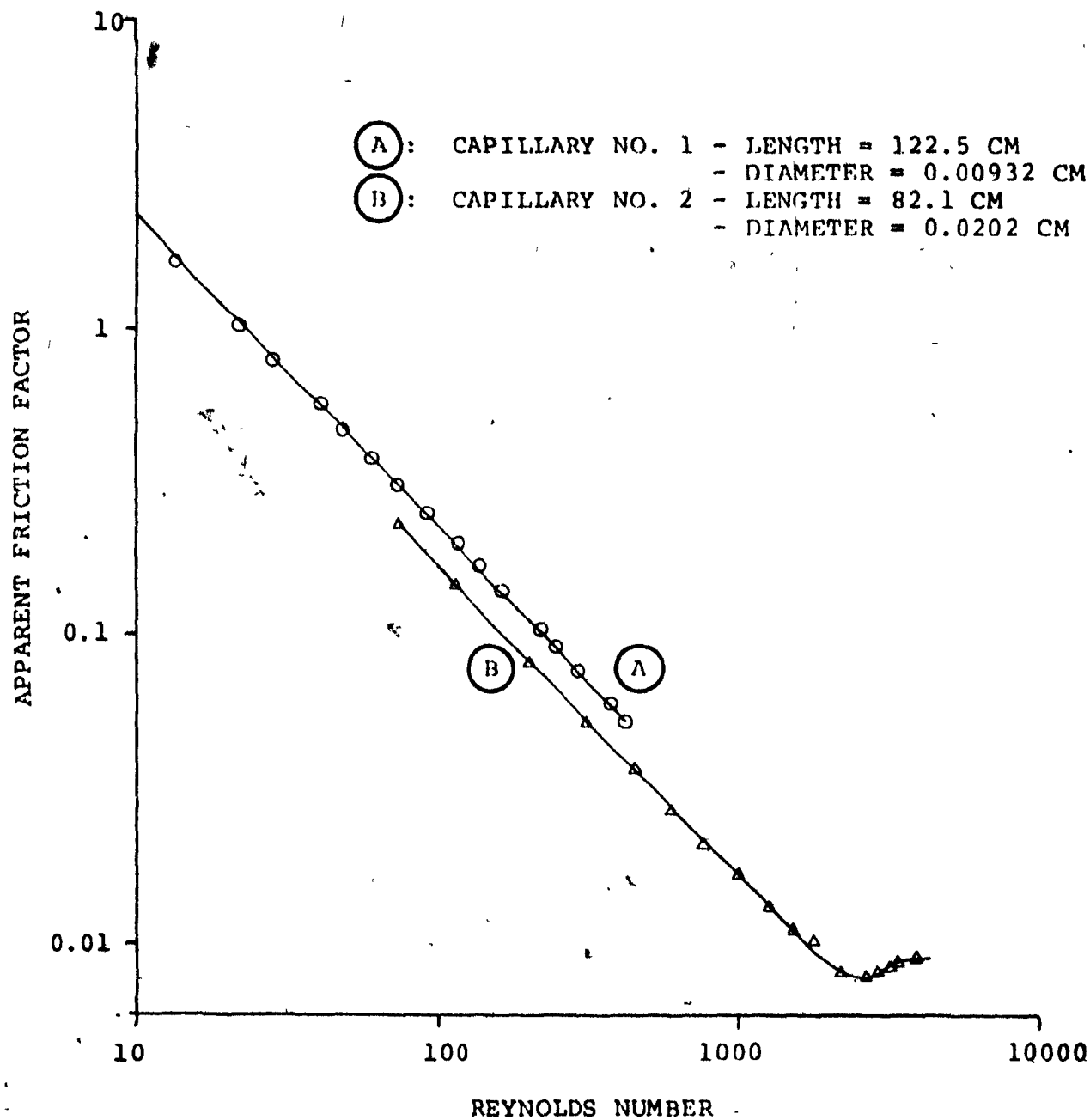


FIGURE 8: APPARENT FRICTION FACTOR VERSUS REYNOLDS NUMBER FOR SMALL CAPILLARIES

were chosen since this is the longest length that could fit inside the piping arrangement from the gas cylinders. Use of shorter meters would require smaller capillary diameters for the same pressure drop. This would result in higher Mach numbers and hence higher end and temperature effects. The meters listed in Table 1 were constructed and calibrated following the procedure described in Appendix A. A polynomial interpolation program was written to interpolate between the calibration points.

Figure 9 shows that actual flow rates were about 15% less than those predicted by the design program for a typical meter. This is probably due to the difference in the lengths of the constructed meter and the long capillaries used to generate the apparent friction factor data. Subsequent analysis of other capillary data not included in this report has shown that friction factors are higher in shorter tubes.

If a higher design accuracy were required, the design calculations would have to be based on friction factor data from capillaries with dimensions closer to those of the final meters. In this case a trial and error procedure would be followed; a crude meter would be constructed using the dimensions calculated from Equations 5, 6, and 7. Then gas flow rates would be measured at several different pressures and a new plot of apparent friction factor versus Reynolds number generated with the analysis program. The new expression for the friction factor would be substituted into the design program and the final dimensions of

-25-

Table 1: Flowmeters for Raney Catalyst Tests

Meter No.	Supply Gas	Capillary Dimensions		Maximum Flowrate cc/min
		length cm	diameter cm	
H-1-A	argon	20	.1105	91
H-1-B	1.2% NO in argon	20	.1105	85
H-2-A	1.2% NH ₃ in argon	20	.13	170

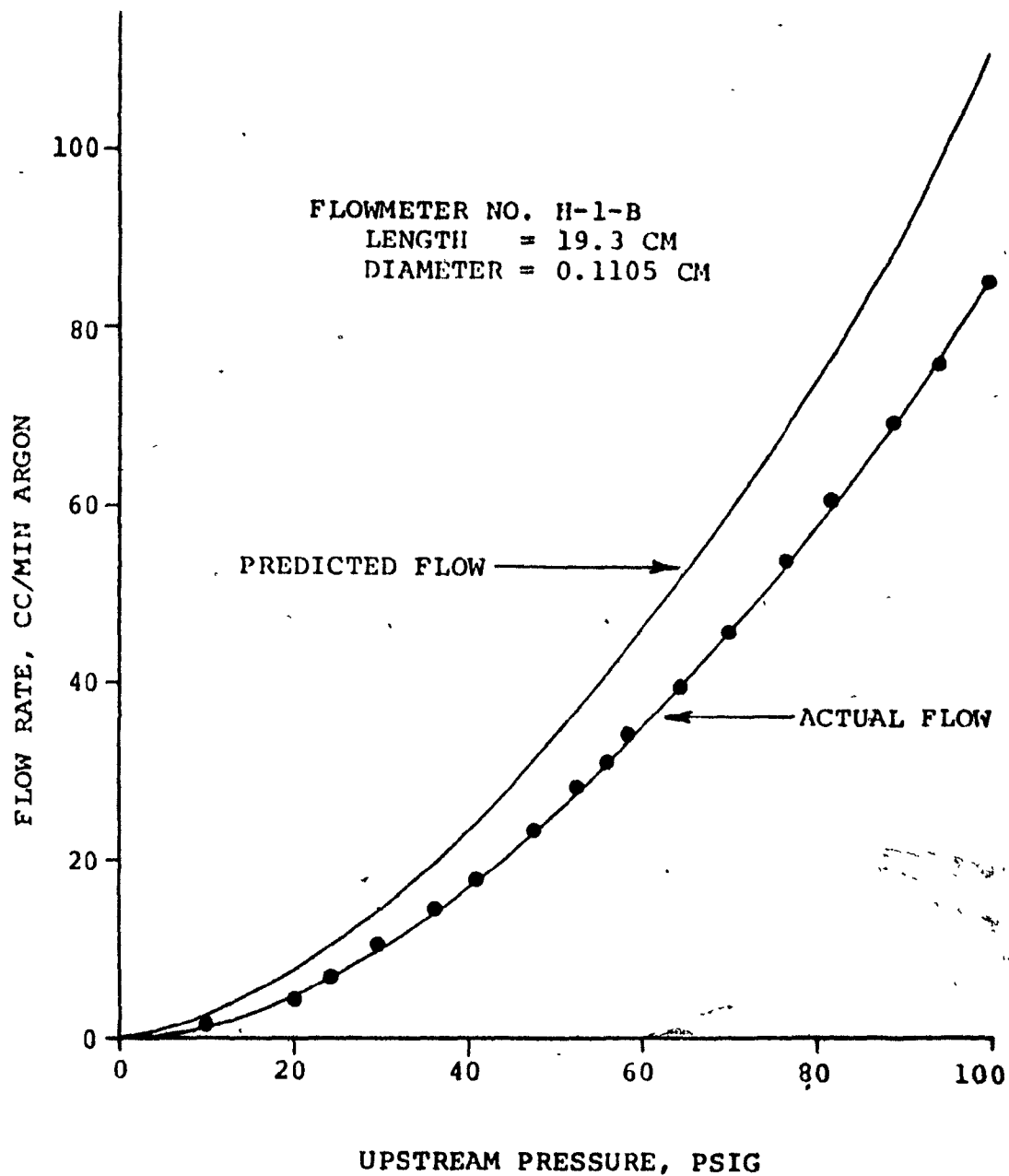


FIGURE 9: PREDICTED AND ACTUAL FLOW RATES
FOR FLOWMETER NO. H-1-B

the new meter established. The actual flow rates would probably be within 2% of the predicted flows. The process could be repeated to give higher accuracy.

The capillaries must be operated free from dirt or other obstructions which could interfere with the flow. Teflon filters were used for this purpose and proved superior to glass wool. Some problems were encountered with deposition of a solid salt in the nitrogen oxide lines. These were solved by scrupulously flushing the lines with inert gas after every test.

The capillary flowmeters provided an inexpensive, accurate, and simple way to supply the gas flows needed for catalyst testing. These meters can be operated in either the sonic or subsonic range. In this work it was convenient to work in the subsonic region because it is not possible to construct meters short enough to achieve sonic flow without excessive pressure drops. As a consequence it was necessary to operate at a low Mach number to minimize temperature and end effects. This ensured that the flow rates calculated from calibration data were within 1% of the actual flows for all the tests reported in this thesis.

Section V: Chemical Analyses

(A) Introduction

The chemical analysis system was originally intended to analyze gaseous samples containing the nitrogen oxides, ammonia, water, argon, oxygen, and nitrogen which would be present in a stream of nitric acid plant tail gas which was being reduced with ammonia.

Quantitative chemical analysis for nitrogen oxides has always been awkward and results often inaccurate. Analysis for individual oxides of nitrogen is difficult because the oxidation state can change in the course of the analysis (14,29). When ammonia is present the difficulties are compounded.

A literature survey of analytical techniques showed that no single method except mass spectrometry had been developed to easily and accurately analyze mixtures of nitrogen oxides and ammonia. Other methods are useful only over limited ranges of concentrations and oxidation states. Mass spectrometry was not available for the present investigation so development of a combined chromatographic and infrared technique was undertaken. Had it proven successful, the infrared method would be less expensive and more convenient than mass spectrometry.

An initial chromatographic technique to separate all the components on Chromsorb 104 packing proved unsuccessful despite literature claims to the contrary. Another method limited to

argon, nitrogen, and nitric oxide was adopted and proved satisfactory. The infrared analyzer gave encouraging preliminary results, but could not be used because its cell windows were attacked by the nitrogen dioxide. These limitations on the chemical analyses restricted the catalyst testing to the non-selective reaction between nitric oxide and ammonia.

(B) Analytical Techniques

Previously reported methods to determine the components in the reaction mixture are wet chemical analyses, infrared spectrometry, ultraviolet spectrometry, mass spectrometry, chromatography, and specialized methods for individual components. The determination of nitrogen oxides will be discussed at greater length because it is the most difficult of the analyses.

Faucett, McRight, and Graham (29) compared the Griess-Hosvay method, the hydrogen peroxide method, and the mixed acid method for determination of total nitrogen oxides in nitric acid plant tail gases. They did not consider the Griess-Hosvay method satisfactory because the nitrite equivalence factor to convert nitrite formed to total nitrogen oxides varied significantly with the nitric oxide/nitrogen dioxide ratio. They also found the hydrogen peroxide method unreliable because small differences in the titration of the sample and the reference blank could lead to large errors in the nitrogen oxide concentration. The most accurate method was the mixed acid procedure in which the

the nitrogen oxides react with a mixture of nitric acid and sulfuric acid to produce nitrosulfuric acid.

Johnson (47) presented a method for determination of high concentrations of nitrogen oxides in air. Markvart (55) determined total nitrogen oxides after removal of ammonia from the sample by sorption on anhydrous $\text{Mg}(\text{ClO}_4)_2$ using a modification of Johnson's procedure.

Fisher and Becknell (31) improved the Saltzman variation of the Griess-Hosvay method by oxidizing the nitric oxide with ozone before using the standard colorimetric technique. Addition of 1% boric acid to the Saltzman reagent eliminated the interference of up to 100 ppm of ammonia in the sample. The boric acid forms a poorly dissociated salt with ammonia.

Determination of oxygen, nitrogen, and argon by chemical methods is more straightforward. Ammonia can be measured by the indophenol method (12,13). Standard techniques are available for oxygen, argon, and nitrogen.

There are other wet chemical methods, but in general a separate analysis must be made for each component. The presence of nitrogen oxides will often interfere with the determination of ammonia and vice versa. However, selective removal of only one component from a gas mixture is not always possible.

The oxidation state of the nitrogen oxides must be fixed before total nitrogen oxide concentrations can be calculated. For best results the nitric oxide is completely oxidized to

nitrogen dioxide before measurement. Oxidizing agents used with varying degrees of success include air, oxygen, MnO_4^- , CrO_7^{2-} , H_2O_2 , and O_3 . Fisher and Becknell (31) reported that ozone gave the most complete and reproducible results.

Each of the methods listed is useful and accurate in certain ranges of concentration and nitric oxide/nitrogen dioxide ratios. However development of a wet chemical method to analyze for all components would be complex and the analyses too time-consuming to be useful for repeated catalyst testing.

Infrared spectroscopy is convenient because several components in one sample can be easily analyzed by scanning at different wavelengths. Noble gases and homopolar diatomic gases have no vibrational infrared spectra and cannot be determined. Taylor (90) used infrared spectroscopy to determine nitrogen oxides in automobile exhaust. Klimish and Taylor (50) used an infrared analyzer to determine nitric oxide and nitrous oxide and an ultraviolet analyzer to determine nitrogen dioxide. Nicksic and Harkins (58) also used ultraviolet spectrometry to measure nitrogen dioxide after all nitric oxide was oxidized with oxygen.

The methods based on radiation absorption are not free from complications. Butcher and Ruff (14) reported that light intensity fluctuations prior to sample analysis could introduce a systematic error by changing oxidation state. This suggests complete oxidation of the sample before analysis should be

considered. Since the radiation absorption is sensitive to the nitrogen dioxide/dinitrogen tetroxide equilibrium, the sample pressure and temperature must be controlled.

Di Martini (24) determined nitrogen dioxide continuously in flowing gas mixtures with a nitrate specific electrode after ozonation of the sample. Results were accurate over a limited range of nitrogen oxide concentrations.

Otto and Shelef (61,62,63) used mass spectra analysis to measure product distributions in the reaction between nitric oxide and ammonia. This is probably the most accurate method to determine all the components in the reaction mixture.

Chromatography has been used to separate mixtures of nitrogen oxides (5,41,43,44,49,53,57,95). It is convenient because other components such as ammonia, nitrogen, oxygen, and water can be measured from the same sample. Porous polymer packings are the most common. Hollis (44) and Wilhite (95) separated nitrogen oxides from air on Porapak Q columns. Cleemput (19) used a similar method. Lamb and Tollefson (51) separated nitric oxide, nitrogen, and hydrogen on a column of Porapak Q and Porapak R in series. Chromsorb 104 has been used for the separation of nitrogen oxides. Available literature data on these porous polymer packings indicated that they could be used to analyze the complete reaction mixture.

Ayen and Amirnazmi (7) studied the reaction of nitrogen dioxide with hydrogen by analyzing for nitrogen, hydrogen, and nitric oxide on a Molecular Sieve 5A column.

The separation of the "permanent gases," i.e., argon, oxygen, and nitrogen has been reviewed by Littlewood (53). Nitrogen can easily be separated from both argon and oxygen on several different column packings, but separation of argon and oxygen is more difficult. The best results were achieved on Molecular Sieve 5A or 13X at dry-ice temperatures (40,42,46,52,60). Jamieson (46) developed a reliable, reproducible, and accurate method of analyzing mixtures containing several percent argon in air. He used a 6 ft column packed with Molecular Sieve 5A at dry-ice temperatures. The argon eluted in five minutes, the oxygen in seven minutes, and the nitrogen would come off when the column was raised to room temperature.

A chemical analysis system to accurately measure the extent of reaction of nitrogen oxides with ammonia had to be chosen from among these methods. Efficient operation of the reactor would require rapid sample analysis. The sample size and sampling technique should be easily adapted to the microreactor system.

On the basis of the literature survey a combined chromatographic and infrared spectrometric technique seemed the most promising. Both methods should be capable of giving accurate results rapidly with relatively small sample volumes. The chromatograph would definitely analyze oxygen, nitrogen, argon, and possibly ammonia and nitrogen oxides. The infrared analyzer could be used for nitrogen oxides, ammonia, and water.

(C) Chromatographic Analysis

The gas samples were analyzed by an F&M Model 700 gas chromatograph with thermal conductivity detectors. The chromatograph column and sampling valves were modified as shown in Appendix B to improve column temperature control and ease and accuracy of gas sampling.

If nitrogen oxides were reduced by ammonia in any commercial process, nitrogen would be present to a large excess from the air used in the process. However it was convenient to use the appearance of the nitrogen peak as a measure of the extent of reaction so another diluent such as argon or helium was considered.

Helium would have been a convenient replacement for nitrogen because it was the carrier gas used in the chromatograph. However, the volume of gas injected per sample varied with the flow rate because of an appreciable pressure drop through the sampling valves. Under these conditions, the analysis of the sample could not be determined from the chromatogram alone because there would have been no peak for helium. Accurate calibration to account for the varying sample size could have been difficult.

The replacement of nitrogen by argon avoided the problem of the varying sample size because argon could be used as an internal standard with the sizes of all other peaks measured relative to the argon peak. The disadvantage of the use of argon is that it requires the separation of oxygen and argon when the selective reaction, containing oxygen, is studied. In

spite of this disadvantage, argon was used instead of helium in order to obtain more accurate analyses.

Available literature suggested that porous polymer packings were best suited to separate all the components, so this method was attempted first (19,43,51). A 10 ft length of 1/8 in outside diameter stainless steel tubing packed with Chromsorb 104 was tested with ammonia, oxygen, argon, nitric oxide, and mixtures of these components. Initial results were satisfactory; peak heights and retention times were reproducible. But after repeated use, unusual peaks and retention times appeared. Tests with nitric oxide in the presence of oxygen demonstrated that the column packing was reacting with the samples. Probably nitrogen dioxide was nitrating the benzene ring of the Chromsorb 104 packing. This effect might have been observed by other workers had they used their columns over a longer period of time or had they used the relatively high nitrogen oxide concentrations of this test work.

These results indicated that the reactivity of the nitrogen dioxide would make development of a chromatographic technique to separate all the components of the reaction mixture difficult. The analysis was further complicated by tailing of the ammonia peak on Chromsorb 104 and on other packings. Ammonia can even be adsorbed on the walls of stainless steel tubing and can exhibit tailing in the absence of a column packing (38). Because of these difficulties, the final chromatographic analysis was limited to

argon, nitrogen, oxygen, and nitric oxide. The other components such as water, ammonia, and nitrogen dioxide were removed from the sample before it reached the column since they would have interfered with the analysis. This final method was based on the work of Jamieson (46) and Ayen (7). Reference to their retention data shows that a Molecular Sieve 5A column of suitable length will separate hydrogen, argon, nitrogen, and nitric oxide when no oxygen is present. When oxygen is present it will probably react with the nitric oxide to form nitrogen dioxide which will then be adsorbed. Hence this analytical method was used for nitric oxide only when the sample contained no oxygen.

A Molecular Sieve 5A column was designed on the data presented by Jamieson (46). Column construction, conditioning, and operating variables are described in Appendix B. A 10 ft long column was used instead of the 6 ft length reported by Jamieson to ensure complete separation of argon and oxygen. Sample volumes and thermal conductivity detector current were adjusted to give a sufficiently large nitrogen peak at nitrogen and nitric oxide concentrations ranging from 0.01 to 0.3%.

The water produced by the reduction of nitric oxide with ammonia would have interfered with the chromatographic separation. It was removed along with the ammonia and nitrous oxide by a Molecular Sieve 13X adsorbent bed in the helium line ahead of the chromatograph column. Design of this bed is discussed in Appendix B. During initial calibration work with pure nitrogen,

oxygen, argon, and nitric oxide the bed was not used so the samples passed directly from the sampling valve to the chromatograph column.

Typical chromatograms are shown in Appendix B. Note the non-symmetrical shape of the argon and nitric oxide peaks. Nitric oxide exhibited slight tailing of the peaks at all concentrations. Argon, oxygen, and nitrogen exhibited slight tailing when samples were large. At lower concentrations or smaller sample volumes of 0.26 cc, the peaks of these three components were virtually symmetrical. Retention times also increased slightly with decreasing sample size or concentration. This behaviour is consistent with a non-linear sorption isotherm on the column packing.

The detector was equally sensitive to argon, oxygen, and nitrogen. Concentrations of these components were calculated from relative peak areas, where the peak area was defined as the product of peak height and width at half the height of the peak. Sensitivity to nitric oxide was considerably less. Nitric oxide concentrations were calculated from the ratio of peak area in one sample to the peak area in another sample of known concentration of nitric oxide. In practice, the amount of nitric oxide in the reactor product stream was found relative to the known concentration in the reactor inlet stream. Tests with mixtures of argon, nitrogen, and nitric oxide confirmed that these methods of sample analysis were accurate within several percent of the absolute amount of each component present.

This analysis technique for argon, nitrogen, and nitric oxide proved reliable, accurate, and reproducible during six months of extensive use. The only maintenance work required was a routine replacement of the adsorbent bed after every hundred samples.

(D) Infrared Analysis

Absorption of infrared radiation by water, ammonia, and nitrogen oxides has been used for quantitative analysis of gas mixtures. Reference to the spectra of these gases will show that it is possible to select frequencies where one component absorbs strongly and the others only weakly (3,9,45,70,81,87). Typical frequencies are 925 cm^{-1} for ammonia, 2250 cm^{-1} for nitrous oxide, 1908 cm^{-1} for nitric oxide, 3000 cm^{-1} for nitrogen dioxide, and 3750 cm^{-1} for water. At these frequencies corrections for absorbances of interfering compounds should be straightforward, so quantitative infrared analysis is feasible.

The analysis of a gas sample containing water, ammonia, and nitrogen oxides would be complicated by possible chemical reactions between the components. Reaction between nitrogen oxides and ammonia is unlikely at room temperature, but would have to be investigated experimentally. Formation of ammonium nitrate would prove troublesome. However oxidation of the nitric oxide to nitrogen dioxide would definitely occur and the nitrogen dioxide/dinitrogen tetroxide equilibrium would have to be accounted for. The oxidation state of the nitrogen oxides might

have to be fixed by a technique such as exposure to oxygen or ozone. This method has proven successful for ultraviolet determination of nitrogen dioxide (58).

To measure ppm concentrations of products and reactants the infrared analyzer must have a long path length; otherwise the absorbance would not be measurable. One such instrument, a Wilks Miran I Infrared Analyzer with long path cell, was purchased for this project. Stephens (88) has discussed the theory of long path cells. Gilby (37) has described this particular instrument. A sample of the gas is introduced into a 5 liter cell with a special mirror at each end. An infrared beam of known wavelength enters the cell through one window, is reflected up and down the length of the cell many times by the mirrors, and finally leaves through another window where its intensity is measured by a detector. With this particular instrument it is possible to vary the wavelength and energy content of the beam, the path length it travels, and the pressure of the gas inside the cell. Maximum path length is approximately 20 m.

Preliminary calibration data established that the analyzer could easily measure ppm concentrations of nitric oxide and ammonia at high path lengths. The samples were admitted into a previously evacuated cell and the absorbances measured after the cell had been isolated. At low path lengths concentrations up to several tenths of a percent could be measured.

Tests with nitric oxide showed that traces of oxygen in the sampling system caused gradual oxidation to nitrogen dioxide over half an hour even when no oxygen was present in the original sample. The problem is serious because the absorbance by nitrogen dioxide is much higher than that by nitric oxide, so even a slight conversion can introduce large errors into quantitative analysis. Other workers have experienced similar difficulties with oxidation of nitric oxide by traces of oxygen during analysis. Complete oxidation of nitric oxide to nitrogen dioxide prior to absorbance measurements would be one possible solution. The other approach would be continuous analysis of gas flowing through the cell at a constant rate. In both cases, the oxidation state would have to be established.

During this preliminary work several instrument problems occurred. The sodium chloride windows of the long path cell became corroded by moisture in the atmosphere and the nitrogen oxides in the gas samples. Some mechanical problems with the instrument also delayed work. The mechanical problems were easily resolved, but the cell window corrosion was serious enough to prevent further use of the instrument. Most standard cell window materials such as sodium chloride, potassium bromide, and cesium iodide are attacked by nitrogen dioxide (4). Others such as barium fluoride and calcium fluoride are suitable for use with nitrogen dioxide but are attacked by ammonia. Perhaps a zinc sulfide or similar material could be used.

Despite its limitations for this particular analysis the infrared spectrometer with long path cell should be a valuable research instrument. Corrosion by atmospheric moisture can easily be eliminated by use in a dry atmosphere. The instrument will become more useful as corrosion resistant cell windows are developed.

Section VI: Catalyst Support

The Raney metal particles are too fine to be used without support in a fixed catalyst bed; they must be dispersed on a substrate to function effectively as catalysts for gas phase reactions. The catalyst support must have certain mechanical properties. It must have sufficient strength to hold the Raney metals in place and to allow convenient grinding, sieving, and handling of the final catalyst. The Raney metals must be uniformly dispersed throughout the bulk of the support to avoid agglomeration of active catalyst particles which might lead to high local reaction rates, overheating, and inaccurate overall activity measurements. The support must have a fine pore structure so that reactants and products can diffuse to and from the active sites without mass transfer limitations to the chemical reactions.

It should not modify or otherwise interfere with the activities of the active metal alloys. The catalyst support can affect the apparent reaction rate by adsorbing or interfering with the transport of reactants, products, or intermediates; it might even have a significant activity for promoting the reaction itself. The support can play a more indirect role by chemically or physically interacting with the active metal during catalyst preparation. Any such interference should be avoided when comparing the inherent activities of different alloys, but might prove useful when trying to improve the activity or selectivity of a specific catalyst.

In short, the Raney metals should be uniformly dispersed throughout the bulk of a strong support which allows diffusion of reactants and products, which does not modify the Raney metals, and which has little or no catalytic activity itself.

Typical catalyst supports are alumina, silica, and zeolites; they are available as commercial products to be used either as catalysts by themselves or as bases for more active components. These commercial products would not be acceptable supports for Raney catalysts because mechanical mixing is the only way that they could be loaded with the Raney metal particles. This would coat the outside of the support particles and the resulting high concentration of metal there could lead to high local reaction rates and temperatures.

The dispersion of the Raney metals in the support must be more intimate than that achieved by mechanical mixing of the separate solid phases. One convenient way of attaining this mixing is introduction of the Raney metals into a colloidal dispersion of the support. The dispersion can then be gelled, dried, calcinated, and further treated if necessary.

Silica, alumina, and silica-alumina gels can be prepared by this method. However, alumina has been known to chemically react with nickel to form nickel aluminates in the preparation of catalysts from nickel oxide. This can significantly change the catalyst properties (56). Silica should prove more suitable as a support because it does not interact in this fashion. Hence, it was chosen as the support for the Raney catalysts.

Silica gels can be prepared by a variety of methods (1,23,71,85). Sing and Madeley (85,86) studied surface properties of gels prepared from sodium silicate and sulphuric acid. Acker (1) reported differences between acid-set and alkali-set silica gels. Depasse and Watillon (23) prepared silica gels from monosilicic acid. Colloidal silica has also been used to prepare silica gels.

Reference to these methods will show that strict adherence to experimental procedures is necessary. Sometimes special care must be taken to achieve specific objectives. Ranganthan, Bakhshi, and Mathews (72) had to use very pure sodium metasilicate because the reaction they were investigating was sensitive to impurities in the silica gel. They also found that rapid drying resulted in a powdery, opaque gel of variable properties. A more gradual drying over several days resulted in a more uniform product. Casey (17) found gellation would sometimes occur at a high pH after only part of the neutralizing acid had been added. Plank (71) found that silica gels which had been allowed long settling times were less sensitive to subsequent treatment than those which had set for only short times.

Several conclusions about the preparation of reproducible silica catalysts can be drawn from the observations of these workers. First, strict adherence to experimental procedures is necessary. Second, gel properties are more easily controlled if gellation and settling occur gradually over a period of at least

one day. Finally, the gels should be dried gradually, preferably over a period of several days.

Several methods of preparing the catalyst support were tried before the final method was developed. Preliminary tests in which sodium metasilicate solution was neutralized by hydrochloric acid were discontinued because control of gellation was poor. The next series of tests were based on Cabosil, a commercial fumed silicon dioxide of very high purity and well-defined particle size. Properties of Cabosil are given in Appendix D. The Cabosil was dissolved in aqueous sodium hydroxide solution and then neutralized with hydrochloric acid. Problems in control of gellation were again encountered. Gel formation was sometimes rapid and sometimes slow; properties of the gels varied from batch to batch. The basic problem is instability of the alkali solutions of the Cabosil. Without stabilization of the silicon dioxide particles in the liquid, reproducible gellation is difficult.

Fortunately a commercial stabilized silicon dioxide suspension, Ludox HS-40, was available for the preparation of the final catalyst support. Some properties of Ludox are listed in Appendix D. Ludox HS-40 is an aqueous colloidal dispersion of discrete spherical particles of surface hydroxylated silica (26). The stability of the suspension is shown in Figure 10, where the dependence of gel time on pH is illustrated. At pH above 9 or below 3 the suspension is stable.

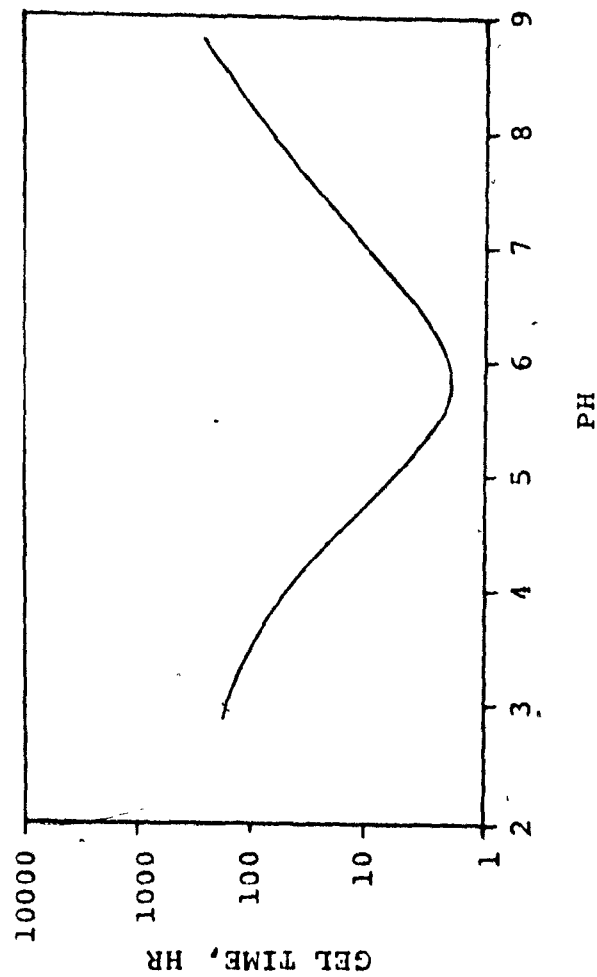


FIGURE 10: STABILITY OF LUDOX HS-40 (26)

The Raney metal powders were dispersed in the Ludox suspension and hydrochloric acid added to lower the pH to about 6, the region of minimum stability. The suspension then gelled and was allowed to settle and dry. Details of the procedure are given in Appendix C.

Several items in this procedure should be noted. The intense mixing of the Waring Blendor is necessary to evenly disperse the Raney metal powders in the Ludox. If a low intensity mixer is used, this dispersion is not achieved; agglomerates of Raney metal particles can be seen when a powerful light is shone through the gel. No such agglomerates are visible after dispersion in the Waring Blendor.

The gels gradually thickened until the liquid started to climb the shaft of the mixer rotating in it. Agitation was continued until the gel was sufficiently viscous that the metal particles would not settle out; usually thirty minutes was satisfactory. The one-day settling time and four-day drying period follow the recommendations of Ranganathan (72). Attempts to shorten the drying time resulted in powdery gels, thus confirming his observations (72).

The Raney metal catalysts were oxidized by heating overnight in a muffle furnace in the presence of air. This treatment generated fines for several of the catalysts, so all catalysts were resieved before use.

Several batches of silica support without Raney metal were prepared so that the activity of the support could be measured. These were prepared by a procedure identical to that in Appendix C, except that no active metal was added.

This method was used successfully over a period of eight months and proved to be a rapid, inexpensive, and reproducible way to prepare silica catalyst supports.

Section VII: Preparation of Raney Alloy Catalysts

(A) Introduction

Raney metals are frequently used to catalyze reactions between liquids and between liquids and gases. When catalyzing gaseous reactions, the Raney powders must be used either in a fluidized bed or supported on an inert substrate in a fixed bed. A typical high temperature application was reported by Field et al. (30) who flame-sprayed Raney nickel on metal plates to catalyze the methanation of synthesis gas. Forney (32) used a fluidized bed of Raney nickel to produce gas from coal via methanation. For the present investigation, the Raney metals were supported on silica according to the procedure described in the previous section.

To prepare a catalyst by the Raney method an aluminum alloy of the active metal is formed, ground to a fine mesh size, sieved, and exposed to an alkali solution which leaches out the aluminum leaving behind a porous structure. It is then washed free of alkali and stored under water or methanol before use.

The physical properties and activity of the final catalyst are determined by the chemical composition and physical properties of the starting aluminum alloy and the leaching, washing, and storage methods. Each of these variables can have a drastic effect on the activity of the final catalyst.

The effect of alloy composition will be considered first. The starting alloy typically contains about 50% by weight aluminum; several discrete phases are present. For example, Anderson, Pieters, and Freel (34,35) reported that an alloy of 50.8% by weight nickel in aluminum consisted of Ni_2Al_3 , NiAl_3 , and a eutectic phase. They found significant differences in the reactivities of NiAl , Ni_2Al_3 , and the eutectic phase to alkali in the preparation of Raney nickel. Petrov et al. (68) suggested the activity of the Raney metal depended on its original phase composition in the aluminum alloy. He supported this claim by correlating the activity of Raney nickel for the hydrogenation of heptene-1 with the content of the NiAl_3 phase in the starting alloy. The importance of the microstructure of the starting alloys has been shown by Davtyan et al. (22) who demonstrated that the lattice parameters of the final Raney nickel can vary substantially with the rate of crystallization and homogenation of the starting alloy.

The leaching process is believed to occur by the reaction of the aluminum in the alloy with alkali solution to yield sodium aluminate and evolve hydrogen according to the following stoichiometry,



The sodium aluminate dissolves in the liquid phase. Residual aluminum left behind with the active metal is usually locked into

the crystal structure or loosely bound as aluminum trihydrate. The active metal forms crystallites which, in the case of Raney nickel, range in size from 25 to 150 Å, and form a network with pore radii in the range of 30 to 100 Å (2, 59, 66). Electron and x-ray diffraction patterns of Raney nickel often correspond to face-centered cubic nickel. The crystallites are held together in a sponge-like mass that has overall dimensions similar to the starting alloy. A thorough discussion of the structure of Raney nickel is given by Anderson, Freel, and Pieters (34, 35, 36, 75, 76) and by Fouilloux et al (33).

The leaching of an aluminum alloy particle is illustrated in Figure 11. The particle is moving relative to the liquid phase and alkali is diffusing into the interior. The hydrogen is diffusing to the surface of the particle from the reaction sites before it bubbles away from the particle. According to the mechanism postulated by Anderson (34) for Raney nickel, the alkali attack advances as a front yielding a sharp boundary between the alloy and the activated catalyst.

The maximum reaction rate possible is determined primarily by the alloy reactivity, the concentration and temperature of the alkali solution, and the surface area available for reaction. Particle size is important since it determines the surface area available and because diffusion resistances into the particle may be significant for larger sizes, especially if hydrogen becomes trapped within the pores.

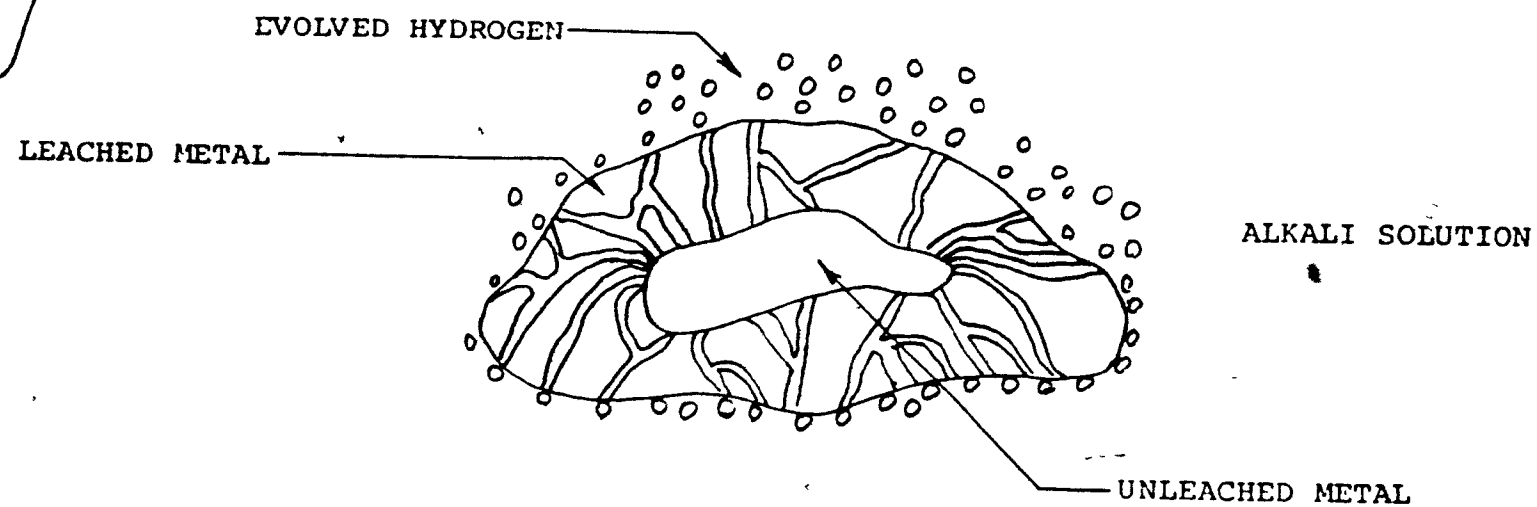



FIGURE 11: FORMATION OF ACTIVE RANEY METAL



Intensity of agitation can affect the leaching rate in two distinct ways. Increased agitation will decrease the diffusion resistance for mass transfer between the bulk of the liquid phase and the surface of the metal particles. However, unless agitation is intense, this effect is probably minor since the particles are merely swept along with the liquid at high liquid velocities. A more important effect is prevention of the agglomeration of partially leached metal particles. The pronounced tendency of leached Raney metal particles to agglomerate can significantly lower the leaching rate unless agitation is intense enough to prevent it.

In summary, the extent of leaching is determined by the reactivity of the starting alloy, the temperature, the concentration of the alkali solution, the intensity of agitation and the extraction time. Raney metals may have from 2% to 60% by weight residual aluminum in the final catalyst (34).

The washing and storage procedures are less complex than the leaching, but can also affect activity. Usually the active metals are washed free of excess alkali with distilled water, but other methods are being introduced. Oxygen is normally excluded from the system during the washing so that chemisorbed hydrogen will not be displaced. In some preparations hydrogen is deliberately bubbled through the liquid in the washing sequence. Final catalysts are stored under water or ethanol.

The importance of leaching conditions and subsequent treatment on catalyst properties was demonstrated by Anderson (34). For example, his results showed the dependence of surface area on extent of leaching illustrated in Figure 12. He also found that exposure to boiling water reduced the specific surface area of one catalyst by a factor of six. o

This general discussion of Raney metals illustrates the factors important to the preparation of the Raney copper-nickel alloy catalysts.

(B) Preparation of Raney Copper-Nickel Alloy Catalysts

The preparation of Raney nickel is well described in the literature (2,22,28,34,59,68,69). Reactivities of nickel-aluminum alloys and the effects of leaching conditions have been described; washing and storage procedures have been developed. The works of Anderson et al. (34,35,36,75,76) and Fouilloux et al. (33) present the basic mechanisms involved in the preparation of Raney nickel. The properties of Raney nickel prepared by most of these standard methods can be predicted from literature data.

Less data are available for Raney copper, but several standard preparation methods are known. A 50% by weight copper in aluminum alloy will react with alkali to yield an active catalyst (66). As yet, there has been no extensive study of the effects of preparation conditions on the properties of Raney copper.

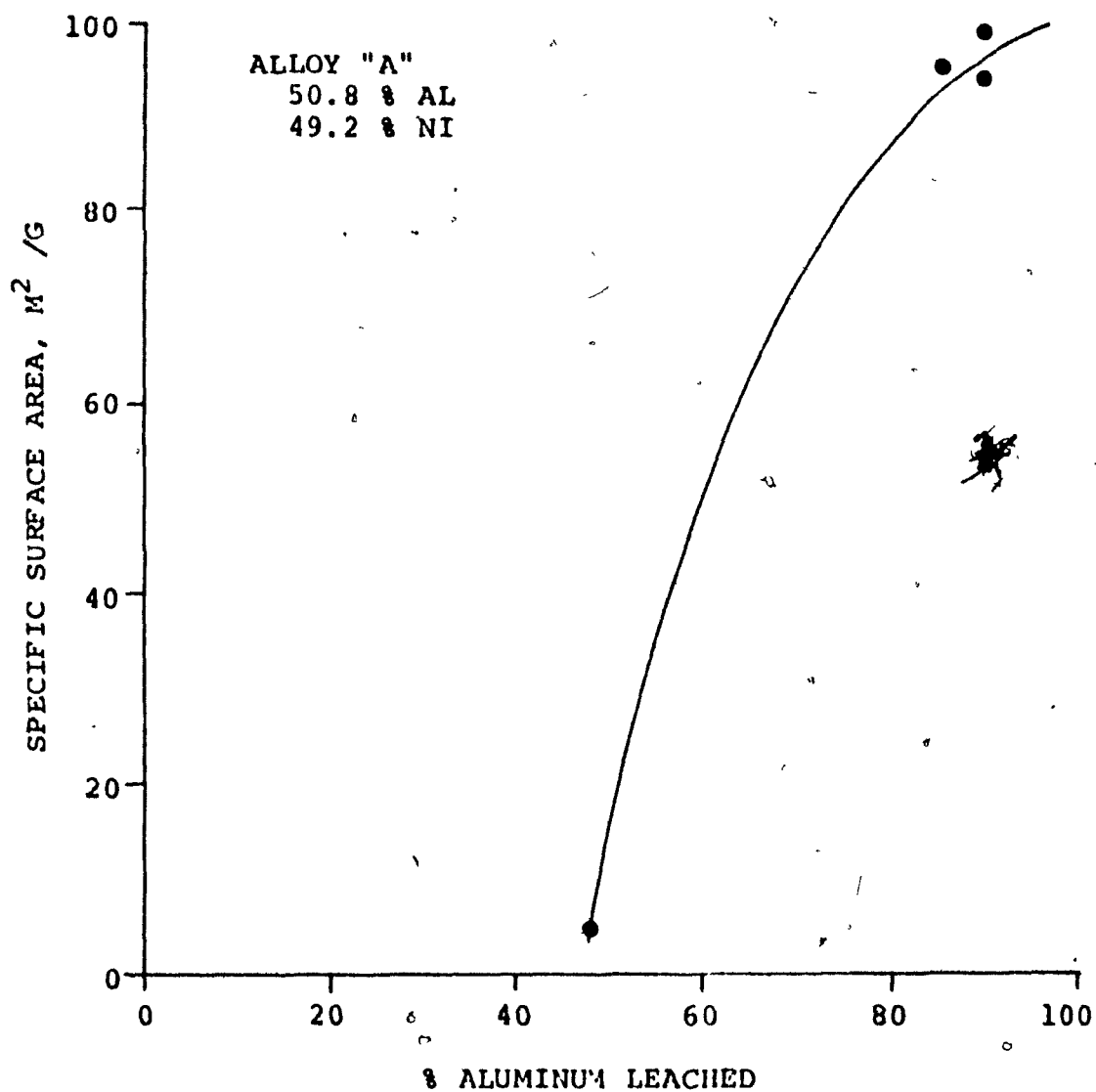


FIGURE 12: DEPENDENCE OF SPECIFIC SURFACE AREA ON EXTENT OF LEACHING OF RANEY NICKEL (34)

Reynolds (73) prepared Raney copper-nickel alloy catalysts by leaching a series of copper-nickel-aluminum alloys in boiling 30% by weight aqueous sodium hydroxide solution. His results in Figures 13 and 14 show the amounts of aluminum leached from the starting alloys, the magnetic susceptibilities, surface areas, the activities of the final catalysts for benzene hydrogenation. Note the high residual aluminum content in some of the intermediate alloys. Further extraction of a 20:30:50 nickel-copper-aluminum alloy in molten sodium hydroxide did not greatly reduce its aluminum content. Reynolds suggested that the catalysts with significant residual aluminum consist of an activated surface covering an unaltered core.

The decrease in magnetic susceptibility with increasing copper content reflects the filling of the vacant d-orbitals of the nickel. The residual aluminum may be significant for some of the alloys. The original copper-nickel-aluminum alloys have negligible magnetic susceptibility.

The variation of specific surface area of the final catalysts reflects differences in crystallite size and structure caused by variations in the reactivities of the starting alloys and the extent of aluminum removal. Anderson's data in Figure 12 suggest that high residual aluminum content is associated with lower specific surface area. In addition, the greater mobility of the copper atoms may result in larger crystallite size and hence lower surface area. Mobility of the metal atoms is important. Raney

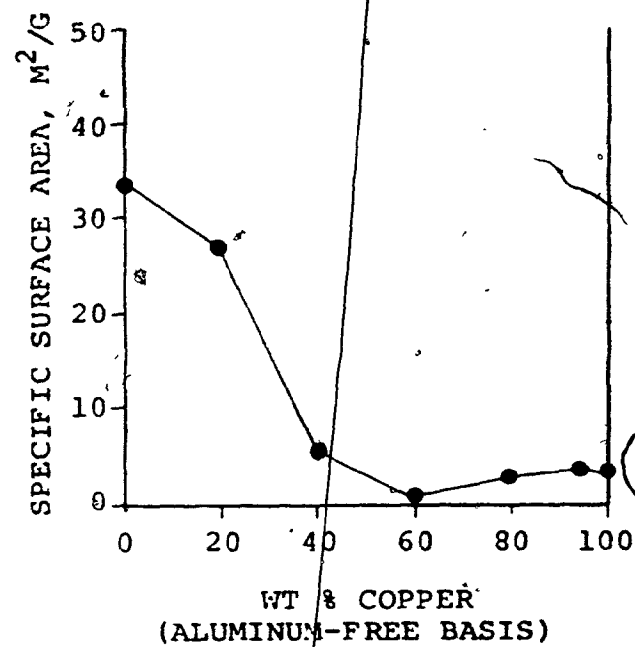
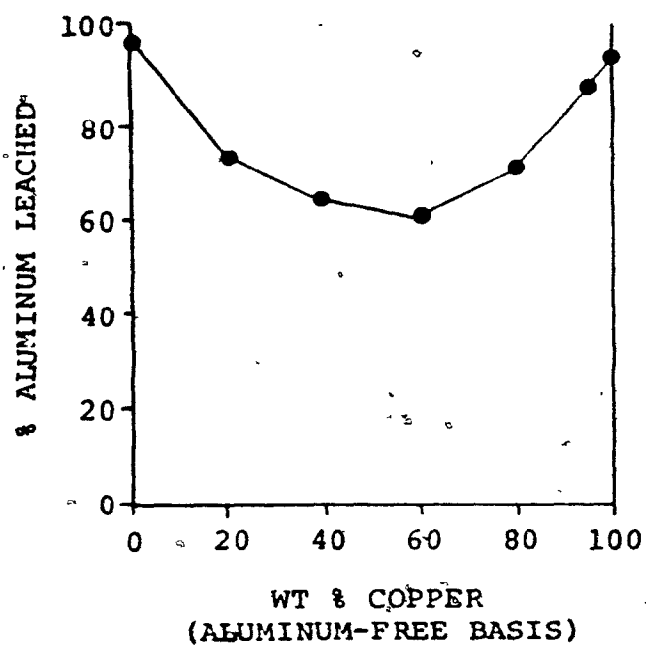
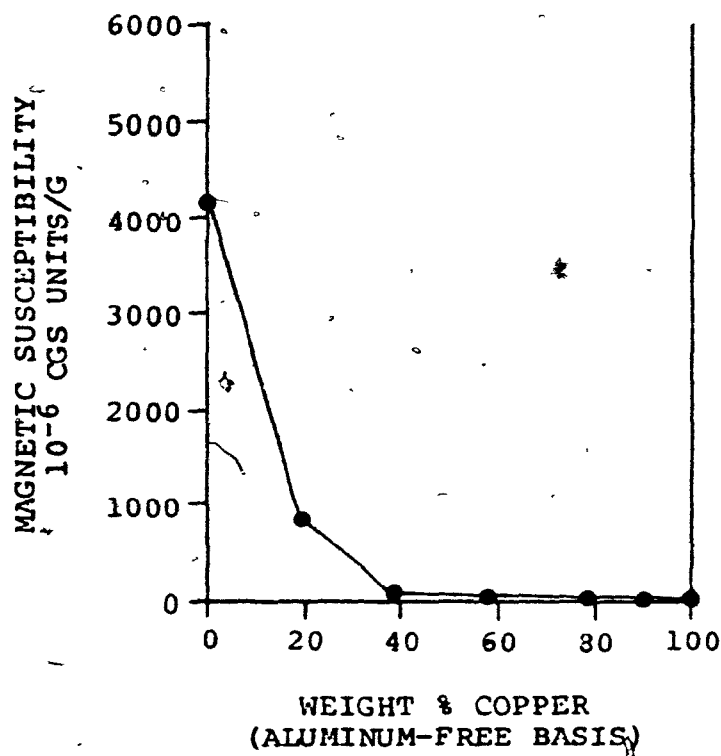


FIGURE 13: ALUMINUM REMOVAL AND SPECIFIC SURFACE AREA OF RANEY COPPER-NICKEL ALLOY CATALYSTS (73)



BENZENE HYDROGENATION
VELOCITY CONSTANT AT 225°C

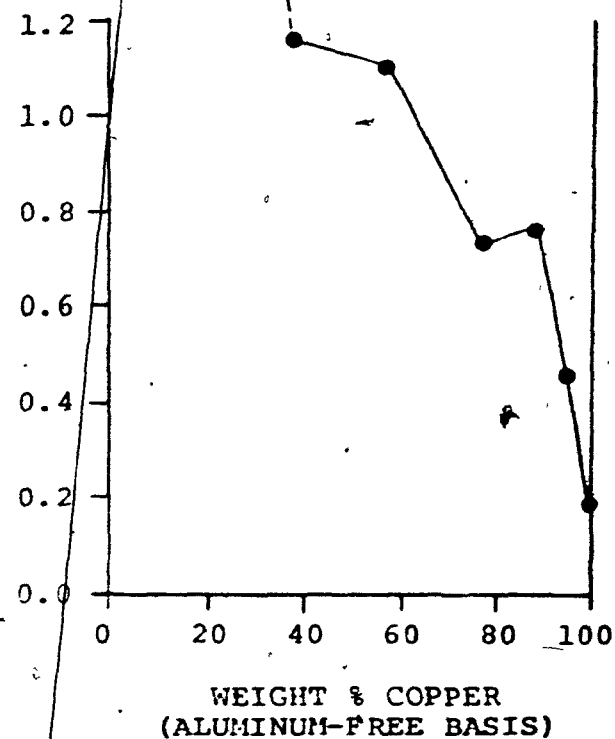


FIGURE 14: MAGNETIC SUSCEPTIBILITIES AND ACTIVITIES OF RANEY COPPER-NICKEL ALLOY CATALYSTS (73)

nickel prepared at a temperature between 50°C and 70°C will form larger crystallites when exposed to boiling alkali (34).

The fall in activity for benzene hydrogenation with increasing copper content may reflect both the decrease in surface area and a lower inherent activity of copper to promote this reaction. In their study of benzene hydrogenation over metal alloy films, van der Plank and Sachtler (92) found nickel was much more active than copper.

A complete investigation into the preparation of Raney copper-nickel alloy catalysts would involve the metallurgical investigation of the phase structure and physical properties of the starting alloys and the ~~leached alloys~~ to establish the dependence of reactivity on phase composition and structure. It would require development of suitable washing and storage procedures and measurement of the properties of the final activated catalysts. A large number of tests would be necessary because initial phase composition can have a drastic effect on catalyst properties. The facilities for such an investigation were not available, so a more limited study was undertaken.

A series of alloys were selected and a standard method which had proven successful for Raney nickel was used to leach them. Table 2 lists the alloys chosen; note that they all contain 50% by weight aluminum. This aluminum content has been used successfully in the preparation of Raney nickel and Raney copper. All these alloys were supplied as -200 mesh powders by W.R. Grace & Company.

Table 2: Compositions of Starting Alloys

Alloy No.	Composition Wt %			Composition Wt % Aluminum-free Basis	
	Cu	Ni	Al	Cu	Ni
R-Ni	0.0	50.0	50	0	100
R-Cu125	12.5	37.5	50	25	75
R-Cu250	25.0	25.0	50	50	50
R-Cu375	37.5	12.5	50	75	25
R-Cu	50.0	0.0	50	100	0

Phase compositions can be predicted from the phase diagram of slowly cooled copper-nickel-aluminum alloys shown in Figure 15 (54). Each alloy consists of at least two phases. Table 3 lists these and presents the relative amounts of each present as computed from Figure 15. Note that this method illustrates only the gross chemical features of the system. Reference to the phase diagrams of the individual copper-aluminum and nickel-aluminum alloys will show the existence of smaller amounts of other phases. Some of these have been found in the alloys used to prepare Raney catalysts. For example, Anderson (34) described a eutectic phase containing 0.05% by weight of nickel in aluminum present in the starting alloy for Raney nickel.

The phases in the copper-nickel-aluminum alloys contain each of the three components. These ternary compounds are not simple mixtures of the binary phases present in the copper-aluminum and nickel-aluminum systems. Their properties should not be directly related to those of the binary alloys; in fact, the data presented by Reynolds (73) suggest they are quite different.

The reactivities of some phases in the binary alloys have been established since active catalysts have been prepared from them. But the reactivities of all phases are not the same. Anderson reported that the order of reactivity to alkali solution in a 50% by weight nickel-aluminum alloy is the following,



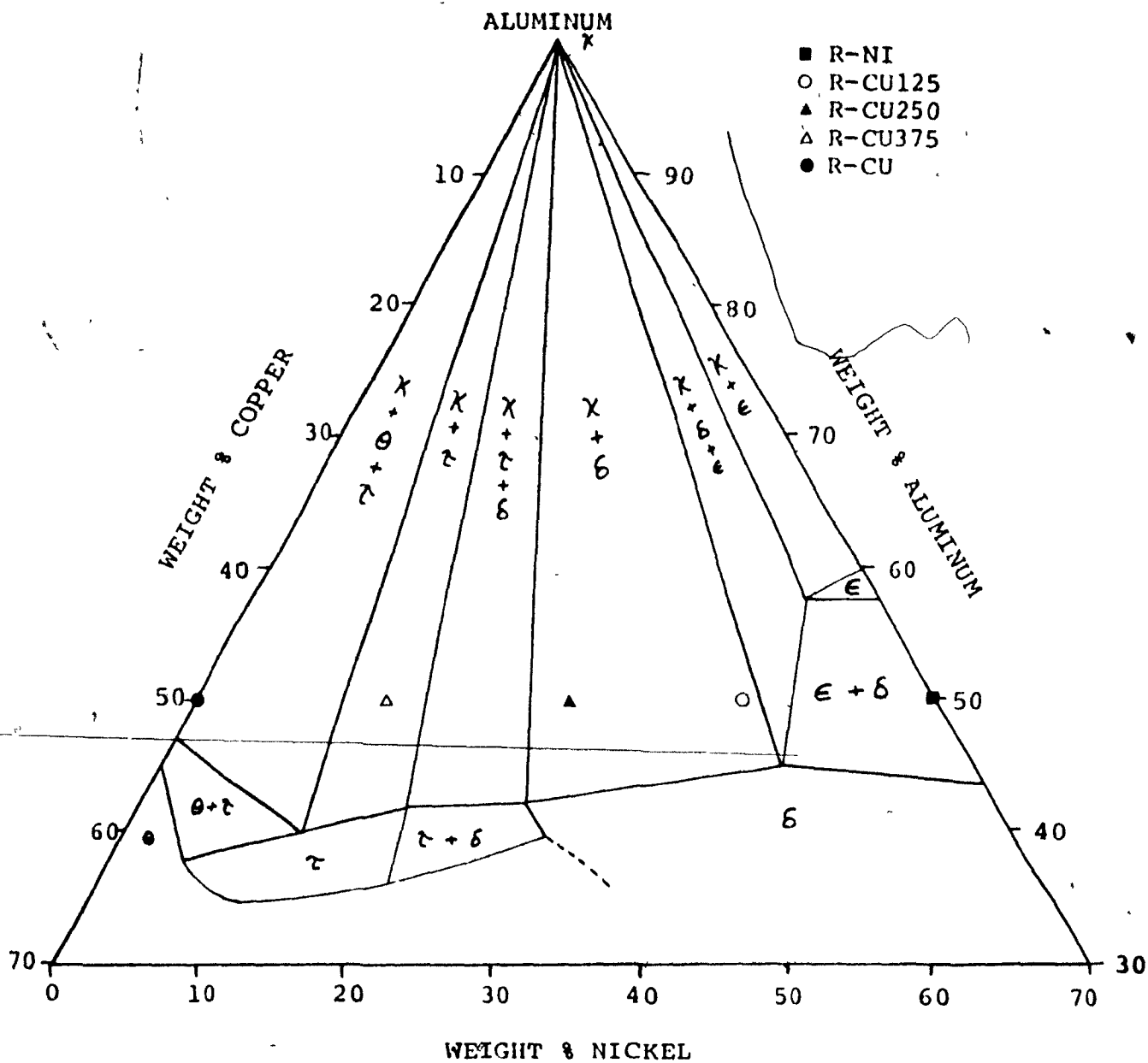


FIGURE 15: PHASE DIAGRAM OF SLOWLY COOLED COPPER-NICKEL-ALUMINUM ALLOYS (59)

Table 3: Phase Compositions of Starting Alloys

Alloy	Phase	Composition Wt %			Weight % Present
		Cu	Ni	Al	
R-Ni	δ	0	56	44	58
	ε	0	42	58	42
R-Cu125	χ	0	0	100	10
	δ	15	41	45	90
R-Cu250	χ	0	0	100	13
	δ	28	29	43	87
R-Cu375	χ	0	0	100	16
	τ	45	14	41	84
R-Cu	χ	0	0	100	6
	θ	47	0	53	94

The eutectic consists of a solid solution of 0.05% nickel in aluminum. Sassoulas (82) reported that NiAl does not react with alkali. The effect of alkali on the individual copper-nickel-aluminum phases is not known.

Many leaching procedures have been developed to prepare Raney nickel. Anderson (34) has discussed some of these and shown their effect on the pore volume, specific surface area, and crystallite properties of the activated catalysts. He grouped the methods into "low pore volume" and "high pore volume" preparations. The low pore volume preparations are leached at approximately 50°C and have a higher surface area and lower pore volume than do the high pore volume preparations which are leached in boiling alkali. The low pore volume catalysts are more active for several reactions.

A low pore volume technique described by Anderson (34) and Nishimura (59) was chosen to leach the copper-nickel-aluminum alloys. It involves the stepwise addition of 120 ml of 50% by weight aqueous sodium hydroxide solution to 30 g of alloy in 180 ml of distilled water at 50°C. Most of the hydrogen is evolved in dilute alkali with the remainder in concentrated alkali. Complete experimental procedures and results are given in Appendix E. Several items should be noted.

The standard alkali addition procedure had to be made more gradual for two of the alloys. Raney copper alloy, R-Cu, evolves hydrogen so rapidly that temperature control is difficult.

Alloy R-Cu250 has a strong foaming tendency when alkali is added.

The bath temperature was maintained at 50°C, but the temperature of the alloy suspensions rose to about 55-60°C during the first half hour of leaching. The large amounts of heat generated could not be removed rapidly enough to maintain the reaction mixture at 50°C. During the last hour of leaching the temperature fell to about 50-52°C. Anderson (34) reported that this method of adding alkali resulted in a fairly constant solution temperature of 50±5°C, but he had used the 30-50 mesh fraction of the starting alloy. The alloys used in this study were -200 mesh. The large difference in particle size and hence surface area probably accounts for the difference in reaction rates and heat evolution.

Reactivity of the alloys to the alkali varied significantly. The fraction of aluminum leached from the alloys was calculated from the volume of hydrogen evolved according to the stoichiometry of Equation 8. Data from Table 27 in the Appendix is plotted in Figure 16, which shows the percentage of aluminum removed for different compositions of the starting alloy.

Virtually all aluminum was removed from the Raney copper alloy; less from the other alloys. Seventy-seven percent of the aluminum was leached from a 50% nickel-aluminum alloy. Anderson (34) reported 90% removal for an alloy of the same composition. This higher reactivity might be due to a difference

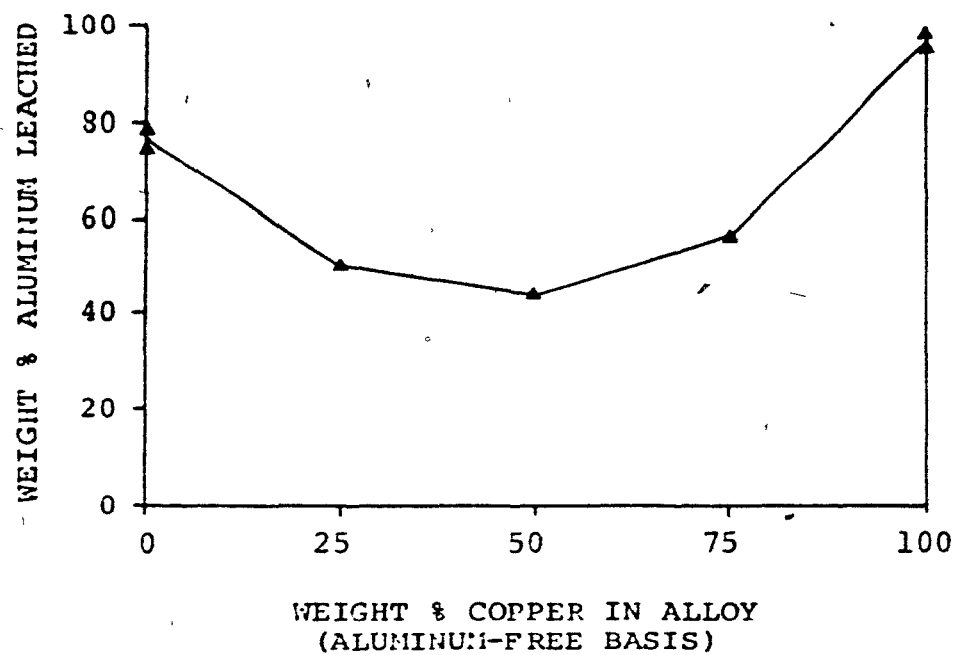


FIGURE 16: ALUMINUM LEACHED FROM COPPER-NICKEL-ALUMINUM ALLOYS

in the microstructure and phase composition of the starting metals. Perhaps the -200 mesh particles used in this test work might have agglomerated more easily than the 35-80 mesh particles used by Anderson. This could have resulted in a diffusion resistance to leaching and hence less aluminum leached. Possibly there was another small, but significant, difference in the leaching procedures.

The low volumes of hydrogen evolved for the three copper-nickel-aluminum alloys suggests that leaching conditions might not have been severe enough to prepare an activated catalyst. To test this hypothesis a small scale test on one alloy was made under severe leaching conditions. Three grams of alloy R-Cu250 was leached in boiling concentrated alkali solution at 107°C until all hydrogen evolution ceased; only 42% of the aluminum was leached out. Within experimental error this is identical to the 45% observed in the large scale leaching. This result confirms the low reactivity of alloy R-Cu250 and is strong evidence that the other two copper-nickel-aluminum alloys also have the low reactivity shown in Figure 16.

The dependence of reactivity on composition is similar to that observed by Reynolds; however about 15% less aluminum was removed from all the alloys except Raney copper. These lower reactivities are more likely due to differences in the physical structures of the starting alloys than to the leaching method since the small scale test confirmed the low reactivity of at least one of the alloys.

The leached alloys were washed to a neutral pH following the procedure described in Appendix E. Oxygen was deliberately bubbled through the slurry to oxidize the catalyst because preliminary activity tests indicated that the catalysts would be oxidized by the reaction mixture.

The activated catalysts were supported on silica according to the procedure in Appendix C. During gellation and drying, colors appeared on the surface of the gels, suggesting the formation of traces of nickel and copper chlorides from the hydrochloric acid used to neutralize the Ludox. Possible interference with catalytic activity was tested in preliminary activity measurements before the final tests.

The presence of some of the Raney metals, especially the copper-rich alloys, accelerated the gellation of the Ludox suspensions. This indicated the presence of nickel and copper ions and is consistent with the fact that divalent cations are able to penetrate the surface hydroxyl ion coverage on the silicon dioxide particles and destabilize the Ludox (26).

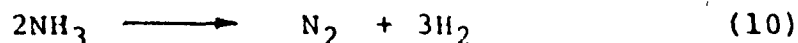
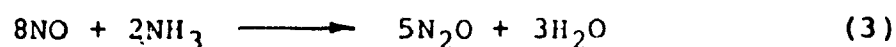
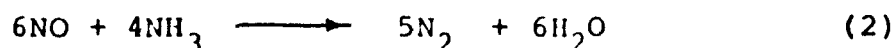
The Raney procedure of catalyst preparation is relatively complex since the reactivity of the starting alloys, the leaching conditions and the washing and support-conditions must be considered. The results presented in this section show a significant variation in the reactivity of the alloys towards the alkali. This is likely to be a source of variation in catalyst activity.

Section VIII: Activity of Raney Catalysts

(A) Introduction

The activity measurements reported in this section are the core of the catalyst tests upon which this thesis is based. The determinations of the inherent activities of the Raney copper-nickel alloys were designed to test the three hypotheses presented in Section II.

The reactor feed was composed of nitric oxide and ammonia in argon. Limitations of the chemical analysis system precluded the presence of oxygen and nitrogen dioxide. The main reactions occurring in a mixture of nitric oxide and ammonia have been presented in Section I.



The reduction of nitric oxide by ammonia can occur at temperatures as low as 150°C. Decomposition of ammonia usually becomes significant only at higher temperatures.

Definitions of conversions by these reactions are given in Appendix G. Total nitric oxide destruction, Y, by Reactions 2 and 3 can be computed directly from the nitric oxide concentrations in the inlet and outlet streams. If ammonia decomposition is negligible, the conversion, X, of nitric oxide to nitrogen by

Reaction 2 can be calculated from the amount of nitrogen formed and nitrous oxide formation can be computed from the difference between nitric oxide destroyed and the nitric oxide reduced to nitrogen.

At higher temperatures, ammonia decomposition becomes significant. Hydrogen cannot be determined with the chromatographic system shown in the Appendix because its thermal conductivity is close to that of the carrier gas, helium. Hydrogen peaks are very small and only qualitative observations can be made. When ammonia decomposition occurs it is not possible to compute the extent of each of the three reactions. Total nitric oxide destruction can still be measured. An upper limit to the reduction of nitric oxide to nitrogen can be calculated from the nitrogen content of the reactor product by assuming that no ammonia decomposition has occurred. This hypothetical conversion can exceed 100% when ammonia decomposition is significant.

The composition of the reactor inlet gas was fixed at 0.3% nitric oxide and 0.6% ammonia in argon unless otherwise stated. If future work is undertaken with nitrogen dioxide, the same feed composition will be used so that comparison between the two sets of data will be straightforward.

Preliminary catalyst testing was designed to point out the proper experimental conditions for the Raney alloy activity tests to follow.

(B) Preliminary Catalyst Testing

The catalyst tests should be designed so that measured conversions are true indications of the inherent activities of the Raney alloy catalysts. The catalyst support should not interfere in any way with measured activities. Radial concentration gradients and mass transfer limitations both inside and outside the catalyst pellets must be negligible. The preliminary test work should also establish any other relevant variables such as oxidation state of the catalyst and conditioning time required in the reaction mixture.

The effect of radial concentration gradients will be negligible if the catalyst pellet dimensions are less than $1/30$ th of the bed diameter. The reactor internal diameter of 0.4 in requires a pellet size of about 0.013 in. All the supported Raney alloy catalysts were ground to a 30-80 mesh size for testing; this corresponds to a particle size range of from 0.007 in to 0.0165 in. Some of the commercial Raney catalysts tested in the preliminary work were larger than this size.

The external diffusion resistance to mass transfer between the bulk of the gas phase and the surface of the catalyst pellet must be negligible in comparison to the reaction rate. This resistance can be calculated from mass transfer correlations for typical operating conditions and is negligible if first order kinetics are assumed for the destruction of nitric oxide. This

calculation is not included here because actual reaction kinetics have not yet been established for the operating conditions of these tests.

The effectiveness factor of the catalyst pellets must be close to unity, i.e., the diffusion resistance to mass transfer inside the catalyst pellets must be small compared to the reaction rates. This resistance cannot be calculated theoretically unless the pore size distribution and the effective diffusivities of each component in the reaction mixture are known. These data are not available, but an indirect test of effectiveness factor was made by varying the catalyst pellet size.

A reduction in catalyst particle size will decrease the total mass transfer resistance between the bulk of the gas phase and the surface of the catalyst pellets and increase the effectiveness factor of the pellet. If a significant reduction in particle size does not increase the conversion, then mass transfer resistances both inside and outside the pellet are negligible.

Catalyst #C1 was prepared by dispersing 5% by weight of W.R. Grace Raney Active Copper Catalyst No. 29 in Ludox using a procedure similar to the standard one described in Appendix C. Two different mesh sizes were separated and the conversion of nitric oxide by ammonia was determined over each. The results in Table 4 show no significant difference in conversion despite the large difference in particle size and external surface area. This shows that both internal and external diffusion resistances are

Table 4: Effect of Catalyst Pellet Size on Conversion

Catalyst: Commercial Raney Copper #Cl
 Reactor Inlet Gas Composition: 0.3% nitric oxide
 0.6% ammonia
 balance argon
 Space Velocity: 2000 hr⁻¹
 Temperature: 300°C

Pellet Mesh-Size:	20-48	8-20
Pellet Size (in):	0.0117-0.0331	0.0331-0.0937
Conversion of NO to N ₂ , %	60	61

negligible at 300°C and a space velocity of 2000 hr⁻¹. The 30-80 mesh particles used for the Raney alloy tests are significantly smaller than the smallest particles used in these tests, so diffusion resistance should be negligible for all the Raney alloy activity measurements.

The possibility of blockage of the Raney metal pores by silica was investigated. A catalyst was prepared by mechanically mixing a dry sample of the same commercial Raney copper with dry silica support to obtain 5% Raney copper on silica. This catalyst reduced 50% of the nitric oxide in an inlet gas stream of 0.3% nitric oxide and 0.6% ammonia in argon at 300°C and a space velocity of 1000 hr⁻¹. Comparison with the data in Tables 4 and 5 shows that this activity is significantly lower than that of the Raney copper catalyst #C1 produced by the standard method. Agglomeration of the metal particles may have reduced the availability of the sites. These data are strong evidence that the silica support is not reducing the activity of the Raney metal.

Once the validity of the activity measurements was established, preliminary testing of commercial Raney copper catalyst #C1 and commercial Raney nickel on silica (W.R. Grace Active Raney Nickel Catalyst No. 28) was started. Each was supported on silica to give a catalyst with 5% by weight of active metal. The support procedure was similar to that in Appendix C; however oxygen was not bubbled through the wash water and the maximum drying temperature was 120°C. These catalysts were not oxidized

to the same extent as the final copper-nickel alloy catalysts were.

At first, activity tests with Raney nickel did not yield consistent results. Initially 100% of the nitric oxide in the inlet gas was reduced by ammonia at 300°C and a space velocity of 1000 hr⁻¹ over a batch of catalyst; after several days of intermittent testing, only 15% of the inlet nitric oxide was destroyed. In general, activity slowly decreased over a period of days at 300°C. It could be increased by reducing the catalyst in hydrogen at 400°C for several hours and lowered by exposing it to oxygen at 300°C. This suggests that the Raney nickel is oxidized by the reaction mixture and that the oxidized catalyst has a much lower activity than the reduced catalyst.

Similar results were obtained with Raney copper. The effect could be observed visually because the supported Raney copper had a dark grey color when not oxidized and a black color when oxidized in air at 400°C. Several batches of unoxidized catalyst were tested in the reactor for different lengths of time at 300°C. Reactor inlet gas composition was 0.3% nitric oxide and 0.6% ammonia in argon. Examination of the beds after testing showed a dark zone at the reactor inlet and a light zone further into the bed. The boundary between the two zones moved down through the catalyst bed as testing proceeded. The zone nearest the inlet appeared identical in color to the catalyst oxidized in air at 400°C, while that further down the bed appeared

identical to the starting unoxidized catalyst. This is strong evidence to support the oxidation of Raney copper by nitric oxide.

Nickel and copper in the bulk are not oxidized by nitric oxide until higher temperatures (65). However the Raney metals have a large surface area and the heat of reaction between the nitric oxide and ammonia might raise the temperature of the active metal sites above the temperature observed in the bulk of the gas phase.

Consistent measurements of Raney catalyst activities can be made on either the completely oxidized or completely reduced metals. The oxidized state was chosen since these catalysts were being tested for possible use in a commercial process to reduce nitrogen oxides. The tail gas from a nitric acid plant contains oxygen and nitrogen dioxide which will oxidize any catalysts which are not resistant to oxidation. In addition, available data indicate that the nitric oxide will oxidize the catalysts even in the absence of oxygen or nitrogen dioxide.

Two batches of commercial Raney copper and Raney nickel were supported on silica following the complete procedure described in Appendix C, except that oxygen was not bubbled through the wash water. These catalysts were oxidized overnight at 350°C and had much lower activities than the unoxidized catalysts. Nitric oxide conversions gradually decreased during the first twelve hours of testing and remained constant thereafter. Activities

were reproducible from batch to batch and did not change when a catalyst bed was tested repeatedly at different dates. The activities of commercial Raney copper catalyst #C1 are given in Table 5; Raney nickel was less active.

Normally oxygen is excluded from the system when Raney metals are being leached and washed to prevent oxidation and displacement of adsorbed hydrogen. However these preliminary activity tests indicated that the Raney catalysts would be oxidized completely in any case. Therefore the common procedure of excluding oxygen during the washing sequence was changed to the procedure described in Appendix C, in which oxygen is bubbled through the wash water to displace adsorbed hydrogen.

This preliminary work demonstrated that radial concentration gradients and mass transfer effects can be neglected, that the Raney catalysts will be oxidized by the nitric oxide, and that the catalysts will require about twelve hours of conditioning in the reaction mixture before steady state conversions are observed.

(C) Activities of Raney Alloy Catalysts

The activity of the catalyst support and the walls of the microreactor for the reaction were measured in the next set of tests. Silica support was prepared by the method described in Appendix C and 2.5 g loaded into the microreactor. Composition of the inlet gas was fixed at 0.3% nitric oxide and 0.6% ammonia

Table 5: Effect of Temperature and Space Velocity on Conversion
over Commercial Raney Copper Catalyst #C1

Reactor Inlet Gas Composition: 0.3% nitric oxide
0.6% ammonia
balance argon

Temperature °C	Space Velocity hr ⁻¹	Conversion of Nitric Oxide to Nitrogen, Y, %
300	400	93
300	1000	82
300	2000	61
300	3000	46
350	1000	96
350	3000	70

in argon. Nitric oxide conversion over the support generally reached its steady state value after one hour of testing. The results presented here were collected after at least two hours of operation at each test point. Space velocity and temperature were varied to give the data in Table 6.

Activity is measured by the nitrogen concentration at the outlet from the reactor. Ammonia decomposition is probably significant at these temperatures so conversions of nitric oxide to nitrous oxide and nitrogen respectively cannot be calculated. An upper limit to conversion of nitric oxide to nitrogen was calculated for each case according to the convention in Appendix G.

These results are plotted in Figure 17. Note that at temperatures of 300°C and higher, conversion of nitric oxide over the silica support is significant for space velocities less than 3000 hr^{-1} .

The final series of tests measured the activities of the supported Raney copper-nickel alloy catalysts. The amount of aluminum leached from the starting alloys varied with alloy composition, so it was necessary to add different amounts of the supported catalysts to maintain the same total weight of copper and nickel in the catalyst bed. Calculations of catalyst loadings are presented in Appendix II.

Catalyst R-Cu-Ni-Mix was prepared by simultaneously dispersing Raney nickel R-Ni-A and Raney copper R-Cu-A on silica to give an overall composition of 2.06% nickel and 2.36% copper by weight on silica.

Table 6: Effect of Temperature and Space Velocity
on Conversion over Silica Support

Catalyst: 2.5 g silica support
Reactor Inlet Gas Composition: 0.3% nitric oxide
0.6% ammonia
balance argon

Temperature °C	Space Velocity hr ⁻¹	% Nitrogen in Reactor Outlet Gas	Maximum Conversion of NO to N ₂ , Y', %
300	5000	.004	1.6
300	3000	.009	3.5
300	1000	.026	10.4
300	500	.043	17.2
300	200	.101	40.5
350	3000	.014	5.7
350	1500	.030	12.1
350	500	.075	30.0
375	5000	.018	7.2

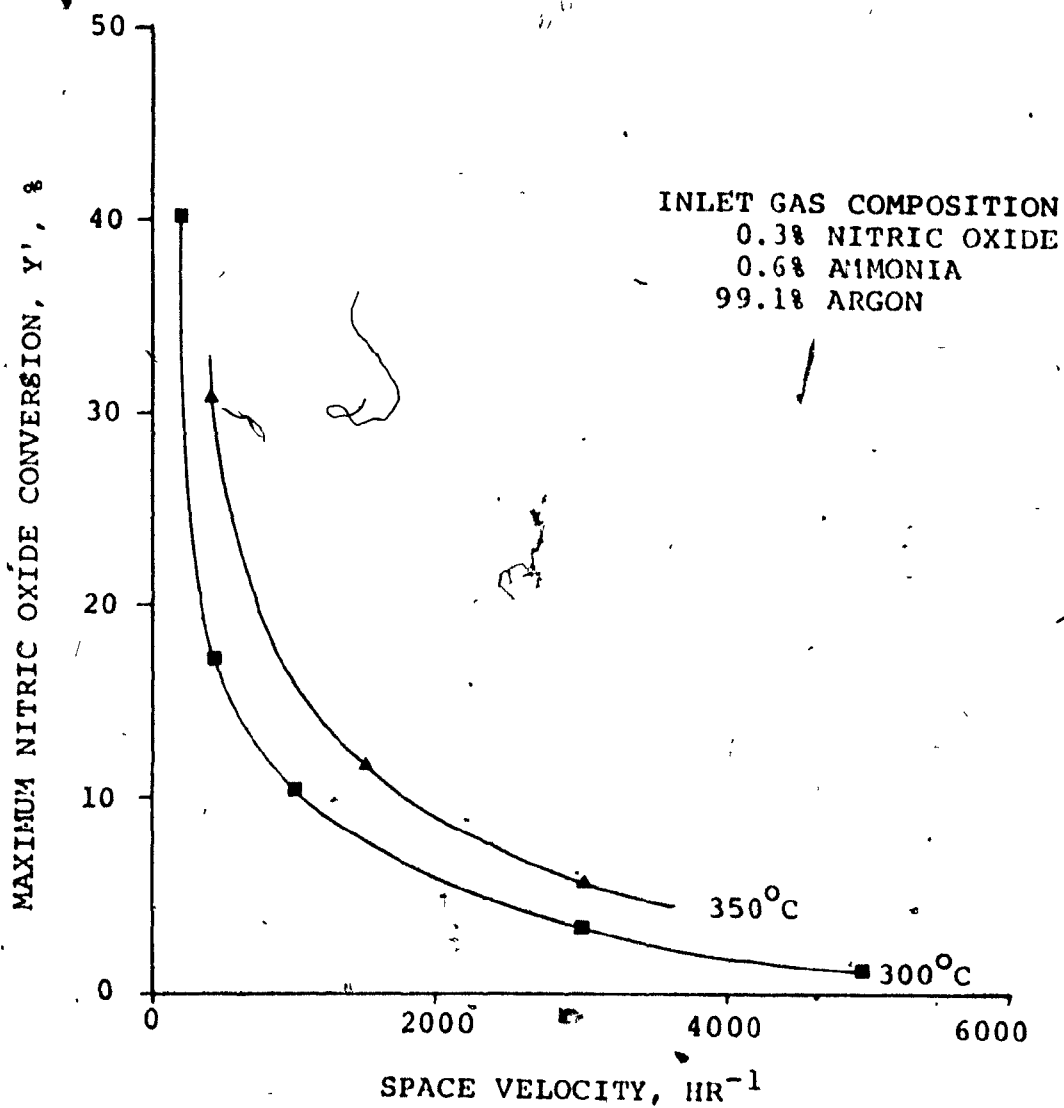


FIGURE 17: ACTIVITY OF SILICA SUPPORT FOR REDUCTION OF NITRIC OXIDE WITH AMMONIA

The activity measurements were straightforward. The supported Raney catalysts and sufficient silica support to bring the total bed weight up to 2.5 g were mechanically mixed and loaded into the reactor. The heater was turned on and the reactants set at their proper flow rates. Usually the individual flow rates were measured at the start of each catalyst test to confirm the accuracy of the flowmeter calibrations. The reactants were analyzed to verify that no nitrogen was present and that the nitric oxide concentration was 0.3%. Then the reactor product gas was analyzed periodically to determine the nitrogen and nitric oxide concentrations. The chromatograph was used exclusively for the chemical analyses.

Typical results are shown in Figure 18 where nitrogen and nitric oxide concentrations are plotted for the testing of catalyst R-Cu375 at 350°C and 500 hr⁻¹ space velocity. Final data were taken after eighteen hours following the start of the run; nitrogen concentrations had remained steady for over four hours prior to the final sample analysis. The other Raney alloy catalysts were tested similarly.

All the Raney alloy catalysts were tested at 350°C and a space velocity of 500 hr⁻¹. Reactor product compositions are listed in Table 7. Conversions were calculated according to the conventions in Appendix H. Note that apparent conversions in excess of 100% over catalysts R-Ni-A and R-Cu-Ni-Mix confirm ammonia decomposition. This reaction is probably occurring over

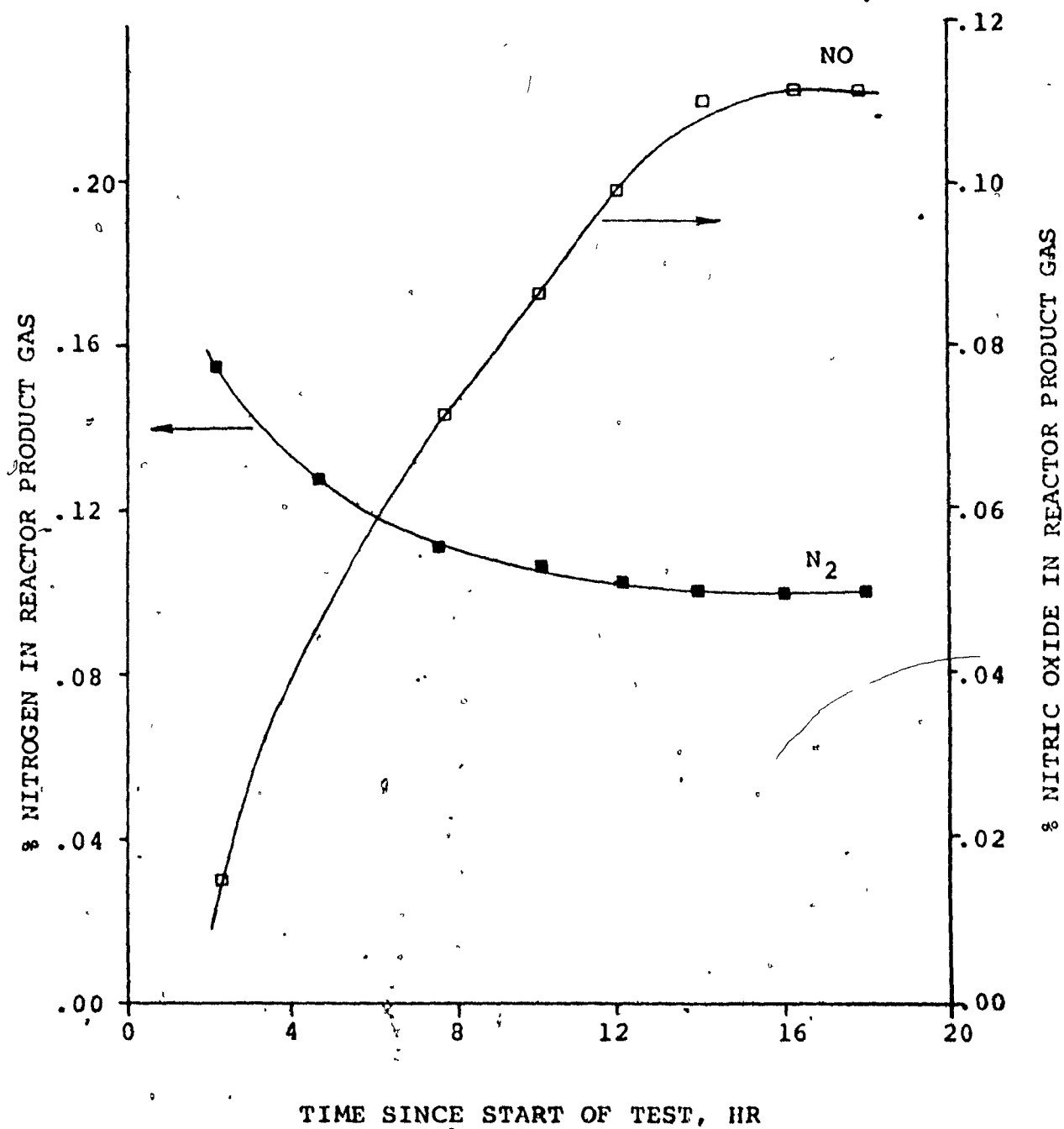


FIGURE 18: REACTOR OUTLET GAS COMPOSITION
OVER CATALYST R-CU375

Table 7: Effect of Alloy Composition on Conversion
Over Raney Copper-Nickel Alloy Catalysts

Reactor Inlet Gas Composition: 0.3% nitric oxide
0.6% ammonia
balance argon
Temperature: 350°C
Space Velocity: 500 hr⁻¹

Catalyst	Reactor Outlet Gas Composition		Conversions	
	% Nitrogen	% Nitric Oxide	Nitric Oxide Destruction X, %	Maximum Conversion of NO to N ₂ Y', %
Silica Support	.077	.224	25	31
R-Ni-A	.391	.000	100	156
R-Cu125	.210	.000	100	84
R-Cu250	.067	.171	44	27
R-Cu375	.101	.122	59	40
R-Cu-A	.140	.104	65	56
R-Cu-Ni-Mix	.270	.000	100	108

the other catalysts, but to a lesser extent. Results are plotted in Figure 19.

The next data set was collected at other space velocities and temperatures, but under less stringent conditions than the basic catalyst tests listed in Table 7. The same catalyst beds were used for this series of tests. Conversions were measured after four hours operation at fixed space velocity and temperature. Results are given in Table 8. Catalysts R-Ni-A, R-Cu125, and R¹-Cu-Ni-Mix were tested at higher space velocities to confirm the order of reactivity suggested by the data in Table 7. Under these conditions, the differences between the catalysts are marked; R-Ni-A is more active than R-Cu-Ni-Mix, which in turn is more active than R-Cu125. Runs 4, 5, and 6 show the effect of space velocity and temperature on conversion of nitric oxide over Raney copper, R-Cu-A. Results are plotted in Figure 20.

The importance of oxidation state of the Raney metals was confirmed in runs 7 and 8. Catalyst R-Cu375A was prepared from a batch of R-Cu375 by reduction in hydrogen at 400°C for eight hours. This treatment significantly increased activity. Catalyst R-Cu375B was prepared by oxidizing R-Cu375A in oxygen at 350°C for eight hours. Its activity is lower than the reduced catalyst.

Ammonia decomposition was evidently occurring over catalyst R-Ni-A and probably over some of the other catalysts. This reaction was studied in greater detail by feeding into the reactor a gas stream consisting of ammonia in argon. Analyses were made

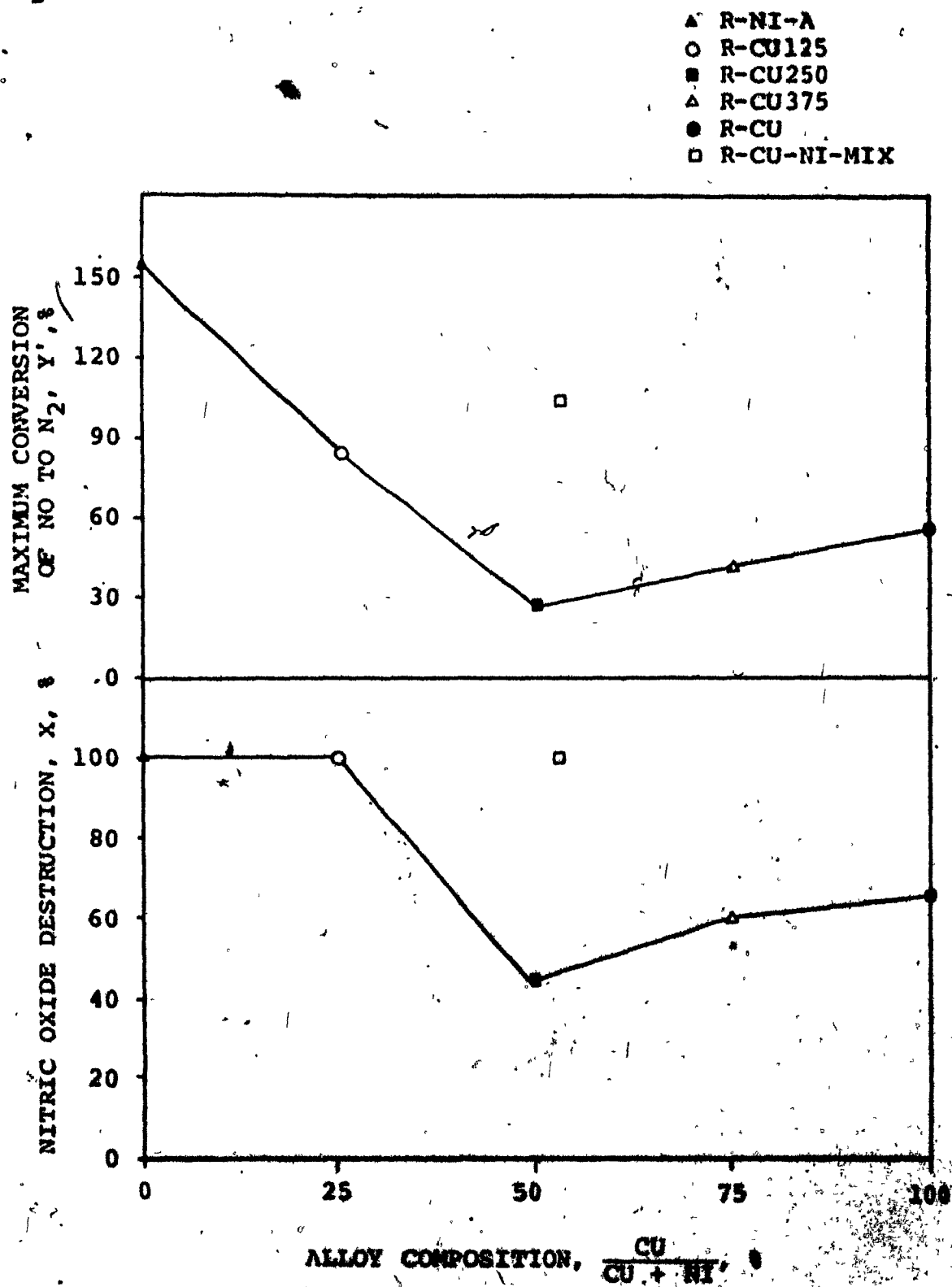


FIGURE 19: ACTIVITY OF RANEY ALLOY CATALYSTS FOR
 REDUCTION OF NITRIC OXIDE WITH AMMONIA AT
 330°C AND 500 HR⁻¹ SPACE VELOCITY

Table 8: Activities of Raney Copper-Nickel Alloy Catalysts

Reactor Feed Composition: 0.3% nitric oxide
0.6% ammonia
balance argon

Run No.	Catalyst	Space Velocity hr ⁻¹	Temp. °C	Composition of		Conversions	
				Reactor	Product Gas	X%	Y%
				%N ₂	%NO		
1	R-Ni-A	3000	350	.293	.000	100	117
2	R-Cu-Ni-Mix	3000	350	.166	.006	98	67
3	R-Cu125	2250	350	.127	.081	73	51
4	R-Cu-A	500	400	.180	.068	78	72
5	R-Cu-A	350	350	.139	.082	73	56
6	R-Cu-A	200	350	.251	.000	100	100
7	R-Cu375-A	3000	350	.114	.136	55	45
8	R-Cu375-B	3000	350	.040	.078	26	16

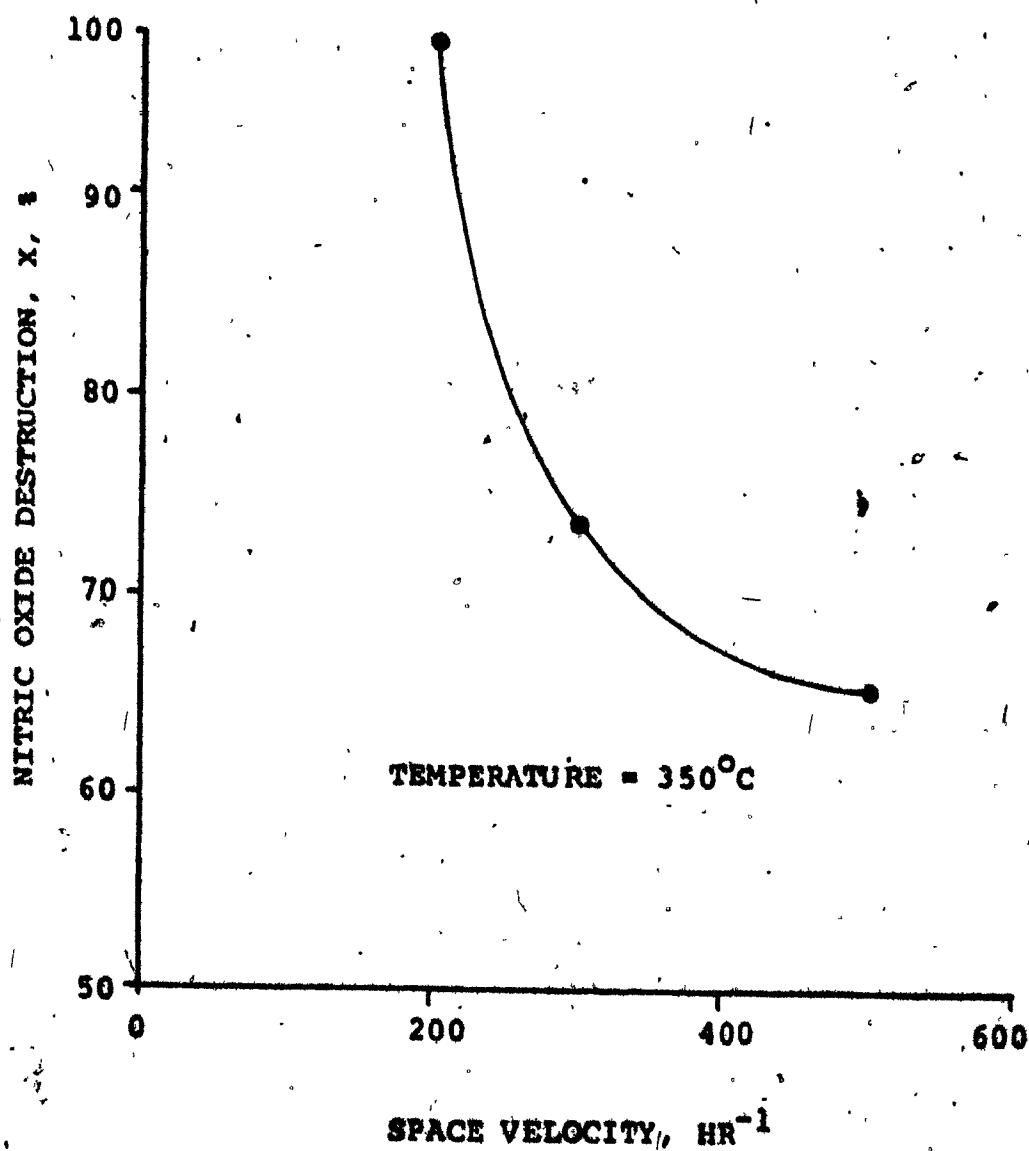


FIGURE 20: EFFECT OF SPACE VELOCITY ON NITRIC OXIDE DESTRUCTION OVER CATALYST R-CU-A

at each operating condition. The results listed in Table 9 confirm that ammonia decomposition is significant over catalysts R-Ni-A and R-Cu-Ni-Mix at the standard test conditions of 350°C and 500 hr⁻¹ space velocity. It is less important over catalyst R-Cu125 and probably negligible over the other three catalysts. Copper does not promote this reaction as well as nickel does (50).

The activities of the Raney catalysts are low compared to other catalysts for this reaction. Jaros and Krizek (8) reported 96% nitric oxide conversion at 260°C and a space velocity of 30000 hr⁻¹ over 0.5% platinum on alumina. Anderson and Keith (8) reported 88% nitrogen oxide conversion at 215°C and a space velocity of 20000 hr⁻¹ over 5.5% nickel on alumina with 5% silica. The commercial Raney copper catalyst C1 does not promote high conversions until the temperature is raised to 350°C and the space velocity lowered to 1000 hr⁻¹. With the exception of catalyst R-Ni-A, the Raney alloys are even less active. In fact, the activities of the Raney metals are so low that there is significant conversion over the silica support at the test conditions of 350°C and 500 hr⁻¹ space velocity. This low activity eliminates Raney copper-nickel alloys from further consideration as commercial catalysts to promote nitric oxide reduction with ammonia.

Alloy composition has two distinct effects, the first on overall activity and the second on catalyst selectivity. Figure 19 shows that activity is strongly dependent on alloy composition. It also shows that catalysts with a high nickel content promote

Table 9: Ammonia Decomposition over Raney
Copper-Nickel Alloy Catalysts

Catalyst	Space Velocity hr ⁻¹	Temperature °C	%NH ₃ in Feed	%N ₂ in Reactor Product Gas	%NH ₃ Decomposed
R-Ni-A	200	150	1.2	0.00	0
R-Ni-A	200	250	1.2	0.14	23
R-Ni-A	200	350	1.2	0.60	100
R-Cu125	500	350	0.6	0.06	19
R-Cu375	500	350	0.6	0.02	5

ammonia decomposition. This reaction becomes more significant on nickel catalysts above 250°C. It is less important over catalysts with a low nickel content. The strong effect of alloy composition suggests that alloy catalysts warrant further investigation. Choice of the proper alloy may result in a catalyst with high activity and selectivity. Among the Raney alloys, catalyst R-Cu125 has almost the same activity as Raney nickel for nitric oxide reduction, but does not strongly promote ammonia decomposition.

Fasman et al. (28) showed that introduction of a further alloying component into the nickel-aluminum alloy can change the activity of the Raney catalyst. For example, molybdenum is not active for the reduction of cotton seed oil, but does increase the activity of Raney nickel for this reaction. No such promotion of Raney nickel by copper was observed for the nitric oxide reduction in the present work.

Petrov et al. (69) found that the specific activity of a Raney manganese-nickel catalyst is 15 to 20% lower than a mechanical mixture of Raney nickel and Raney manganese of the same overall composition. The activity of the mechanical mixture was found to be the same as the weighted sum of the activities of the separate catalysts. The results observed here for nitric oxide reduction are similar; the alloy catalyst is less active than the mechanical mixture.

Section IX: Nitrate-Based Mixed-Oxide Catalysts

The Raney alloy catalysts are not suitable for a commercial process to reduce nitrogen oxides with ammonia because their low activities necessitate high temperatures for satisfactory conversion. Ammonia decomposition makes the process even less practical. A second series of copper-nickel catalysts was prepared by a different method which results in much higher activity.

Catalysts to promote the reduction of nitric oxide by ammonia should not be liable to deactivation by oxidation, as are the Raney catalysts. Ideally, the catalysts should consist of fine metal crystallites well dispersed over the inert support. If these crystallites are separated from each other, oxidation should not result in agglomeration and a drastic decrease in surface area available for reaction.

Such catalysts can be produced by several standard methods (56,62,93). One of the simplest is impregnation of a support with the metal nitrates, followed by heating and reduction.

Van Hardeveld and Hartog (93) calculated crystallite dimensions of reduced nickel catalysts prepared by impregnating aerosil with nickelous nitrate. The typical crystallite dimension was 48 Å, with a corresponding metal surface area of 150 m²/g. This surface area was decreased to 39 m²/g by pyrolyzing the catalyst in air at 450°C prior to reduction.

Reynolds (73) prepared copper-nickel alloy catalysts by mixing copper and nickel nitrates with kieselguhr and precipitating the metal salts with ammonium hydrogen carbonate. The catalysts were reduced at 500°C. His results, shown in Figure 21, indicate a decrease in specific surface area with increasing copper content. This may result from the high mobility of the copper atoms at the reduction temperature of 500°C. The effect may be similar to the decrease in nickel surface area due to pyrolyzing at 450°C observed by Van Hardeveld and Hartog (93). Presumably catalysts rich in copper should be reduced at a lower temperature to produce crystallite dimensions as small as those of the nickel.

The data presented by Reynolds and Van Hardeveld suggest that, at low metal loadings, the metal nitrate procedure should result in catalysts whose surface area is high and will not decrease drastically with oxidation. This nitrate procedure was adopted in this investigation as a second means of preparing copper-nickel catalysts.

The catalysts listed in Table 10 were prepared by adding solutions of copper and nickel nitrates to Ludox HS-40 to yield 1% metal on silica. The Ludox was then gelled with acetic acid, dried at 120°C, sieved, and finally oxidized at 400°C. Details of the procedure are given in Appendix F. Note that the catalysts contained copper and nickel nitrates after drying at 120°C. They were then left overnight in the presence of air at 400°C. This

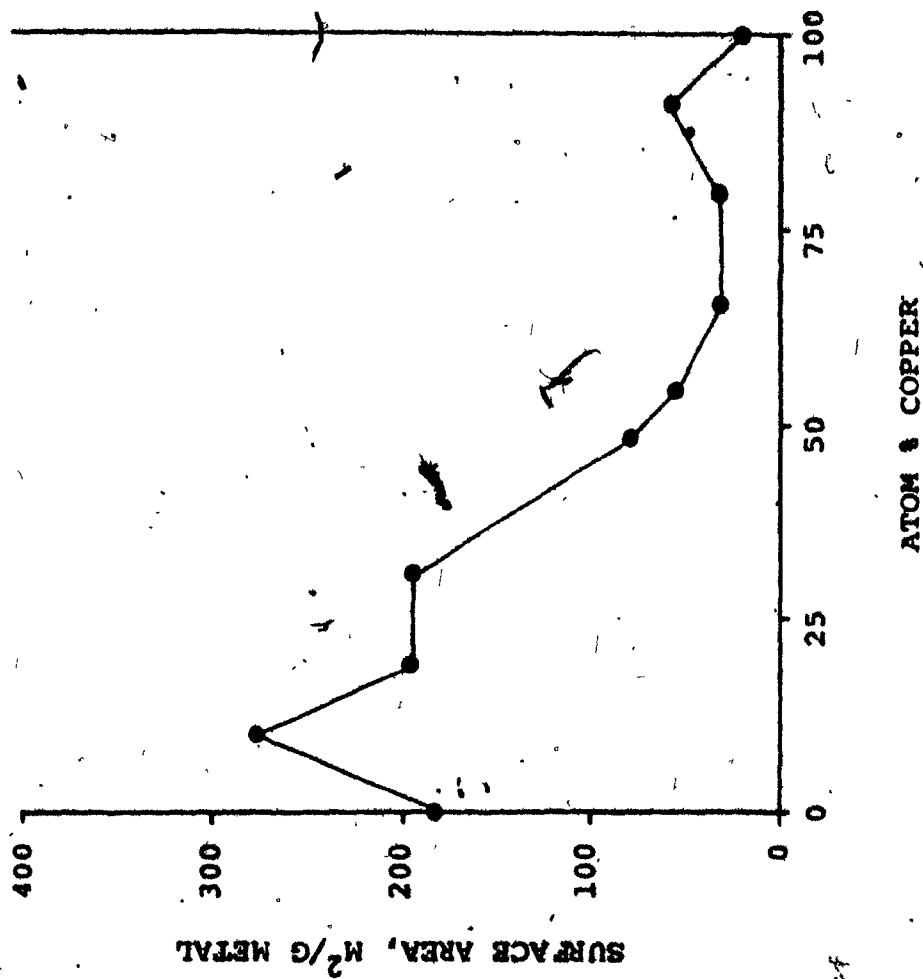


FIGURE 21: SURFACE AREAS OF COPPER-NICKEL ALLOY CATALYSTS (73)

Table 10: Composition of Nitrate-Based Mixed-Oxide Catalysts

Catalyst	Wt % Ni	Wt % Cu	$\frac{\text{Cu}}{\text{Cu} + \text{Ni}}$ %
N-Ni	1.000	0.000	0
N-Cu250	0.750	0.250	25
N-Cu500	0.500	0.500	50
N-Cu750	0.250	0.750	75
N-Cu875	0.125	0.875	88
N-Cu	0.000	1.000	100
N-Mix	0.125	0.875	88

temperature is high enough to decompose the metal nitrates with evolution of nitrogen oxides and subsequent formation of metal oxides. It should also result in sufficient surface migration over the silica support for the copper and nickel oxide crystallites to be in intimate contact. These catalysts are referred to as "mixed-oxide" catalysts, rather than as alloy catalysts, because they were not reduced to produce copper-nickel alloys. Takasu (89) has shown that exposing copper-nickel alloy plates to oxidative-reductive treatment results in pronounced changes in the surface composition. Copper-rich alloys were enriched on the surface by nickel while the surface of nickel-rich alloys was enriched by copper. Subjecting the mixed-oxide catalysts to an oxidative-reductive cycle would form copper-nickel alloys which would then be oxidized, but would introduce the added complication of changes in surface composition. To avoid this, the mixed-oxide catalysts were not reduced.

Catalyst N-Mix, was prepared by mixing 87.5% by weight of catalyst N-Cu with 12.5% by weight of catalyst N-Ni. Its activity will be compared to the mixed-oxide catalyst with the same overall composition of 0.875% copper and 0.125% nickel on silica.

This catalyst preparation method is much less complex than the Raney procedure. It is more flexible since aluminum alloys do not have to be formed and leached. Mixed-oxide catalysts of a wide range of metals can easily be prepared by

starting with the corresponding metal nitrates. Metal loadings can be varied by changing the concentration of the nitrate solution. At low metal loadings, this method should result in a fine dispersion of small metal crystallites on the support.

These catalysts proved to be much more active than the Raney metal alloys. The activity determinations lasted only three hours, so data collected are not applicable to fully conditioned catalysts. However the effect is small, and since all catalysts were tested under identical conditions, comparisons between catalysts are justified. The space velocity was raised to 3000 hr^{-1} and the reactor temperature lowered to 200°C . Figure 17 shows the activity of the silica support is negligible under these operating conditions. Figure 22 shows reactor product composition over catalyst G-Cu250; note that conditioning of the mixed-oxide catalyst is much more rapid than that of the Raney catalysts. Activity data for all the catalysts are given in Table 11 and in Figures 23 and 24. Conversions and product distributions were calculated according to the conventions in Appendix G. Ammonia decomposition was later shown to be negligible at 200°C so calculations of conversions to nitrous oxide are justified.

Activity is strongly dependant on composition. Nickel has virtually no activity while copper is quite active. The most active catalyst is G-Cu875. The mechanical mixture of the same overall composition, G-Mix, is almost as active as this

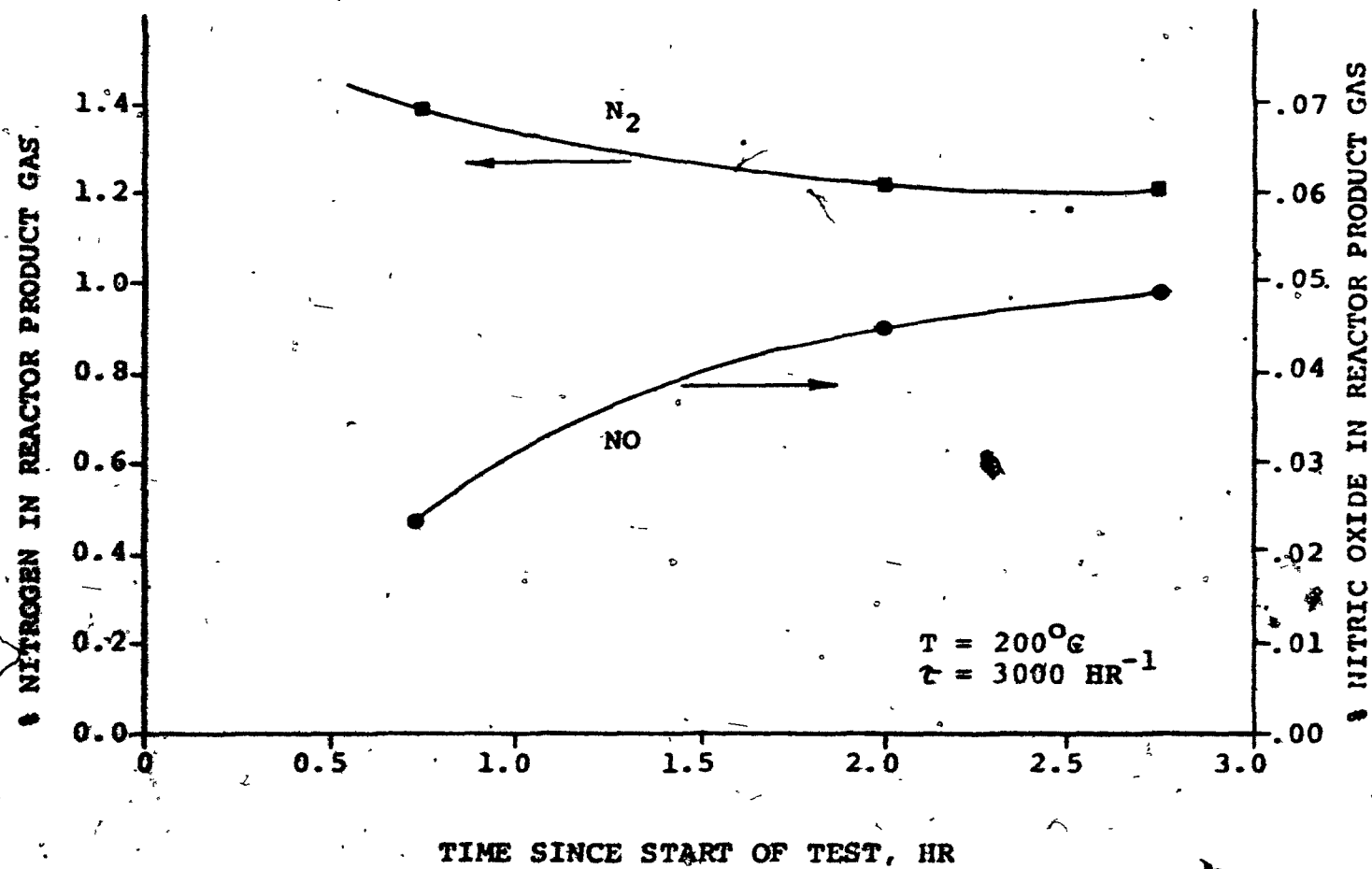


FIGURE 22: CONVERSION OVER CATALYST G-CU250

Table 11: Effect of Composition on Conversion over Nitrate-Based Mixed-Oxide Catalysts

Reactor Feed Composition: 0.3% nitric oxide
0.6% ammonia
balance argon
Temperature: 200°C
Space Velocity: 3000 hr⁻¹

Catalyst	Reactor Product Composition		Conversions			Product Distribution Ratio, R, %
	%N ₂	%NO	X, %	Y, %	Z, %	
N-Ni	.003	.285	0	1	0	-
N-Cu250	.122	.048	84	49	35	58
N-Cu500	.043	.212	29	17	12	58
N-Cu750	.040	.205	32	26	16	50
N-Cu875	.187	.000	100	75	25	75
N-Cu	.143	.000	100	58	43	58
N-Mix	.177	.000	100	71	29	71

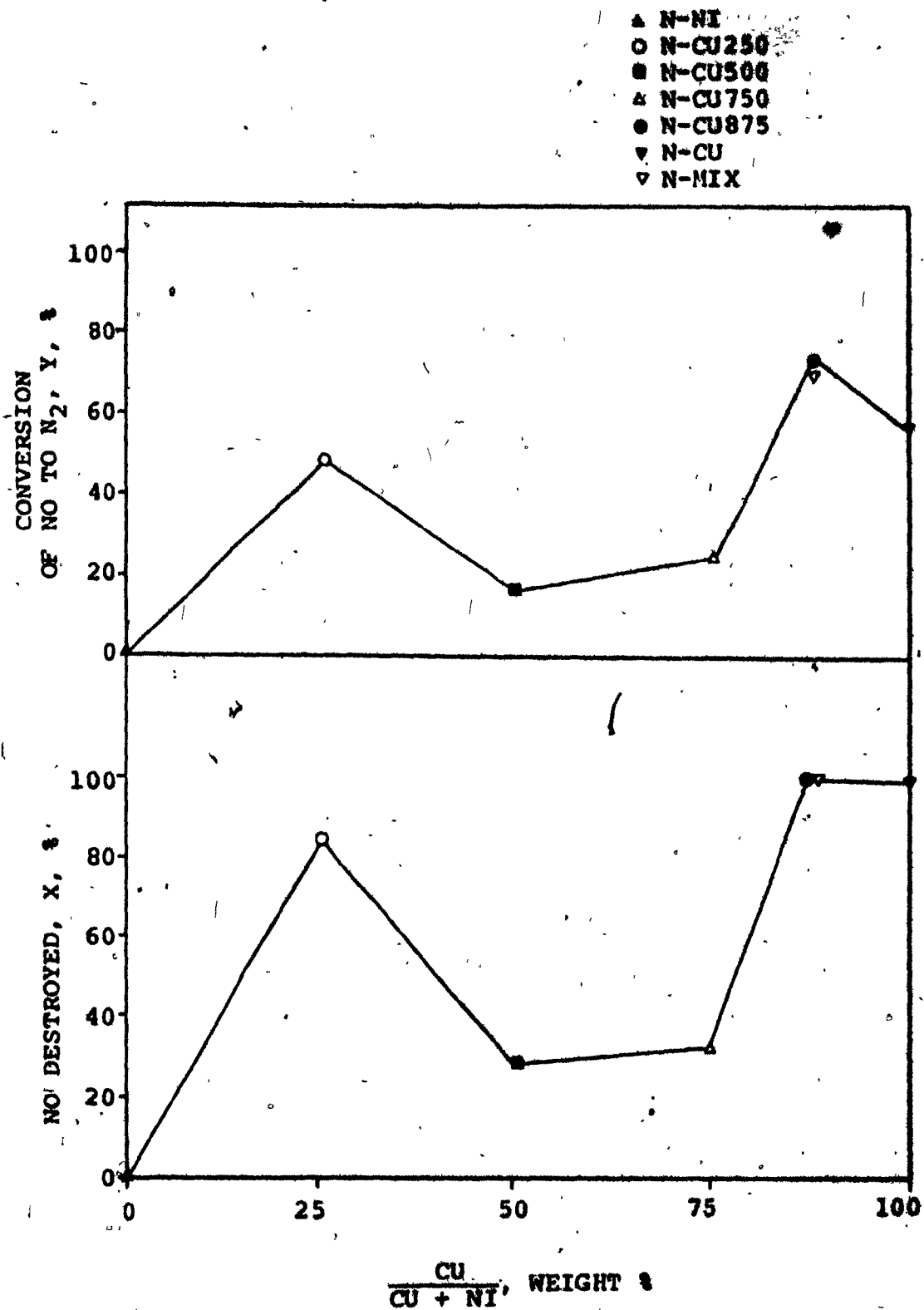


FIGURE 23: ACTIVITY OF NITRATE-BASED CATALYSTS FOR
 REDUCTION OF NITRIC OXIDE WITH AMMONIA AT 200°C
 AND 3000 HR⁻¹ SPACE VELOCITY

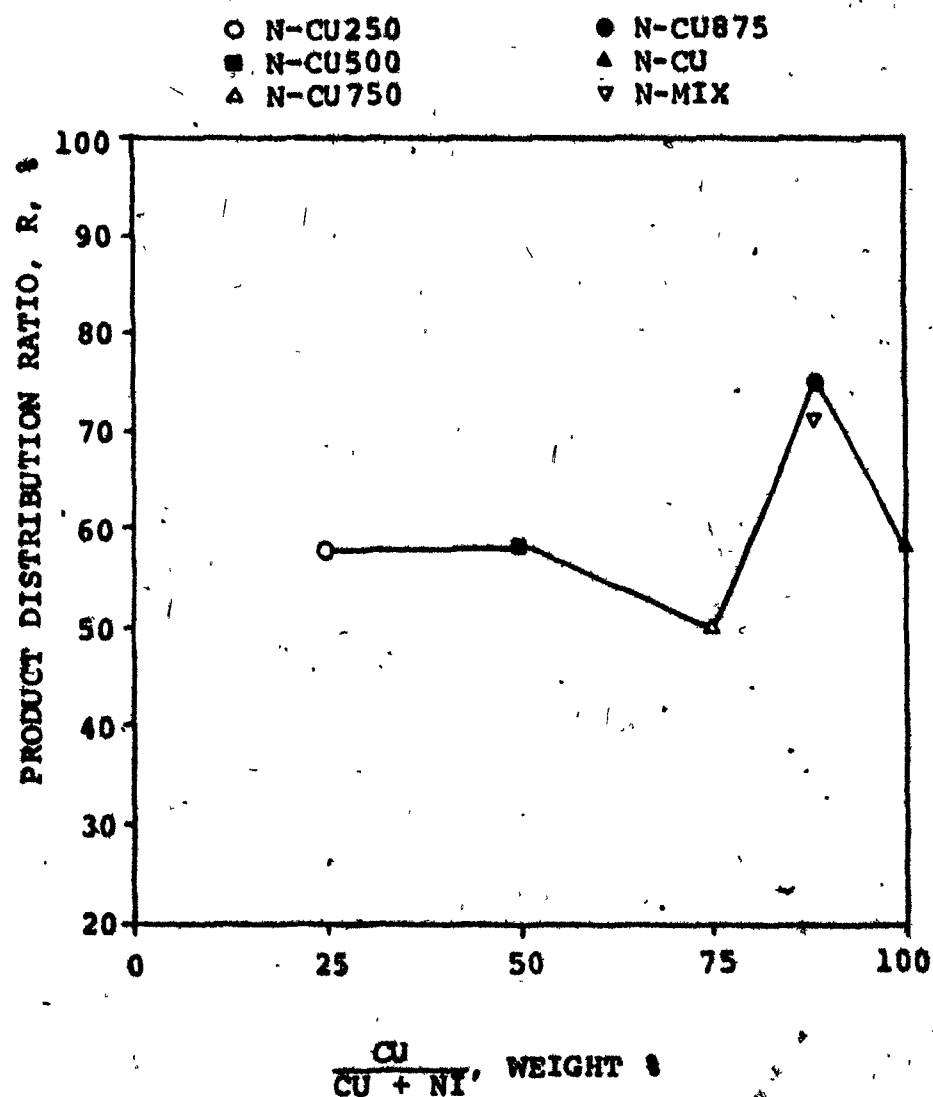


FIGURE 24: EFFECT OF METAL COMPOSITION ON PRODUCT DISTRIBUTION RATIO FOR NITRIC OXIDE REDUCTION OVER NITRATE-BASED CATALYSTS

mixed-oxide catalyst. The product distribution ratio shown in Figure 24 is significantly higher for these two catalysts than it is for all the others; this suggests a difference in mechanism.

The effect of temperature on conversion was determined in a second series of tests whose results are presented in Table 12. The most active catalysts were tested at 150°C. Even at this low temperature catalysts N-Cu875 and N-Mix convert 95% of the inlet nitric oxide. There is a shift in the product distribution ratio with greater reduction to nitrous oxide and less to nitrogen. The less active catalysts were tested at the higher temperature of 300°C. There is a definite increase in conversion with complete elimination of nitric oxide over two of the mixed-oxide catalysts. The nickel catalyst, N-Ni, is the least active; its activity is probably comparable to that of the Raney nickel catalyst R-Ni-A. Product distribution ratios were not calculated at this temperature because of possible ammonia decomposition.

Ammonia decomposition over catalyst G-Mix was measured at 200°C and at 300°C; data are presented in Table 13. The reaction is insignificant at 200°C and rapid at 300°C. This confirms the importance of maintaining a low reaction temperature for the reduction of the nitric oxide.

Activities of the nitrate-based catalysts are much higher than those of the Raney metals. This is illustrated in Table 14 by comparison to catalysts reported by other workers (8). The activity of catalyst N-Cu per unit weight of metal is probably close to that of the commercial nickel catalyst.

Table 12: Activities of Nitrate-Based Mixed-Oxide Catalysts

Reactor Feed Composition: 0.3% nitric oxide
0.6% ammonia
balance argon
Space Velocity: 3000 hr⁻¹

Catalyst	Temperature °C	Reactor Product Gas Composition		X, %	Conversions		Product Distribution Ratio, R, %
		%N ₂	%NO		Y, %	Z, %	
N-Cu	150	.091	.077	74	37	37	51
N-Cu250	150	.048	.169	44	19	24	44
N-Cu875	150	.127	.015	95	51	44	53
N-Mix	150	.143	.015	95	58	38	60
N-Ni	300	.067	.181	40	28	-	-
N-Cu500	300	.176	.000	100	70	-	-
N-Cu750	300	.178	.000	100	72	-	-

Table 13: Effect of Temperature on Ammonia Decomposition over Nitrate-Based Catalyst #N-Mix

Reactor Feed Composition: 1.2% ammonia in argon
Space Velocity: 800 hr⁻¹

Temperature	%Ammonia Decomposed
200°C	.47
300°C	92

Table 14: Comparison of Catalyst Activities for Reduction of Nitrogen Oxides with Ammonia

Catalyst	R-Cu-A	N-Cu	Ni on alumina	Pt on alumina
Reference No.	-	-	8	8
Wt % Metal	3.3	1.0	5.5	0.5
Temperature, °C	350	200	215	260
Space Velocity, hr ⁻¹	500	3000	20000	30000
% Nitrogen oxides destroyed	65	100	88	96

The results of these preliminary tests are quite promising. High activities have been shown at low reaction temperatures where ammonia decomposition is negligible. Metal composition has a strong effect on activity and selectivity. Further investigation of this system would proceed by study of more catalysts, especially those with nickel contents between 0% and 25% by weight. Catalyst testing over extended periods of time would be the next step. Finally the metal loadings would be increased to permit operation of the reactor at high space velocities. This increase in metal loading should be achieved without a large increase in metal crystallite dimensions so that the extra metal added will result in a corresponding increase in surface area available for reaction.

Section X: Discussion of Apparatus and Procedures

Development of the microreactor, the flowmeters, and the analytical systems was crucial to accurate measurement of catalyst activities. The microreactor and flow controllers were relatively straightforward, but the analytical systems were severely limited by the difficulties previously discussed.

The capillary flowmeters served the dual function of flow control and measurement. They would be particularly useful in the control of very small gas and liquid flows, especially at extreme temperature ranges. For example, volumetric flow rates of 0.33 cc/min argon can be metered through a capillary which is 20 cm long and 0.02 mm internal diameter at a differential pressure of 100 psi. Flow rates of several cc/hr can be controlled with this meter at smaller differential pressures.

These meters would be useful at high temperatures because most high temperature commercial valves cannot handle such low flow rates. For example, flow control at 500°C requires highly specialized valves, such as bellows valves in which the stem packing is isolated from the process fluid. These valves are expensive and even with micrometering stems would not be suited for control of gas flows of less than 1 cc/min. The temperature range of the capillary flowmeters used in this work was limited by the epoxy resin used to hold the capillary in place inside the tube. Since then, several other meters have been constructed

with ordinary solder holding the glass in place. They performed well during tests at room temperature. Use of high temperature solder and glass would probably extend the operating temperature of these meters up to at least 500°C.

Capillary flowmeters could be used for direct metering of a gas or liquid into a localized area such as the center of a catalyst pellet. They would make excellent point sources for micro-diffusion studies.

The importance of the flow controllers to the catalyst tests is their simple and accurate control of the reactor inlet stream composition and flow rate.

The difficulties in the chemical analyses of nitrogen oxides have been encountered by other workers. Several avoided part of the problem by simply measuring nitric oxide destruction without determining extents of reduction to nitrous oxide and nitrogen (6,55). The combined infrared and chromatographic analysis originally planned in this project should be capable of a complete analysis of the reaction mixture.

The chromatographic determination of argon, nitrogen, and nitric oxide proved satisfactory over a period of many months. Gas chromatography can probably be utilized more extensively than it was in this project. For example, hydrogen can be determined by using argon as the carrier gas in the second chromatograph column. This would introduce baseline drift during non-isothermal operation, but would measure the extent of the ammonia decomposition

reaction. The analysis might be extended to include nitrous oxide by adsorbing the ammonia and water on anhydrous $\text{Mg}(\text{ClO}_4)_2$ rather than on Molecular Sieve 13X. Use of cold traps and a second analysis column might permit extension of the analysis to nitrogen dioxide, water, and ammonia. Considerable development work would be required for any of these alternate analyses.

Infrared analysis of the gas mixture is feasible despite the problems encountered with the Miran I Infrared Analyzer. The preliminary results demonstrated that ammonia and nitrogen dioxide can be determined down to the ppm levels. However, the Miran I Infrared Analyzer with long path cell requires two important improvements before it can be used for this analysis. The windows of the long path cell should be constructed of a corrosion resistant material, even at the expense of limiting the usable region of the spectrum. The instrument resolution should be increased from low to at least medium to permit accurate analysis of complex mixtures.

An ultraviolet spectrometer equipped with a long path cell would allow precise measurement of nitrogen dioxide levels and perhaps several other components. Quartz windows could be used on the long path cell to solve the corrosion problem.

Ludox HS-40 is a versatile catalyst support with a fine pore structure and a high specific surface area. It was used successfully in this work to support the Raney alloy catalysts and to prepare the nitrate-based mixed-oxide catalysts. Other catalysts have been supported on it. It can be cogelled with

alumina to yield an aluminosilicate support (26). Alternatively, active metals can be precipitated as hydroxides or carbonates on the Ludox (93).

Ludox provides a gel stability and reproducibility that other methods of silica gel preparation are unable to. Impurity levels can be minimized by proper choice of preparation conditions. For example, Ludox AS is stabilized by ammonium ions rather than by sodium ions; it could be gelled by acetic acid. Both the ammonium and acetate ions would leave on drying to produce a high-purity gel.

Proper selection of the drying method is an important step in the catalyst preparation procedure. It is not critical in the support of the Raney metals because the active catalyst centers are present before the gel is dried; the silica is merely acting as a base for the metal particles. However, this is not the case for the nitrate-based catalysts. The metal nitrate solution is drawn to the surface by the surface tension forces developed in the drying. The result is a higher concentration of metal near the surface of the gel. The effect is not important in a preliminary study such as the one undertaken here for the nitrate-based catalysts. However, in any precise work, the metal should be uniformly deposited throughout the bulk of the catalyst support. It could be deposited as an insoluble salt such as hydroxide or carbonate before the gel is dried. Alternately, the gel could be

spray-dried so that any non-uniformities would be on the microscopic scale.

There is no evidence that the catalyst support was interfering with the activity measurements on either the Raney catalysts or the nitrate-based catalysts. The Ludox was neutralized with hydrochloric acid when the Raney metals were supported. The chloride ions should not have affected the activity determinations since they were locked into the silica support without a means to diffuse to and agglomerate on the Raney metal particles. Experimentally, Raney copper was more active when dispersed in the silica according to the standard procedure than when it was mixed with the silica support mechanically. Presumably this effect was due to improved dispersion. When the nitrate-based catalysts were prepared, the Ludox was gelled with acetic acid. Since the acetate ion leaves during the catalyst drying, no interference should be expected.

The Raney metals were prepared by a standard technique which results in active nickel catalysts. Unfortunately it can result in a variation of physical and chemical properties when applied to different starting alloys. The results of this investigation agree with the observations of Reynolds (73). The reactivity of the copper-nickel-aluminum alloy varies strongly with composition; large amounts of residual aluminum remain in the activated copper-nickel catalysts. The higher levels of residual aluminum observed

in this investigation as compared to that of Reynolds may reflect a difference in the structure of the starting alloys or the less severe leaching conditions employed in this work.

None of the experimental data supported Reynolds' theory that catalysts with significant residual aluminum consist of an activated surface covering an unaltered core. A better explanation is that a fraction of the aluminum atoms are locked in a solid solution with the copper and nickel and are simply not reactive to alkali. The leaching of the starting alloy will cease after all available aluminum has been removed. Microscopic examination of sections of activated catalysts would test these alternate explanations.

Reynolds observed a large variation in specific surface area of the activated catalysts with composition of the starting alloy. There is probably a similar variation in this investigation.

This variability in extent of leaching, surface area, and pore size will prevent interpretation of the conversion data over the Raney alloy catalysts in terms of simple models of inherent activities of the Raney alloys.

Section XI: Discussion of Catalyst Activities

The aim of this investigation is to test the three research hypotheses on Raney alloy catalyst activities presented in Section II. As a result of this work with the Raney catalysts, further experiments were undertaken with a series of nitrate-based copper-nickel catalysts.

The results of the experimental work, and in particular, the data in Figure 19 and Tables 7 and 8, justify the following conclusions regarding the research hypotheses.

- (A) The Raney method can be used to prepare copper-nickel alloy catalysts active for the reduction of nitric oxide with ammonia. However, all catalysts have low activities and one catalyst of 50% by weight copper has virtually no activity.
- (B) Activity measurements on commercial Raney copper and nickel and on alloy catalyst R-Cu375 demonstrated that oxidation of the Raney catalysts decreases activity drastically.
- (C) The activity of the mechanical mixture of Raney copper and Raney nickel differs from that of the corresponding Raney alloy. Unfortunately this difference cannot be interpreted in terms of reaction mechanism or inherent activities.

The low activities of the Raney catalysts may be due to low inherent activities of the Raney metals, to low surface areas, to deactivation when oxygen was bubbled through the wash water, to poisoning of the surface by adsorbed NH_2 from ammonia decomposition, or to low activities of the oxide form of the Raney metals.

Several of these mechanisms are probably not significant. The nitrate-based catalysts were oxidized, but still active. Similarly, NH_2 is likely to be adsorbed on the nitrate-based catalysts if it is adsorbed on the Raney catalysts. The high activities of the nitrate-based catalysts show this is unlikely. Deactivation by the oxygen bubbled through the wash water cannot be the major factor because even the commercial Raney nickel and copper had low activities; these catalysts had not been exposed to oxygen during the leaching of the aluminum alloys.

The surface areas of Raney metals are high. If the surface were active for nitric oxide reduction, significant conversion should be observed at temperatures much lower than 350°C .

The low activities are most likely due to low inherent activities reduced even further by pore blockage from oxidation. The following calculation illustrates the effect of oxidation in reducing surface area available for reaction. Consider a typical Raney metal particle which is assumed to be a cube of 0.01 mm on each side. If the specific surface area is $50 \text{ m}^2/\text{g}$ and the density is 9 g/cc , then the total surface area of the cube is the following,

$$\begin{aligned} A_t &= 9 \text{ g/cc} \times (10^{-3})^3 \times 50 \text{ m}^2/\text{g} \\ &= 4.5 \times 10^{-7} \text{ m}^2 \end{aligned}$$

If the internal pores are blocked, leaving only the external surface available for reaction, the surface area is reduced to the following,

$$A_{\text{ext}} = 6 \times (10^{-5} \text{ m})^2$$

$$= 6 \times 10^{-10} \text{ m}^2$$

The ratio of external to internal surface area is 1.3×10^{-3} . Blockage of the pores by oxidation will drastically reduce the activity.

Pore blockage is likely if the metal oxide has a significantly larger specific volume than the metal. The ratio of the specific volume of CuO to Cu is 1.39, while the ratio of the specific volume of NiO to Ni is 1.25 (67). Since the porosities of Raney metals are typically 0.1 cc/g (34), conversion from the pure metal to the oxide should result in pluggage of the pores.

However, even the reduced Raney metals such as R-Cu375-A and the unoxidized commercial Raney nickel and copper have activities low compared to commercial catalysts and the nitrate-based mixed-oxide catalysts. This demonstrates that even reduced Raney metals have a low inherent activity for the reduction of nitric oxide with ammonia.

The low experimental conversions over the oxidized Raney metals are probably due to both low inherent activities and low specific surface area caused by oxidation.

This suggests that any catalysts to promote reduction of nitrogen oxides with ammonia should be resistant to pore pluggage either from oxidation or adsorption of reactants. The active metal should be well dispersed as small crystallites over an inert support of high pore size and volume and low specific surface area.

The variation of activity with composition of the starting alloy may be due to differences in the microstructure and chemical composition of the starting alloys, to variations in the amount of aluminum leached, to variations in the specific surface area of the active metals, to changes in oxidation state with composition, and to variations in the inherent activities of the alloy catalysts. All of these factors are probably contributing to the observed conversions.

The starting alloys differ not only in chemical composition, but also in microstructure. The chemical aspect is important because it determines the elemental composition of the final catalyst. The physical structure of the initial alloys may be equally important. Final catalyst properties will definitely be affected by crystalline microhardness, grain structure, and relative proportions of the aluminum phases in the starting alloys (21,22).

Variations in the amount of aluminum leached will affect the chemical composition, surface area, and pore structure of the final catalyst. The presence of aluminum in the copper-nickel matrix will change the number and nature of the sites available for reaction. Physical properties will also be influenced. Anderson (34) has shown a significant change in the surface area of Raney nickel as the amount of aluminum leached is varied from 50% to 98%. Reynolds (73) has shown a strong dependence of alloy specific surface area on composition.

2

There may also be variations in the amount of metal converted to oxide. The pure metals may be more or less easily oxidized than the alloys. Also, since the pore volume of the copper-nickel alloys is significantly less than that of Raney nickel and copper, oxidation is likely to cause more extensive pore blockage.

All of these factors prevent interpretation of observed conversions in terms of inherent metal activities and any meaningful conclusions from comparison of the activity of alloy catalyst R-Cu250 to the mechanical mixture R-Cu-Ni-Mix. The Raney nickel and Raney copper present in R-Cu-Ni-Mix are probably acting independently since the activity is intermediate between those of the two Raney metals. Catalyst R-Cu250 has very little activity.

The nitrate-based catalysts are much more active. They should consist of very fine metal oxide crystallites scattered over the silica support. The crystallite dimensions are probably of the same order of magnitude as the crystallite dimensions of Raney nickel or the nickel catalysts described by Reynolds (73). If these nitrate-based catalysts were reduced, they should be much less susceptible to deactivation by oxidation than are the Raney catalysts because the surface area will not be drastically lowered. This method is superior to the Raney procedure to prepare catalysts to reduce nitric oxide with ammonia.

The activity could be further increased by both increasing the metal loading and by producing smaller crystallites. The

metal loading of 1% could easily be increased to above 15%. At the same time the support procedures could be changed to reduce the crystallite size. The calcination temperature could be lowered to below 400°C or another method used to decompose the nitrates. High calcination temperatures produce large crystallite sizes because of the high mobility of the copper atoms.

The dependence of activity on composition shown in Figure 23 is different from that of the Raney alloy catalysts in Figure 19. Although no aluminum is present to complicate the interpretation, there can be significant variations in specific surface area, crystallite size, and oxidation state between catalysts. There are similarities between the activities of the Raney and nitrate-based catalysts. In both cases, there is a region of low activity at a composition of 50% copper. The overall shape of the activity-composition curve of the nitrate-based catalysts is similar to that reported by Campbell and Emmett (16) for the hydrogenation of ethylene over copper-nickel films.

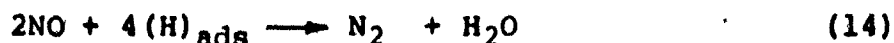
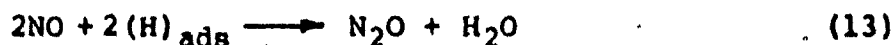
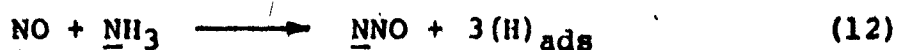
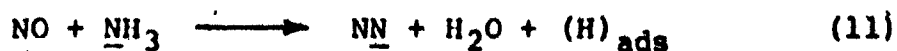
Since the specific surface areas of the catalysts were not measured, conversions cannot be converted to inherent catalytic activities per unit surface of metal. However, the nickel oxide crystallites should be no larger than the mixed-oxide crystallites since the greater mobility of the copper is likely to result in larger crystallites at the calcination temperature of 400°C. Surface areas of all the mixed oxide catalysts are probably of the same order of magnitude, so activities per unit

surface area probably vary with composition in a fashion similar to the overall conversion-composition curve in Figure 23. Note that Reynolds' data in Figure 21 show that the surface areas of reduced oxide on kieselguhr catalysts do not monotonically decrease with copper content of the alloy. One of the local peaks in the surface area-composition curve in Figure 21 falls close to the peak of the conversion-composition curve in Figure 23.

The most active catalyst is 12.5% nickel in copper. The presence of relatively small amounts of nickel increases the activity of the copper. This promotional effect could be due to formation of special copper-nickel sites, to changes in surface structure and area from inclusion of the nickel into the copper matrix, to surface diffusion of reaction intermediates between copper and nickel sites, or to a gas-phase intermediate between copper and nickel sites. The increase in the product distribution ratio at this composition shown in Figure 24 suggests that the reaction mechanism being catalyzed is different from that being promoted over the other mixed-oxide catalysts. However, the available conversion data are not extensive enough to allow any conclusions on the nature of the promotion mechanism.

The mechanical mixture of the copper and nickel catalysts, N-Mix, is just as active as the mixed-oxide catalyst N-Cu875, and its product distribution ratio is almost as high. The only interaction between the copper and nickel sites possible in this mixture of two catalysts is by diffusion of a gas-phase intermediate through the bulk of the reaction mixture. Gas-phase intermediates have been demonstrated for other systems, but have not been postulated in current theories of the reaction between nitric oxide and ammonia.

Otto and Shelef (61,62,63) studied the reduction of nitric oxide with ammonia over platinum and copper catalysts; reactants were alternately labelled by the ^{15}N isotope. They proposed the following reaction sequences,



where $\underline{\text{N}}$ refers to the nitrogen introduced with the ammonia and N refers to the nitrogen introduced with the nitric oxide.

They found (11) and (13) to be the major and (12) and (14) to be the minor paths over a platinum catalyst at 200°C . On a copper oxide catalyst mixed nitrogen by (11) was the only product. They also found that the copper oxide catalyst is reduced to metallic copper after exposure to the reaction mixture. Activity increases with extent of reduction. The metallic copper catalyst is four times as active as platinum per surface atom. The reaction mechanism and product distribution are strongly dependent on the chemical composition and oxidation state of the catalyst. Table 15 presents the product distribution ratio at 200°C .

They found the reaction order is zero, indicating that the rate-determining step is in the adsorbed layer. A kinetic isotope effect results when ND_3 is substituted for NH_3 . This supports

**Table 15: Product Distribution Ratio for Reduction
of Nitric Oxide with Ammonia***

Catalyst	Product Distribution Ratio, R, % % of NO reduced to N₂
CuO	100
Cu₂O	84
Cu	69
Pt	50

* based on data presented by Otto & Shelef (63)

their theory that the rate-determining step is the surface dissociation of ammonia in Reactions (11) and (12),



The promotional effect of small amounts of nickel on copper can be rationalized within this mechanism. Nickel is known to be much more active than copper for ammonia decomposition (11,50). Klimisch and Taylor (50) studied the reduction of nitric oxide with hydrogen and carbon monoxide over alloy catalysts containing nickel in combination with copper, platinum, and palladium. They demonstrated that the ammonia decomposition function resides primarily in the nickel while the reduction activity is derived from the other metal.

If ammonia decomposition is the rate-determining step, then addition of small amounts of nickel to copper should increase the rate of ammonia decomposition and hence the overall activity. The low activity of the nickel catalyst, N-Ni, is in agreement with the low reduction activity reported by Klimish and Taylor (50). Addition of copper to nickel should increase its activity for nitric oxide reduction because copper promotes the reduction. These hypotheses can explain why all mixed-oxide catalysts should be more active than nickel. They do not explain the decrease in activity in the region of 50% copper. However, at this composition the d-band vacancies of nickel are filled by electrons donated by copper. Reynolds (73) has shown the magnetic susceptibility of

copper-nickel alloys falls to zero at this composition. Figure 1 shows that electrical and thermal conductivities are also low. Similarly, minima in activity-composition curves have been observed for other reactions catalyzed by copper-nickel alloys of this composition (16,83). The phenomena is a fairly general one which may be related to the formation of an inactive copper-nickel alloy.

The proposed explanation does not account for the high activity of the mechanical mixture of the copper and nickel catalysts because adsorbed ammonia cannot reach a copper site from a nickel site by surface diffusion. A gas-phase intermediate is a likely hypothetical explanation.

The difference between the product distribution ratios for the nitrate-based catalysts and the copper catalysts studied by Otto and Shelef are probably due to differences in catalyst preparation and crystallite size. Their copper oxide catalyst was a sample of "Specpure" copper oxide of surface area $0.88 \text{ m}^2/\text{g}$. It is probably more chemically pure than the copper-on-silica prepared for this investigation. This difference in chemical composition may account for the fact that their catalyst produces only mixed nitrogen, while catalyst N-Cu produces only 58% nitrogen when nitric oxide is reduced by ammonia.

Another possible explanation is that the change in product distribution ratio with catalyst composition shown in Table 15 is actually correlated with changes in crystallite size. Under

the experimental conditions employed by Otto and Shelef, dimensions of the catalyst crystallites probably decrease as the sample is reduced; the platinum catalyst likely has a very small crystallite size. The decrease in nitrogen formation with reduction of the catalyst may be correlated with crystallite dimensions, rather than simply chemical composition. The product distribution ratio observed over N-Cu may indicate that its crystallite dimensions are close to the dimensions of the reduced copper oxide tested by Otto and Shelef (63).

There is no evidence of reduction of either the Raney or nitrate-based catalysts studied in this work. Both were oxidized before use. The slight decrease in activity after exposure to the reaction mixture may be due to poisoning of the surface by ammonia (61). Otto and Shelef reported that their copper oxide catalyst becomes more active as the reduction proceeds. Figures 18 and 22 show a decrease in activity with time over both Raney and nitrate-based catalysts; this suggests no reduction is occurring.

The overall results of this investigation are quite promising. The Raney catalysts are not suitable for any commercial application. However, testing this series of catalysts demonstrated the importance of alloy composition and oxidation state, and the necessity to prepare a catalyst which cannot be easily deactivated by oxidation. The investigation of the nitrate-based mixed-oxide catalysts was more fruitful. Activities are high and both activity and product distribution are dependent on composition.

Optimization of activity and selectivity by further testing is feasible.

Interpretation of conversion results in terms of inherent catalyst activity requires knowledge of the specific surface of the copper and nickel alloys, of the crystallite characteristics, and of the surface composition of the active metal sites. The adsorptive characteristics of the reactive species and the reaction mechanism are also required. Facilities to undertake these measurements were not available for this investigation. However, these limitations do not detract from the demonstration that formation of copper-nickel alloys and mixed-oxides is a powerful tool in the preparation of catalysts to reduce nitrogen oxides. Similar techniques should prove useful for studying other reactions.

Appendix A: Capillary Flowmeters

The reactants were metered from their supply cylinders through capillary glass flowmeters to the microreactor. The fluid flow in these meters is compressible, subsonic flow in the laminar, transition, and turbulent regions. It is also adiabatic, although an isothermal flow model is used to describe it.

The flow through the capillaries is two-dimensional since fluid velocity, temperature, and pressure are functions of both radial and axial coordinates. If the flow were turbulent, this might not be important. However, most of the meters were designed for low space velocities which corresponded to the laminar and transition flow regimes. A one-dimensional model might not be sufficiently accurate when the velocity profile is approximately parabolic.

The flow is highly compressible because the inlet pressure is generally several times the outlet. The resulting Mach number increase from inlet to outlet causes a temperature drop along the tube. The meters were operated in the subsonic region to minimize the end and temperature effects associated with high Mach numbers.

The two-dimensional nature of the flow complicates estimation of the heat transfer to the gas flowing inside the capillaries from the surroundings. Since the Mach number is

higher at the center of the tube than near the wall, the temperature in the center of the tube will be lower. The wall temperature cannot be calculated without knowing the details of fluid flow inside the capillary. If the wall temperature is at least several centigrade degrees cooler than the surroundings, heat transfer may be significant.

The first step in the analysis of the fluid flow is an enthalpy balance between any two points on a streamline inside the capillary. According to the development of Owczarek (64), the following relation for adiabatic one-dimensional flow of an ideal gas expresses the temperature drop in terms of the change in the Mach number,

$$T_2 = T_1 \frac{1 + \frac{\gamma-1}{2} M_1^2}{1 + \frac{\gamma-1}{2} M_2^2} \quad (16)$$

where T_1 and T_2 are absolute temperatures

M_1 and M_2 are the Mach numbers

γ is the ratio of specific heats

This equation can be modified to apply to two-dimensional flow by expressing the kinetic energy across a section of the capillary in terms of the average velocity at that section as follows,

$$T_2 = T_1 \frac{1 + \frac{\gamma-1}{2} KM_1^2}{1 + \frac{\gamma-1}{2} KM_2^2} \quad (17)$$

$$K = \frac{\int \rho v^2 dv}{\int \rho dv} \quad (18)$$

where v is the fluid velocity at a point

dv is the element of volume

ρ is the fluid density

For laminar flow K is 2.00, while for turbulent flow it is 1.07. If section 1 is at the capillary inlet while section 2 is at the outlet, it can be assumed that $M_1^2 \ll M_2^2$, and Equation 17 simplified,

$$T_2 = \frac{T_1}{1 + \frac{\gamma-1}{2} KM_2^2} \quad (19)$$

Figure 25 shows the theoretical downstream temperature corresponding to an inlet temperature of 25°C for an ideal gas of specific heat ratio 1.668. The temperature drop becomes significant as the Mach number rises.

Entrance and exit losses for incompressible flow are usually expressed in terms of the average fluid velocity and density,

$$\Delta P = K_L \left(\frac{1}{2} \rho V^2 \right) \quad (20)$$

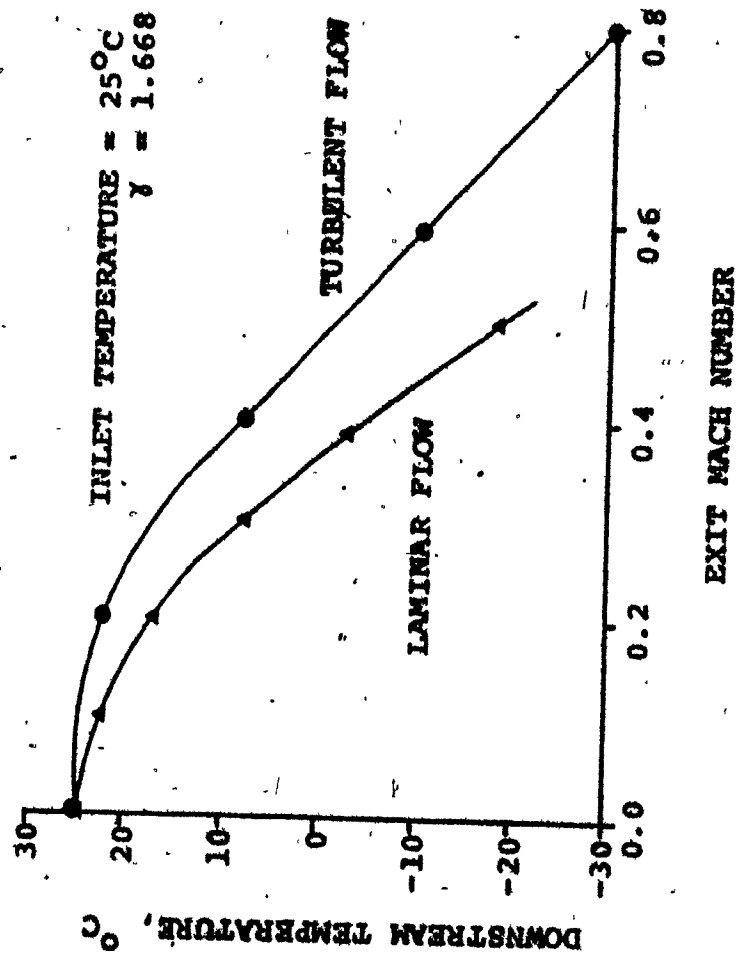


FIGURE 25: EFFECT OF EXIT MACH NUMBER ON DOWNSTREAM TEMPERATURE FOR IDEAL, ADIABATIC FLOW

where V is the average fluid velocity,

ρ is the average fluid density

K_L is the pressure loss coefficient

Pressure loss coefficients presented by Rimberg (74) and Perry (67) are listed in Table 16.

Typical exit losses for the incompressible flow of argon at 1 atm and 25°C are shown in Figure 26. Results are for illustrative purposes only because the flow cannot remain incompressible when the pressure falls. However, the pressure losses can be large at high Mach numbers.

The model of one-dimensional, isothermal, compressible fluid flow presented by Bennet and Myers (10) was used to correlate the data. Their Equation 17-47 was modified by the introduction of the kinetic energy correction factor to yield the following,

$$Q^2 = \frac{\pi^2}{16} \frac{RTg_c}{M} \frac{P_1^2 - P_2^2}{P_0^2} \frac{1}{1 + \frac{4.61}{4fL/D} K \log_{10}(P_1/P_2)} \frac{D^4}{4fL/D} \quad (5)$$

where all symbols are defined in Section IV of the text.

The friction factor is a function of the local Reynolds number. It is assumed constant despite temperature and density variations in the capillary and is calculated assuming isothermal flow at 25°C.

Table 16: Entrance and Exit Loss Coefficients
in Incompressible Flow

Flow Regime	Laminar	Turbulent
Entrance Coefficient	1.072	0.5
Exit Coefficient	1.000	1.0
Reference No.	74	67

Table 17: Dimensions of Test Capillaries

Capillary No.	1	2
Length, cm	122.5	82.1
Diameter, cm	0.0932	0.202
L/D	13100	4060

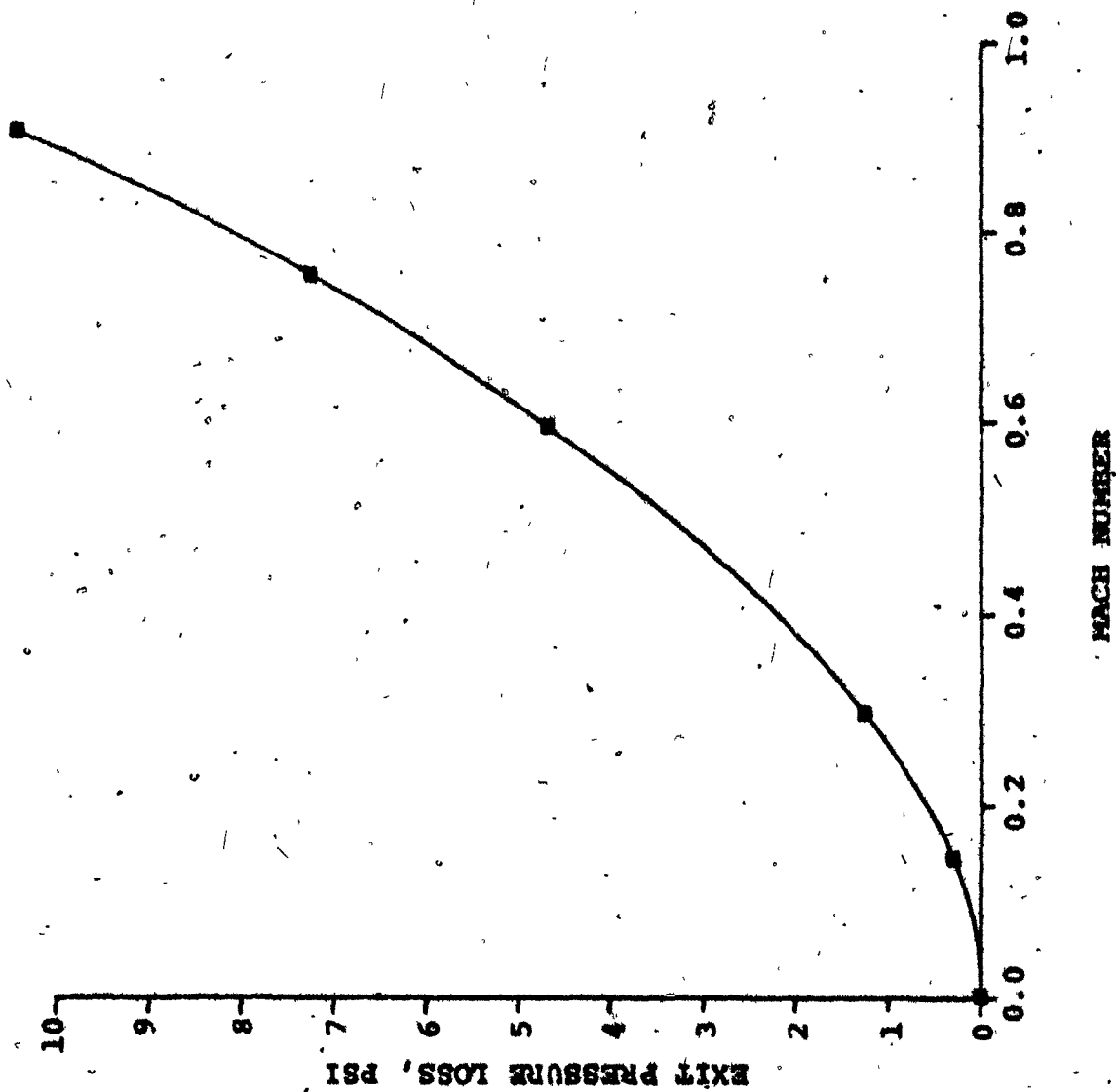


FIGURE 26: EXIT PRESSURE LOSSES FOR LAMINAR AND TURBULENT INCOMPRESSIBLE FLOW

Use of Equation 5 requires the tube dimensions, the fluid properties, and the friction factor corresponding to the Reynolds number of the flow. The tube dimensions can be measured and the fluid properties are known. The friction factor can be estimated from standard correlations such as that in Figure 5-25 of Perry (67). However, data are not given for the transition regime, the relative roughness of the capillaries is not known, and the applicability of these friction factors to very small capillaries has not been established for highly compressible flow.

The dependence of the friction factor on the Reynolds number was measured experimentally by flowing argon through two separate glass capillaries whose dimensions are given in Table 17. These capillaries were made very long to minimize temperature and end effects. Volumetric flow rates were measured by displacement of water; inlet and outlet pressures were measured on gauges.

Results are given in Tables 18 and 19. Inlet and outlet pressure losses were computed and appropriate corrections made. The calculations of the adiabatic temperature loss show that this effect should be small. Results are plotted in Figures 7 and 8 of the text.

For discharge pressures less than 10 psig, the data from capillary #1 can be represented by the relation,

$$f = 23/Re \quad (21)$$

Table 18: Preliminary Capillary Test Data

Test Capillary No. -1
Capillary Length: 122.5 cm
Capillary Diameter: 0.00932 cm

Gas: Argon
Temperature: 25°C

[illegible]

Table 18 (Cont'd): Preliminary Capillary Test Data

Test Capillary No. 1
 Capillary Length: 122.5 cm
 Capillary Diameter: 0.00932 cm

Gas: Argon
 Temperature: 25°C

Data Point No.	8	9	10	11	12	13	14
Inlet Pressure, P_1 , psig	32.6	50.0	39.3	59.0	44.4	73.5	52.0
Discharge Pressure, P_2 , psig	0.0	25.3	0.0	29.8	0.0	37.8	0.0
Volumetric Flowrate, Q , cc/min argon at 1 atm	1.55	1.84	2.10	2.39	2.55	3.40	3.25
$(P_1^2 - P_2^2)$, (atm abs) ²	9.3	12.0	12.5	16.0	15.2	23.2	19.6
Exit Mach Number	.010	.005	.014	.005	.017	.006	.022
Inlet Pressure Loss, ΔP_{in} , psig	.001	.001	.001	.001	.001	.001	.002
Outlet Pressure Loss, ΔP_{out} , psig	.002	.001	.003	.002	.005	.002	.007
Reynolds Number	28.8	34.2	39.1	44.4	47.4	63.2	60.4
Friction Factor	.768	.698	.559	.552	.460	.397	.366
Adiabatic Discharge Temperature, °C	25.0	25.0	25.0	25.0	24.9	25.0	24.9

Table 18 (Cont'd): Preliminary Capillary Test Data

Test Capillary No. 1
 Capillary Length: 122.5 cm
 Capillary Diameter: 0.00932 cm

Gas: Argon
 Temperature: 25°C

Data Point No.	15	16	17	18	19	20	21
Inlet Pressure, P_1 , psig	59.0	89.0	70.0	80.0	90.0	100.0	110.0
Discharge Pressure, P_2 , psig	0.0	45.8	0.0	0.0	0.0	0.0	0.0
Volumetric Flowrate, Q , cc/min argon at 1 atm	3.90	4.72	5.00	6.30	7.60	9.10	11.70
$(P_1^2 - P_2^2)$, (atm abs) ²	24.1	32.8	32.2	40.5	49.7	59.9	71.0
Exit Mach Number	.026	.008	.033	.042	.051	.061	.078
Inlet Pressure Loss, ΔP_{in} , psig	.002	.002	.003	.005	.006	.008	.012
Outlet Pressure Loss, ΔP_{out} , psig	.011	.003	.018	.028	.041	.059	.097
Reynolds Number	72.5	87.8	93.0	117.2	141.3	169.2	217.6
Friction Factor	.313	.291	.254	.201	.170	.143	.102
Adiabatic Discharge Temperature, °C	24.9	25.0	24.8	24.7	24.5	24.3	23.8

Table 18 (Cont'd): Preliminary Capillary Test Data

Test Capillary No. 1
 Capillary Length: 122.5 cm
 Capillary Diameter: 0.00932 cm

Gas: Argon
 Temperature: 25°C

Data Point No.	22	23	24	25	26
Inlet Pressure, P ₁ , psig	120.0	130.0	140.0	150.0	160.0
Discharge Pressure, P ₂ , psig	0.0	0.0	0.0	0.0	0.0
Volumetric Flowrate, Q, cc/min argon at 1 atm	13.40	15.64	17.74	20.60	22.60
(P ₁ ² - P ₂ ²), (atm abs) ²	83.0	95.9	109.8	124.5	140.2
Exit Mach Number	.089	.104	.118	.137	.151
Inlet Pressure Loss, ΔP _{in} , psig	.015	.019	.023	.029	.033
Outlet Pressure Loss, ΔP _{out} , psig	.127	.173	.223	.300	.361
Reynolds Number	249	291	330	383	420
Friction Factor	.091	.077	.069	.058	.054
Adiabatic Discharge Temperature, °C	23.4	22.9	22.2	21.3	20.5

Table 19: Preliminary Capillary Test Data

Test Capillary No. 2
 Capillary Length: 82.1 cm
 Capillary Diameter: 0.0202 cm

Gas: Argon
 Temperature: 25°C

Data Point No.	1	2	3	4	5	6	7
Inlet Pressure, P_1 , psig	7.3	10.3	16.2	22.0	28.2	34.3	39.8
Discharge Pressure, P_2 , psig	0.0	0.0	0.0	0.0	0.0	0.0	0.0
Volumetric Flowrate, Q , cc/min argon at 1 atm	8.6	13.4	24.0	38.0	54.0	72.0	92.0
$(P_1^2 - P_2^2)$, (atm abs) ²	1.23	1.89	3.42	5.23	7.52	10.1	12.7
Exit Mach Number	.012	.019	.034	.054	.077	.102	.131
Inlet Pressure Loss, ΔP_{in} , psig	.002	.004	.009	.020	.034	.053	.078
Outlet Pressure Loss, ΔP_{out} , psig	.002	.006	.018	.046	.093	.166	.271
Reynolds Number	74	115	206	326	463	618	789
Friction Factor	.234	.148	.083	.051	.036	.027	.021
Adiabatic Discharge Temperature, °C	25.0	25.0	24.8	24.4	23.8	22.9	21.6

Table 19 (Cont'd): Preliminary Capillary Test Data

Test Capillary No. 2
 Capillary Length: 82.1 cm
 Capillary Diameter: 0.0202 cm

Gas: Argon
 Temperature: 25°C

Data Point No.	8	9	10	11	12	13	14
Inlet Pressure, P_1 , psig	46.8	53.8	60.0	70.0	80.0	90.0	100.0
Discharge Pressure, P_2 , psig	0.0	0.0	0.0	0.0	0.0	0.0	0.0
Volumetric Flowrate, Q , cc/min argon at 1 atm	117	147	175	210	255	300	325
$(P_1^2 - P_2^2)$, (atm abs) ²	16.5	20.7	24.8	32.2	40.5	49.7	59.9
Exit Mach Number	.166	.209	.249	.298	.362	.426	.462
Inlet Pressure Loss, ΔP_{in} , psig	.112	.159	.207	.263	.347	.203	.217
Outlet Pressure Loss, ΔP_{out} , psig	0.44	0.69	0.98	1.41	2.08	2.89	3.39
Reynolds Number	1004	1261	1501	1802	2188	2574	2789
Friction Factor	.017	.013	.011	.010	.008	.007	.008
Adiabatic Discharge Temperature, °C	19.6	16.6	13.2	8.3	1.0	6.8	3.9

Table 19 (Cont'd): Preliminary Capillary Test Data

Test Capillary No. 2
 Capillary Length: 82.1 cm
 Capillary Diameter: 0.0202 cm

Gas: Argon
 Temperature: 25°C

Data Point No.	15	16	17	18	19	20
Inlet Pressure, P_1 , psig	110	120	130	140	160	180
Discharge Pressure, P_2 , psig	0.0	0.0	0.0	0.0	0.0	0.0
Volumetric Flowrate, Q , cc/min argon at 1 atm	338	356	380	400	456	514
$(P_1^2 - P_2^2)$, (atm abs) ²	71.0	83.0	95.9	109.8	140.2	174.4
Exit Mach Number	.480	.506	.540	.568	.648	.730
Inlet Pressure Loss, ΔP_{in} , psig	.216	.222	.235	.244	.280	.320
Outlet Pressure Loss, ΔP_{out} , psig	3.66	4.06	4.63	5.13	6.67	8.47
Reynolds Number	2900	3054	3260	3432	3912	4411
Friction Factor	.008	.009	.009	.009	.009	.009
Adiabatic Discharge Temperature, °C	2.3	0.0	-3.1	-5.8	-13.9	-22.7

Data from capillary #2 can be represented by the following relations,

$$f = 16/Re \quad Re < 2300 \quad (22)$$

$$f = 0.009 \quad 2300 < Re < 5000 \quad (23)$$

Data from the larger diameter capillary agree well with the correlation presented by Perry (67).

For design purposes, the following dependence of the friction factor on the Reynolds number was assumed,

$$f = 23/Re \quad Re < 2300 \quad (24)$$

$$f = 0.01 \quad Re > 2300 \quad (25)$$

In the laminar regime, data from capillary #1 were used as the basis because most of the meters to be used in this work will have diameters closer to 0.1 mm than to 0.2 mm. A computer program was written to predict the flow properties of capillaries of known dimensions from Equations 18, 19, 20, 24, and 25. A typical output is shown in Table 20 for flowmeter #H-1-B which was used in catalyst testing. Figure 9 (text) shows a plot of the flow rate versus the supply pressure.

A series of capillary dimensions was chosen and the corresponding flow properties calculated. A survey of some of these preliminary design calculations is given in Table 21, where capillary dimensions, pressure drops, and Mach numbers at maximum flow rates are given. Note that a wide range of gas flows can be controlled by these meters. With small diameter capillaries,

Table 20: Design of Capillary Flowmeter No. H-1-B

Length: 20 cm
 Diameter: 0.01105 cm
 Discharge Pressure: atmospheric
 Designed for maximum flow rate of 100 cc/min argon at 25°C

Data Point No.	1	2	3	4	5	6	7
Flow rate, cc/min at 1 atm	10	20	30	60	70	80	90
Reynolds Number	158	316	475	950	1109	1267	1425
Exit Mach No.	.052	.103	.207	.310	.362	.414	.466
Friction Factor	.145	.073	.048	.024	.021	.018	.016
Inlet pressure, psig	21.7	34.8	45.2	69.7	76.6	83.2	89.4
$\frac{P_1^2 - P_2^2}{(atm abs)^2}$	5.2	10.4	15.6	32.0	37.6	43.3	49.2
Inlet Pressure Loss, psi	.014	.043	.079	.224	.282	.344	.409
Outlet Pressure Loss, psi	.038	.153	.345	1.38	1.88	2.46	3.10
Adiabatic Discharge Temperature, °C	24	23	17	7	1	-5	-12

Table 21: Summary of Flowmeter Designs

Design No.	Capillary Dimensions		Typical Flow Conditions		
	diameter	length	Mach No.	Inlet Pressure,	Flowrate
	mm	cm	at Exit	psig	cc/min
1	0.02	2	0.16	88	1
2	0.02	10	0.08	100	0.5
3	0.02	20	0.05	100	0.3
4	0.05	2	0.63	75	25
5	0.05	10	0.21	91	8
6	0.05	20	0.11	91	4
7	0.09	2	0.79	51	100
8	0.09	10	0.66	96	84
9	0.09	20	0.39	100	50
10	0.13	2	0.86	38	230
11	0.13	10	0.86	88	230
12	0.13	20	0.72	101	191
13	0.17	2	0.79	30	360
14	0.17	10	0.79	68	360
15	0.17	20	0.79	98	360
16	0.20	2	0.90	33	630
17	0.20	10	0.90	72	630
18	0.20	20	0.90	102	630

Note: Discharge pressure of 1 atm abs was assumed for all designs.

flows of several cc/hr are feasible; with larger diameters flows of up to several liters/min are possible. In practice, high flow rates would probably be handled by meters operating in the sonic region.

The initial data were screened and the process repeated with new capillary dimensions and flow rates. After several runs of the program, sufficient data were available to select the capillary dimensions needed to construct the flowmeters for catalyst testing. The next step was actual construction of the meters.

The glass capillaries are the most critical feature of the flowmeters. The inside bore must be uniform and free from solid deposits of any kind. Attempts to produce such a capillary by hand drawing a glass tube in a Bunsen burner were not successful. Fortunately a glass-drawing machine was available and several sets of machine-drawn capillaries were produced. The internal diameters of these were measured on a microscope with a travelling platform and found to be uniform within 0.002 mm.

Previous workers on this project had experienced difficulties in handling the fragile glass capillaries. This problem was avoided in the current work by using a heavy-walled Pyrex capillary of 1 mm internal diameter as the starting tube. Even when this was drawn down to an internal diameter of 0.1 mm, it was still strong enough to be easily handled.

Once the tubes were drawn, their internal diameters were measured and found to be close to, but not identical with,

the diameters used in the original flow calculations. The computer program was again used to predict what lengths should be cut. The capillaries were over-designed by 20% so that the required flow rates could definitely be obtained. The capillaries were cut to length and held inside a stainless steel tube fitting with epoxy resin. A wad of Teflon filter paper on the inlet side removed any dirt particles from the incoming gas. The entire assembly is shown in Figure 27.

The meters were assembled into the flow control system shown in Figure 6 (text) and calibrated under conditions identical to those later used in the catalyst testing. This eliminated any errors due to inaccuracies in pressure regulators and gauges. Each data point was checked at least four times to verify that the calibration was accurate.

Table 22 lists the meters constructed for the catalyst tests and compares design parameters to actual performance of the meters. Figure 9 (text) compares actual and predicted flow rates for one of the meters.

A special spline fit interpolation program was written to interpolate between the data points. It proved to be more accurate than several standard polynomial interpolation methods. The output of the program was used exclusively for obtaining the proper flow rates during the experimental work, thereby eliminating the errors associated with reading data from graphs.

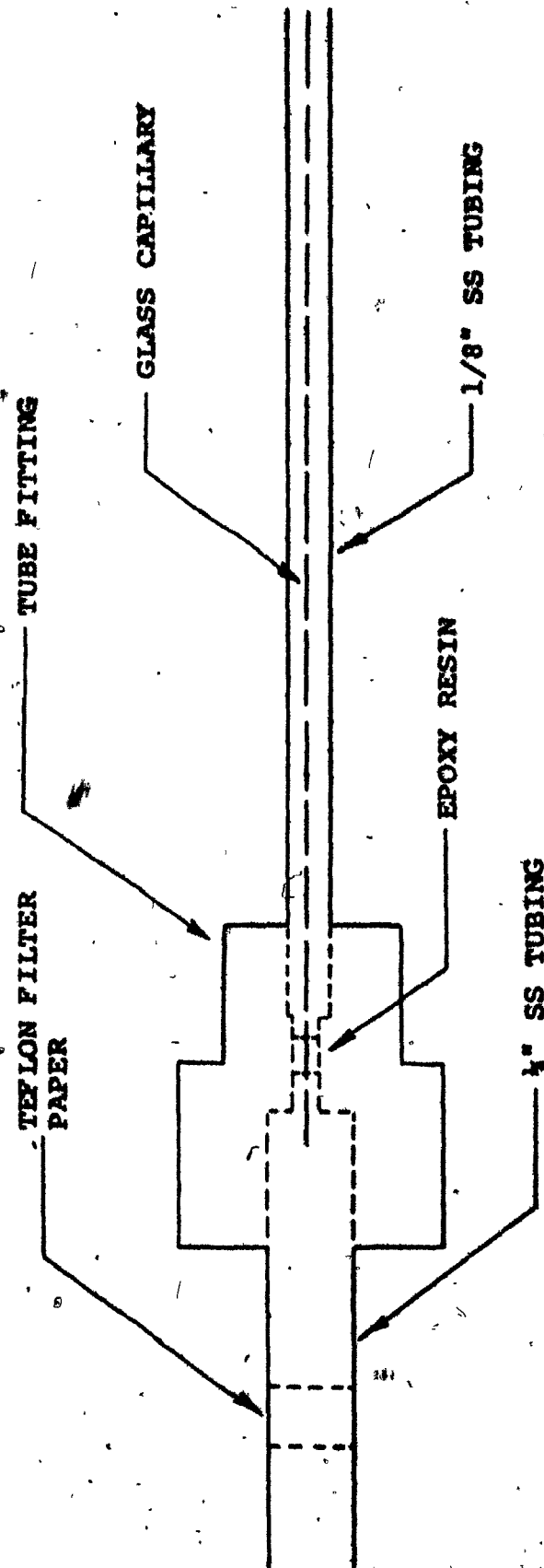


FIGURE 27: CAPILLARY FLOWMETER CONSTRUCTION

**Table 22: Design Parameters for Capillary Flowmeters
Used for the Raney Catalyst Tests**

Composition of Final Gas Stream: 0.3% nitric oxide
0.6% ammonia
balance argon
Space Velocity Range: 30 - 3200 hr⁻¹
Total Flow Rate Range: 3 - 320 cc/min

Meter No.	H-1-A	H-1-B	H-2-A
Maximum Flow Desired at 100 psig Supply, cc/min	80	80	160
Gas to be Metered	argon	1.2% NO in argon	1.2% NH ₃ in argon
Design Parameters			
Max. Flow, cc/min at 1 atm	100	100	192
Gas Supply Pressure at Max. Flow Rate, psig	95	95	101
Capillary length, cm	20	20	20
Capillary Diameter, mm	.1105	.1105	.13
Constructed Flowmeters			
Length, cm	19.3	20.0	20.0
Diameter, mm	.1105 ± .001	.1105 ± .001	.13 ± .005
Max. Flow, cc/min at 1 atm	91	85	170
Gas Supply Pressure at Max. Flow Rate, psig	100	100	94

Appendix B: Chromatographic Analysis

A Hewlett-Packard F&M Model 700 chromatograph was modified in the following ways to make analysis of the microreactor products and reactants easier and more accurate.

To permit isothermal operation at -80°C , the columns were removed from the normal location inside the chromatograph oven and wound into seven-inch diameter coils held outside the chromatograph and connected to it with $1/8$ in outside diameter stainless steel tubing. This allowed complete immersion of the columns in a dry ice acetone bath at -80°C .

Fritted glass filters were placed in the helium lines just before the detector to prevent particles from reaching it. This action was taken after a serious noise problem with the detector output appeared during the initial test work. Fines from the catalyst bed in the microreactor had worked their way through the system and lodged on the detector filaments where they were clearly visible under a microscope.

The helium supply to one of the columns passed through two sampling valves to allow accurate and reproducible gas sampling. Ammonia, water, nitrous oxide, and nitrogen dioxide were removed from the gas samples ahead of the columns by an adsorbent bed in the helium line.

The gas sampling system is shown in more detail in Figure 28. The reaction mixture passes through one sample valve, the micro-

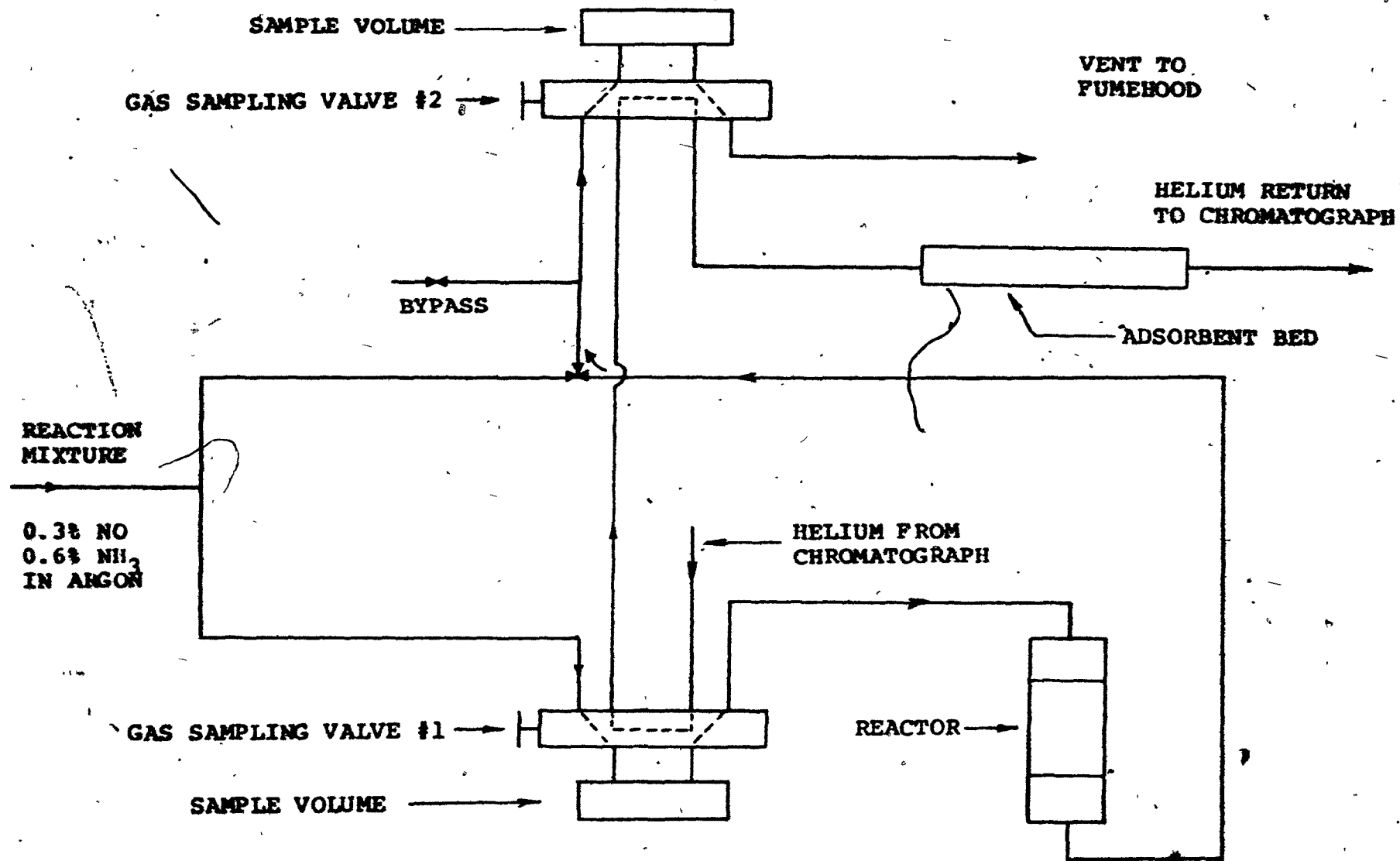


FIGURE 28: CHROMATOGRAPH SAMPLING SYSTEM

reactor, another sample valve, and finally out to vent into a fumehood. Simultaneously helium from the chromatograph is flowing through both sampling valves and returning to the chromatograph. When the plunger of one of the sample valves is pushed, the contents of the sample volume are flushed into the helium line and flow to the chromatograph.

To separate oxygen and argon, the columns were immersed in a dry ice acetone bath at -80°C . The sample was taken after the baseline was steady. Two minutes after the maximum of the oxygen peak, the dry ice acetone bath was replaced by an acetone bath at room temperature to return the column temperature to 25°C for the nitrogen to elute.

During catalyst activity measurements, the reactor inlet gas was analyzed from sample volume #1 and the reactor products from sample volume #2. Operational variables of the chromatograph are listed in Table 23. Typical chromatograms are illustrated in Figure 29.

Peak heights and retention times were very reproducible. For example, the standard deviations of the peak heights for repeated analyses of air samples were less than 1.5% of the mean peak heights.

The design of the adsorbent bed was based on the work of Joithe, Bell, and Lynn (48) who used Molecular Sieve 13X at room temperature to remove nitrogen oxides from a gas stream. They demonstrated that molecular sieves have a high adsorptive

Table 23: Chromatograph Operational Variables

Chromatograph: F&M Model 700

Detector: Thermal Conductivity Type WX
Filament Current of 175 ma
Detector Temperature of 110°C

Carrier Gas: 50 cc/min helium, reduced to 25°C and 1 atm

Columns: 10 ft long x 1/8 od, stainless steel 316
Molecular Sieve 5A packing
Conditioned at 300°C in helium flow for 24 hrs
Operating Temperatures:
25°C normal
-80°C to separate O₂ and A

Sampling Valves: Varian Aerograph Model 57-000034

Sample Volumes: 4.5 cc normal
0.26 cc and 0.75 cc used for special purposes

Retention Times: For a sample volume of 4.5 cc
O₂ and A: 2.6 min at 25°C
N₂: 6.4 min at 25°C
O₂: 16.6 min at -80°C
A: 12.2 min at -80°C
NO: 13 min at 25°C

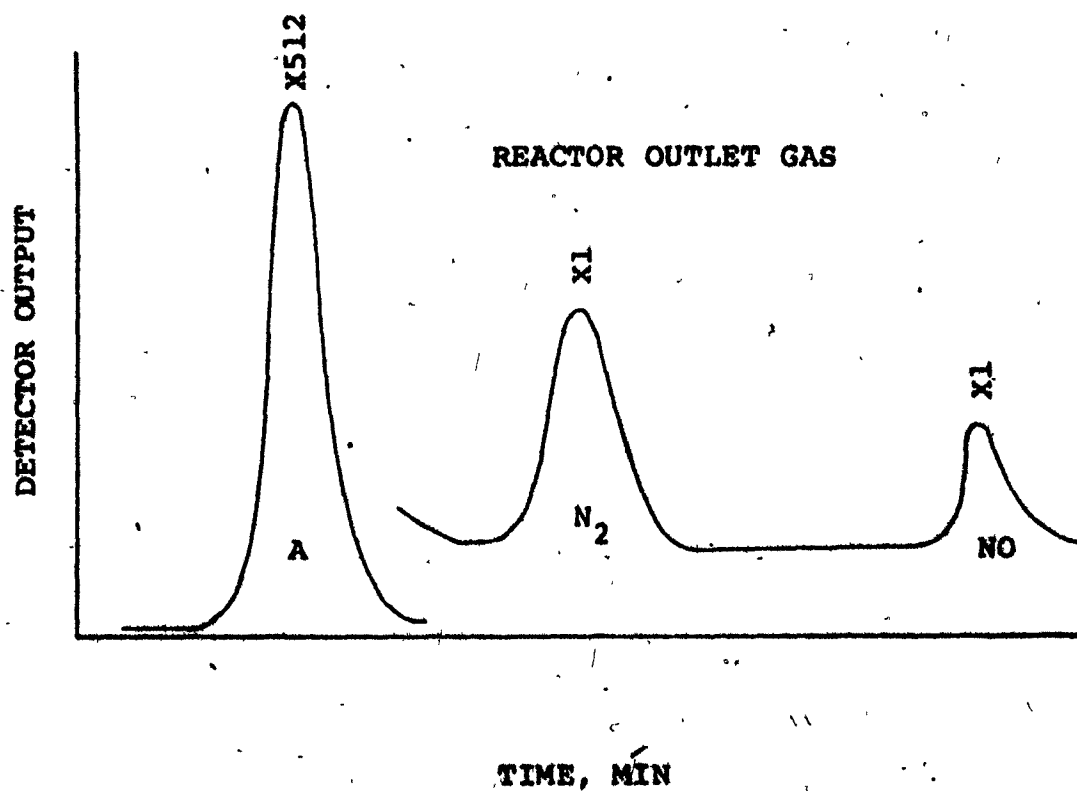
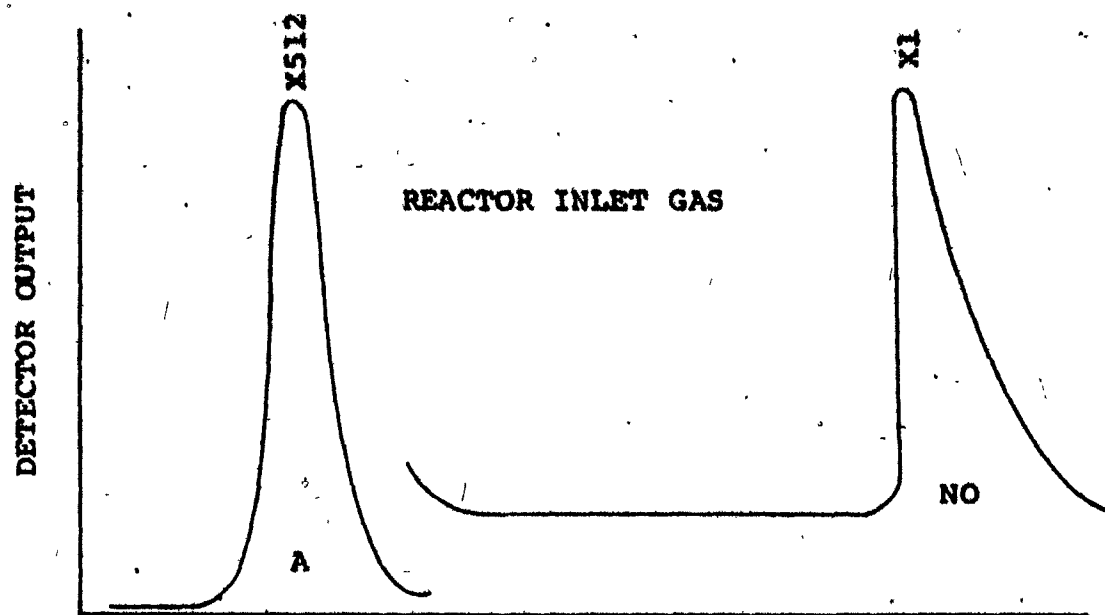


FIGURE 29: TYPICAL CHROMATOGRAMS OF REACTOR INLET AND OUTLET GASES

capacity for nitrogen dioxide, but essentially no capacity for adsorbing nitric oxide by itself. However in the presence of oxygen, molecular sieves catalyze the conversion of nitric oxide to nitrogen dioxide which is then adsorbed.

Molecular sieves also have a good capacity to adsorb ammonia, nitrous oxide, and water. This indicates that ammonia, nitrous oxide, and water will be selectively removed from a gas stream containing argon, nitrogen, nitric oxide, nitrous oxide, and water. Whenever oxygen is present in the sample, analysis for nitric oxide will not be possible. This problem might be avoided by operating the bed at a low temperature where the catalytic conversion of nitric oxide to nitrogen dioxide may not occur.

The adsorbent bed was constructed from $\frac{1}{4}$ in outside diameter stainless steel 316 tubing packed with Molecular Sieve 13X. It was designed to have a mass transfer resistance and residence time similar to the bed used by Joithe (48). Bed characteristics are listed in Table 24.

The molecular sieve packing was replaced after every hundred samples to prevent bed saturation. Actual bed capacity is at least several times larger and depends on the sample size and composition. In preliminary test work, deliberate saturation of the bed was easily identified by distortion of the argon and nitric oxide peaks.

The overall chromatographic analysis system performed well over a period of six months. Analyses were rapid, routine, and accurate.

Table 24: Adsorbent Bed Characteristics

Length:	6 in
Outside Diameter:	0.25 in
Inside Diameter:	0.146 in
Volume:	1.46 ml
Weight of Molecular Sieve Type 13X Bed:	1.55 g
Operating Temperature:	25°C
Operating Pressure:	10. psig (approximately)
Carrier Gas Flow Rate:	50 cc/min helium reduced to 1 atm and 25°C
Residence Time in Bed:	3 sec

Appendix C: Preparation of Silica Support For Raney Metals

The following standard method was used to prepare 5% by weight Raney metal on silica catalysts. The yield is approximately 85 g of catalyst. All gellation, mixing, and settling are done at the room temperature of $25 \pm 1^{\circ}\text{C}$.

- a) Measure out 5 g of dried active Raney metal and place in the bottom of a Waring Blendor.
- b) Add 182 cc of Ludox HS-40 colloidal silica. Mix with a glass stirring rod to wet the metal with the Ludox.
- c) Turn on the blendor. Leave for 1 min at low speed and for 1 min at high speed.
- d) Turn off the blendor and transfer its contents to a 400 ml beaker.
- e) Place the agitator of a Fisher Dynamix stirrer below the liquid surface and turn on the mixer.
- f) Wait 2 min; then add 35 cc of 1N hydrochloric acid to neutralize the Ludox. Test with indicator paper to verify that the pH is between 6 and 7.

The solution will thicken as gellation occurs and will start to climb up the shaft rotating in it.

- g) When the liquid vortex about the rotating shaft has disappeared and the liquid surface is approximately horizontal, turn off the agitator.

The gel time is affected by the nature of the Raney metal present. Table 28 lists the gel times for all the Raney metal catalysts prepared. After gellation the liquid is sufficiently viscous that the Raney metal particles will not settle out.

- h) Pour out the liquid into a 6 in x 9 in aluminum pan.
- i) Let settle for 1 hr and then score the surface into 1 cm squares with a sharp knife.
- j) Let settle for one day.
- k) Dry for two days at 60°C in a draft oven with air flow.
- l) Increase the temperature in the oven to 120°C and dry for two more days.
- m) Remove from the oven.
- n) Crush the catalyst into small particles and separate out the +20, 20-35, 35-80, and -80 fractions on Tyler sieves.
- o) Oxidize overnight at 350°C in a muffle furnace in the presence of air.
- p) Remove from the furnace and cool to room temperature.
- q) Place in a vacuum oven and evacuate to a pressure of less than 1 torr.
- r) Heat to 200°C for 2 hr and then turn off the heat to allow the catalyst to cool to room temperature.
- s) Fill the oven with argon and then remove the catalysts.
- t) Resieve the 35-80 mesh fraction and store in a sealed jar for activity tests.

**Appendix D: Properties of Cabosil Fumed Silicon Dioxide
and Ludox Colloidal Silica**

**Table 25: Properties of Cabosil Fumed Silicon
Dioxide Grade M-7***

Silicon Dioxide Content:	+99%
Nominal Particle Size:	0.012 microns
Specific Surface Area:	200 m ² /g
Bulk Density:	4 lb/ft ³

*Manufactured by Cabot Corporation, Massachusetts

**Table 26: Properties of Ludox Colloidal Silica
Type HS-40 (26)**

Stabilizing Counter Ion:	Sodium
Particle Size:	13 - 14 μ m
Specific Surface Area:	210 - 230 m ² /g
Weight Percent Silica:	40
pH at 25°C	9.1
Titrateable Alkali,	
Calcd. as Na ₂ O, Wt %:	0.43
SiO ₂ /Na ₂ O, by Weight:	93
Chlorides, Weight %,	
Calcd. as NaCl:	0.01
Sulfates, Weight %,	
Calcd. as Na ₂ SO ₄ :	0.06
Viscosity at 25°C:	17.5 cp
Weight/Gallon, at 60°F:	10.8 lb

Appendix E: Preparation of Active Raney Alloys

(A) Experimental Method

The copper-nickel-aluminum alloys were leached inside a 1 liter round bottom Pyrex flask partially immersed in a large water bath as shown in Figure 30. A temperature controller maintained the bath at $50 \pm 0.2^\circ\text{C}$. A three-necked flask was used to facilitate agitation, temperature measurement, escape of hydrogen, and alkali addition.

The alkali solution addition was controlled by a valve on the discharge line from the supply reservoir. The evolved hydrogen escaped up one of the necks of the flask to a condenser which removed the water vapor. It then flowed to displace the water inside an inverted 20 liter tank. Total hydrogen evolved was read from the tank level.

The temperature of the solution was measured by a thermometer which extended through one of the necks to below the liquid level. The liquid was kept agitated by a Teflon stirrer at the end of a Pyrex glass shaft which passed through an o-ring seal in the central neck of the flask. The shaft was driven by a Fisher Dynamix stirrer.

The following procedure was used to leach the Raney alloys.

- a) Turn on the temperature controller and allow the water bath to reach 50°C .

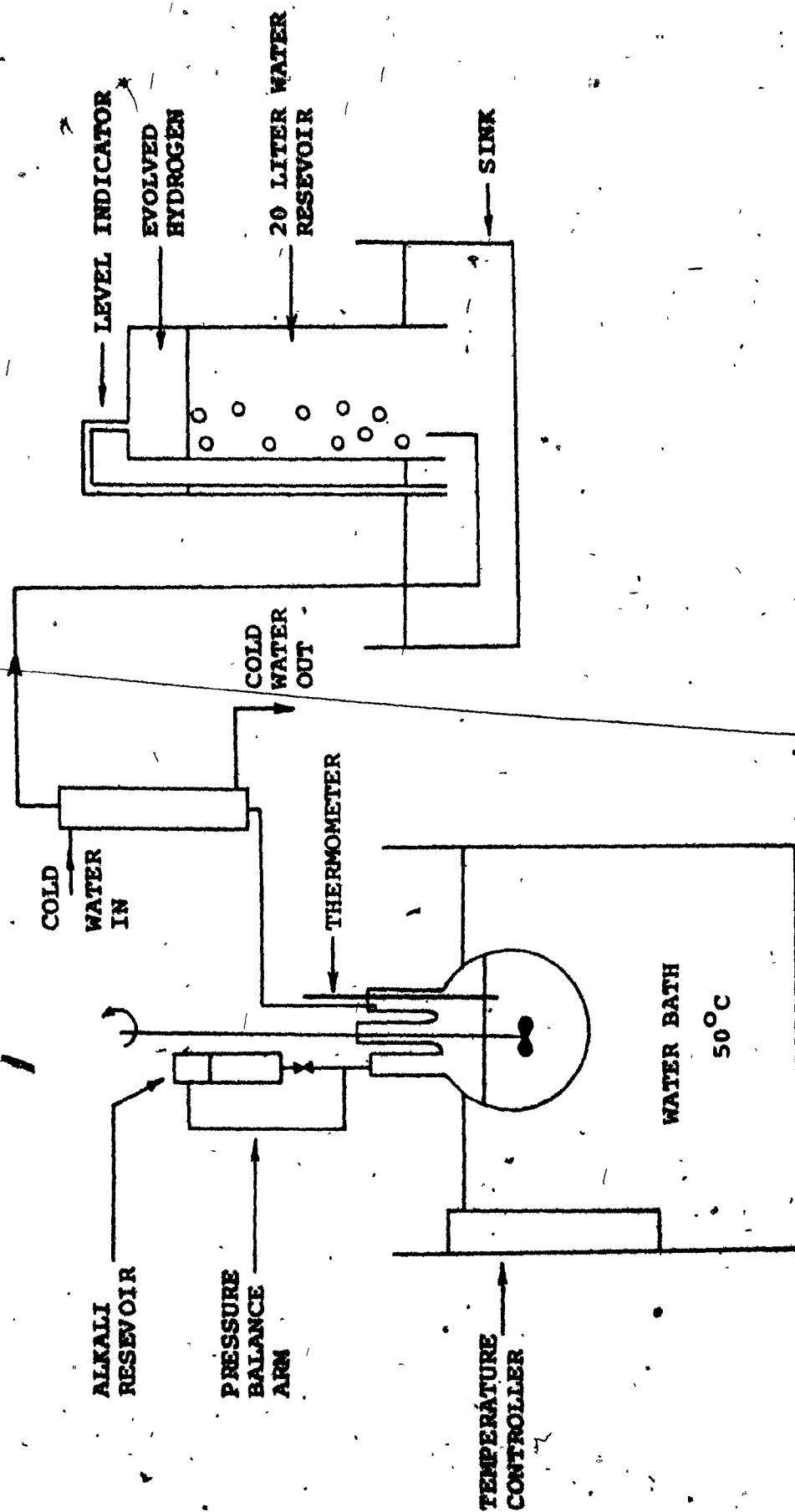


FIGURE 30: APPARATUS TO LEACH RANEY METAL ALLOYS

- b) Measure out 30 g of copper-nickel-aluminum alloy into a clean aluminum pan.
- c) Pour the metal powder into the three-necked flask. Do not spill any metal on the sides of the flask.
- d) Rinse all the metal powder down into the bottom of the flask with 180 cc of distilled water.
- e) Lower the flask into the water bath until the liquid level inside the flask is well below the water level of the bath.
- f) Insert the agitator into the flask. The flask, agitator, shaft, and drive must be properly aligned.
- g) Pour 120 g of 50% by weight aqueous sodium hydroxide solution into the alkali reservoir. Place the reservoir onto one neck of the flask with the discharge valve closed.
- h) Into the remaining neck of the flask insert the thermometer and the outlet to the condenser and collection chamber.
- i) Turn on the cold water to the condenser.
- j) Check that all glass joints are properly sealed. Apply vacuum grease to the fittings if necessary.
- k) Turn on the agitator.
- l) Apply a slight positive air pressure from the discharge line and inspect the system for leaks with a soap solution. Proceed if there are no leaks.
- m) Vent the air pressure and place the discharge line from the condenser below the 20 liter collection chamber which is held full of water in a sink.

- n) Allow the temperature of the liquid in the flask to rise to 50°C.
- o) When the temperature is steady at 50°C, add alkali solution according to the following schedule,

Time, min	Total volume of NaOH 50% soln. added, ml
0	2
8	4
16	6
24	8
32	10
40	30
42	50
44	70
46	90
48	120

After each addition of alkali, record the temperature, the volume of hydrogen evolved, and any other observations of interest.

- p) Allow the contents of the flask to digest at 50°C until 1½ hr from the start of the alkali addition.

This concludes the leaching procedure used to prepare the Raney metals. The active metals were then immediately washed as follows,

- a) Rinse out the contents of the flask with 1 liter of distilled water into a 3 liter glass beaker.
- b) Agitate the contents of the beaker with a stirrer while bubbling oxygen through a fine glass nozzle near the bottom of the beaker at a rate of 175 cc/min.

- c) After 5 min turn off the agitator and the oxygen flow. Allow the suspension to decant.
- d) After 10 min the Raney metal should have settled to the bottom of the flask. Remove the water with a small vacuum aspirator. Test the wash water with pH paper.
- e) Add 1 liter of distilled water to the beaker and repeat steps b, c, and d.
- f) Wash the catalyst a total of seven times. After the fifth wash, the wash water should be at neutral pH.

This concludes the washing sequence used for the Raney metals. The active catalysts were then dried and stored as follows,

- a) After the final rinse, decant and remove the water as usual. Then add a small amount of distilled water to the 3 liter beaker and rinse the Raney metal particles into the bottom of a 6 in by 9 in aluminum pan.
- b) Allow the suspension to decant and remove the excess water with the vacuum aspirator.
- c) Place in a draft oven at room temperature and gradually increase the temperature to reach 140°C at the end of 24 hr.
- d) Remove from the draft oven and dry in a vacuum oven at 210°C for 4 hr at less than 1 torr absolute pressure.
- e) Turn off the heat to the vacuum oven and allow the Raney metal to cool down to room temperature. Then admit argon gradually to pressurize the oven to atmospheric pressure.

f) Remove the Raney metals from the oven and store in sealed glass bottles until use.

(B) Results

The volumes of hydrogen evolved when the copper-nickel-aluminum alloys were leached are listed in Table 27. Duplicate determinations on Raney copper and Raney nickel agreed within five percent. The fraction of aluminum leached was calculated from the hydrogen evolution according to the stoichiometry of Equation 8. The fraction of active metal in the final catalyst was calculated as the total weight of copper and nickel expressed as a percent of the total metal present. The following observations of the leaching process are worth noting.

Most of the hydrogen evolution occurred during the first 40 min of leaching. Reaction was rapid when alkali was added and gradually slowed down until the next addition of alkali. This showed that the alkali was quickly consumed when added; most of the hydrogen was evolved in dilute alkali while the final amounts were evolved in concentrated alkali.

The wide variation in alloy reactivity towards the alkali necessitated a slight change in the leaching procedure. The standard leaching procedure just described was followed for alloys R-Ni, R-Cu125, and R-Cu375. However, alkali addition for

Table 27: Reactivities of Copper-Nickel-Aluminum Alloys Towards Alkali Solution

Starting Alloy	Catalyst Produced	Volume H ₂ evolved, liters ² at 25°C and 1 atm	% Aluminum Leached	% Active Metal
R-Ni	R-Ni-A	16.0	79	83
R-Ni	R-Ni-B	15.2	75	80
R-Cu125	R-Cu125	10.0	50	67
R-Cu250	R-Cu250	9.0	45	64
R-Cu375	R-Cu375	11.2	56	69
R-Cu	R-Cu-A	19.0	94	94
R-Cu	R-Cu-B	19.8	98	98

R-Cu and R-Cu250 was more gradual. The standard procedure of adding 2 cc of alkali every eight minutes at the start of the leaching was changed to adding 1 cc of alkali every four minutes. This was necessary for alloy R-Cu because it reacted so rapidly that large volumes of hydrogen were generated in a short time and the temperature of the suspension rose from the heat generation. Although alloy R-Cu250 did not evolve hydrogen rapidly, it did have a pronounced foaming tendency which became severe during rapid hydrogen formation. The more gradual alkali addition resulted in better control of the process in both cases.

Alloy R-Ni was evolving hydrogen at a rate of less than 1 cc/min even at the end of the ninety minute leaching process. It continued to evolve gas even during the washing sequence. This phenomena was not observed with any of the other alloys. In these other cases, the hydrogen evolution ceased after sixty minutes of leaching, but the alloys were allowed to digest for the full ninety minutes.

In a small scale test, 3 g of alloy R-Cu250 was leached in boiling alkali. Only 42% of the aluminum was removed; this confirmed the low reactivity of this copper-nickel-aluminum alloy.

The leached alloys were supported on silica by the method described in Appendix C. In each case, 5 g of activated Raney metal was supported on 95 g of silica. Gel times of the Ludox suspensions of the activated catalysts are shown in Table 28. Note that the presence of copper accelerated the gellation process. This indicates the presence of at least traces of copper ions.

Table 28: Gel Times of Ludox Suspensions
of 5% Raney Metals

Raney Metal	Gel Time, min ± 20%
none	45
R-Ni-A	45
R-Ni-B	40
R-Cu125	12
R-Cu250	10
R-Cu375	8
R-Cu-A	5
R-Cu-B	5

During the gelling and drying processes, slight colors appeared on the surface of some of the gels. Most of these colors disappeared on overnight oxidizing at 300°C. They indicated the presence of traces of copper and nickel chlorides.

One unusual observation was that alloy R-Cu250 did not mix well with Ludox during the support procedure. However, it was effectively dispersed by mixing for an extra ten minutes in the Waring Blendor and appeared normal in further processing. This abnormal behaviour may be related to the low activity of the catalyst.

Appendix F: Preparation of Nitrate-Based Mixed-Oxide Catalysts

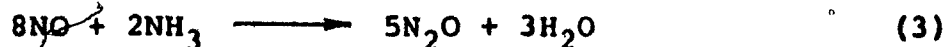
The following procedure was followed in the preparation of all the nitrate-based mixed-oxide catalysts. The yield is approximately 85 g of supported catalyst with 1% by weight of active metal.

- a) Prepare the following two metal nitrate standard solutions.
Solution A: 37.2 g of $\text{Cu}(\text{NO}_3)_2 \cdot 6\text{H}_2\text{O}$ in 200 cc of distilled water; 29.65 g of solution contains 1 g copper
Solution B: 39.84 g of $\text{Ni}(\text{NO}_3)_2 \cdot 6\text{H}_2\text{O}$ in 200 cc of distilled water; 29.96 g of solution contains 1 g nickel
- b) Mix together sufficient volumes of solutions A and B to contain 1 g of metal with the desired proportions of copper and nickel.
- c) Measure out 190 cc of Ludox HS-40 and pour into the Waring Blendor.
- d) Turn on the blender; leave for 1 min at low speed and 1 min at high speed.
- e) Turn off the blender and transfer its contents to a 400 ml beaker.
- f) Place the agitator of a Fisher Dynamix stirrer below the liquid surface and turn on the stirrer.
- g) Wait 2 min; then add 10.5 cc of 20% acetic acid to neutralize the Ludox. Test with indicator paper to verify that the pH is between 6 and 7.

- h) Wait 1 min, then pour in the mixture of the metal nitrate solutions.
- i) The suspension will thicken as gelation occurs and will start to climb up the rotating shaft.
When the liquid vortex about the rotating shaft has disappeared and the liquid surface is approximately horizontal, turn off the agitator.
- j) Pour out the liquid into a 6 in x 9 in aluminum pan.
- k) Let settle for 1 hr and then score the surface into 1 cm squares with a sharp knife.
- l) Allow to settle for one day.
- m) Dry for two days at 60°C in a draft oven with air flow.
- n) Increase the temperature in the draft oven to 120°C and dry for two more days.
- o) Remove from the oven and allow to cool.
- p) Crush the catalyst into pieces and separate out the +20, 20-35, 35-80, and -80 fractions on Tyler sieves.
- q) Oxidize for two days at 400°C in a muffle furnace in the presence of air.
- r) Remove from the furnace and cool to room temperature.
- s) Place in a vacuum oven and evacuate to a pressure of less than 1 torr absolute. Heat to 200°C for two hours and then turn off the heat to allow the catalyst to cool to room temperature. Fill the oven with argon and then remove the catalyst.
- t) Resieve the 35-80 mesh fraction and store for catalyst tests.

Appendix G: Definition of Conversions

The reactor feed gas of nitric oxide and ammonia in argon may undergo the following reactions,



Let X be the fraction of inlet nitric oxide destroyed by the first two reactions. It is calculated directly from the nitric oxide concentrations in the reactor feed and product gases.

$$X(\%) = \frac{C(\text{NO})_{\text{in}} - C(\text{NO})_{\text{out}}}{C(\text{NO})_{\text{in}}} \times 100 \quad (26)$$

$C(i)$ is the concentration of the i th component in mole percent.

Let Y be the fraction of the nitric oxide in the feed that is reduced to nitrogen by Reaction 2. If no ammonia decomposition is occurring, Y can be calculated directly from the concentration of nitrogen in the reactor product gas.

$$\begin{aligned} Y(\%) &= \frac{C(\text{N}_2)_{\text{out}}}{C(\text{NO})_{\text{in}}} \times \frac{6 \text{ moles of NO destroyed}}{5 \text{ moles of N}_2 \text{ produced}} \times 100 \\ &= \frac{C(\text{N}_2)_{\text{out}}}{C(\text{NO})_{\text{in}}} \times 120 \end{aligned} \quad (27)$$

Let Z be the percent of nitric oxide in the feed which is converted into nitrous oxide by Reaction 3. Then,

$$Z = X - Y \quad (28)$$

Let the product distribution ratio, R , be the fraction of nitric oxide destroyed which is reduced to nitrogen. Then,

$$R(\%) = 100 Y/X \quad (29)$$

If ammonia decomposition is occurring, then only nitric oxide destruction can be computed accurately. However an upper limit to the conversion of nitric oxide to nitrogen, Y' , can be calculated by assuming that all the nitrogen found in the reactor product was produced by the reduction of nitric oxide with ammonia and using Equation 27. This hypothetical conversion may exceed 100% if ammonia decomposition is significant.

Appendix H: Calculation of Raney Catalyst Bed Weights

All the supported catalysts contained 5% by weight Raney metal on silica, but the content of aluminum in the Raney metal varied. Aluminum is not known to catalyze the reaction. To maintain a constant weight of active metal in the bed, the amount of the supported catalyst was varied and silica support added to keep a constant bed weight of 2.5 g. Catalyst R-Cu250 was chosen as the basis because it contained the most aluminum. The calculation of active metal content of the Raney metals is illustrated below; results are summarized in Table 29.

(1) Calculation of weight % active metal in catalyst R-Cu250

Basis: 100 g of alloy R-Cu250

wt of Al present	= 50 g
wt of Cu present	= 25 g
wt of Ni present	= 25 g

From Table 27, 45% of the aluminum was leached. The weights of metal present in the activated catalysts are the following,

wt of Al	= 50 g x .55	= 27.5 g
wt of Cu		= 25 g
wt of Ni		= 25 g
total wt of metal		= 77.5 g
wt of (Cu + Ni)		= 50 g
wt % of active metal in		
leached alloy		= $100 \times 50/77.5$
		= 64.3%

The maximum bed weight which can be conveniently tested in the microreactor is 2.5 g. This was chosen as the standard bed weight for all catalyst tests.

- (2) Calculation of weight of active metal in 2.5 g of catalyst R-Cu250

wt % Raney R-Cu250 on silica = 5%

wt % (Cu + Ni) in activated

catalyst R-Cu250 = 64.3%

wt % (Cu + Ni) on silica = $5 \times .643$

= 3.22%

wt of (Cu + Ni) in 2.5 g catalyst

bed = 2.5×0.0322

= 0.0806 g

The bed weight of all other catalysts was varied to give 0.0806 g of active metal, (Cu + Ni). The calculation of this amount is illustrated for catalyst R-Ni-A.

- (3) Calculation of bed weight for catalyst R-Ni-A

from Table 27, wt % aluminum leached = 79%

as before, wt % (Cu + Ni) in leached alloy = 82.6%

wt % active metal on silica = $5 \times .826$ = 4.13%

bed weight to contain 0.0806 g of active metal

= $0.0806 / 0.0413$ = 1.95 g

wt of silica support required to increase bed

wt to 2.5 g = $2.5 - 1.95$ = 0.55 g

Table 29: Calculations of Raney Metal Catalyst Bed Weights

Catalyst	Aluminum Leached, %	Active Metal In Raney Metal %	% Raney Metal on Silica	% Active Metal on Silica	Weight Catalyst Bed, g	Weight Silica g
R-Ni-A	79	82.64	5	4.132	1.95	.55
R-Cu125	50	66.49	5	3.325	2.42	.08
R-Cu250	45	64.31	5	3.215	2.50	.00
R-Cu375	56	69.25	5	3.462	2.32	.18
R-Cu-A	94	94.34	5	4.717	1.70	.80

Note: For all catalysts, the total bed weight was 2.5 g and the weight of active metal in the bed was 0.0806 g.

BIBLIOGRAPHY

- 1) Acker, E.G., "The Characterization of Acid-Set Silica Hydrosols, Hydrogels, and Dried Gel," J. Colloid Interfac. Sci., 32, 41 (1970)
- 2) Adkins, H., and H.R. Billica, "The Preparation of Raney Nickel Catalysts and Their Use Under Conditions Comparable with those for Platinum and Palladium Catalysts," J. Amer. Chem. Soc., 70, 695 (1948)
- 3) Alpert, N.L., W.E. Keiser, and H.A. Szymanski, "Theory and Practice of Infrared Spectroscopy," Plenum Publishing, New York (1970)
- 4) Altshuller, A.P., and I.R. Cohen, "Window Materials for Use in Infrared Analyses Involving Nitrogen Dioxide," Anal. Chem., 31, 628 (1959)
- 5) Amirnazmi, A., J.E. Benson, and M. Boudart, "Oxygen Inhibition in the Decomposition of NO on Metal Oxides and Platinum," J. Catal., 30, 55 (1973)
- 6) Andersen, H.C., W.J. Green, and D.R. Steele, "Catalytic Treatment of Nitric Acid Plant Tail Gas," Ind. Eng. Chem., 53, 199 (1961)
- 7) Ayen, R.J., and A. Amirnazmi, "Catalytic Reduction of Nitrogen Dioxide with Hydrogen," Ind. Eng. Chem. Process. Des. Develop., 9, 247 (1970)
- 8) Bartock, W., et al., "Systems Study of Nitrogen Oxide Control Methods for Stationary Sources. II.," U.S. Govt. Res. Develop. Rep., 70, 131 (1970)
- 9) Begun, G.M., "Infrared and Raman Spectra of $N_2^{14}O_4$ and $N_2^{15}O_4$," J. Mol. Spectrosc., 4, 388 (1960)
- 10) Bennett, C.O., and J.E. Myers, "Momentum, Heat, and Mass Transfer," p. 229, McGraw-Hill, New York (1962)
- 11) Blyholder, G., and R.W. Sheets, "Electronic Factors in Chemisorption: NH_3 Adsorption," J. Catal., 27, 301 (1972)
- 12) Bolleter, W.T., C.J. Bushman, and P.W. Tidwell, "Spectrophotometric Determination of Ammonia as Indophenol," Anal. Chem., 33, 592 (1961)

- 13) Boltz, D.F., and M.G. Mellon, "Light Absorption Spectrometry," Anal. Chem., 44, 300R (1972)
- 14) Butcher, S.S., and R.E. Ruff, "Effect of Inlet Residence Time on Analysis of Atmospheric Nitrogen Oxides and Ozone," Anal. Chem., 43, 1890 (1971)
- 15) Cadenhead, D.A., and N.J. Wagner, "The Surface Composition of Reduced Oxide Copper-Nickel Alloys," J. Catal., 27, 475 (1972)
- 16) Campbell, J.S., and P.H. Emmett, "The Catalytic Hydrogenation of Ethylene on Nickel-Copper and Nickel-Gold Films," J. Catal., 7, 252 (1967)
- 17) Casey, E.J., C.W.M. Grant, and C.L. Gardner, "Methyl Radicals on Doped Silica Gel Surfaces," Can. J. Chem., 47, 3367 (1969)
- 18) Clark, A., "The Theory of Adsorption and Catalysis," p. 332, Academic Press, New York (1970)
- 19) Cleemput, O.V., "Gas Chromatography of Gases Emanating from the Soil Atmosphere," J. Chromatogr., 45, 315 (1969)
- 20) Cooke, N.E., O.M. Fuller, and R.M. Pitblado, "Preliminary Investigation of the Selective Catalytic Reduction of the Oxides of Nitrogen with Ammonia," unpublished communication, McGill University, Montreal, Canada (1970)
- 21) Davtyan, O.K., and R.I. Makordei, "Catalytic Activity of Transition Metals used as Hydrogen Electrode Catalysts: I. Structure and Catalytic Activity of Raney Nickel Prepared from Intermetallic Phases of a Nickel-Aluminum Alloy," Elektrokhimiya, 7, 1881 (Russ.) (1971)
- 22) Davtyan, O.K., E.G. Mixyuk, and R.I. Makordei, "Effect of the Composition and Structure of Nickel-Aluminum Alloys on the Structure and Catalytic Activity of Raney Nickel. I. Relations among the Composition, Alloy Structure, and Structure of Raney Nickel," Elektrokhimiya, 7, 1595 (Russ.) (1971)
- 23) Depasse, J., and A. Watillon, "The Stability of Amorphous Colloidal Silica," J. Colloid Interface Sci., 33, 430 (1970)
- 24) Di Martini, R., "Determination of Nitrogen Dioxide and Nitric Oxide in the Parts Per Million Range in Flowing Gaseous Mixtures by Means of the Nitrate-Specific-Ion Electrode," Anal. Chem., 42, 1102 (1970)

- 25) Dirksen, H.A., and H.R. Linden, "Pipeline Gas From Coal by Methanation of Synthesis Gas," Inst. Gas Technol. Res. Bull. No. 33, Chicago (1963)
- 26) E.I. Dupont de Nemour & Co., "Dupont Ludox Colloidal Silica Technical/Product Information"
- 27) Emmett, P.H., and P. Sabatier, "Catalysis: Then and Now," p. 36, Franklin Publishing, Englewood (1965)
- 28) Fasman, A.B., et al., "Modifications of Raney Nickel Catalyst by Additions of Transition Metals. I. Mechanism of Promotion by Molybdenum," Russ. J. Phys. Chem., 40, 56 (1966)
- 29) Faucett, H.L., T.C. McRight, and H.G. Graham Jr., "Analysis of Gases for Nitric Oxide, Nitrogen Dioxide, and Oxygen in a Pressure Nitric Acid Plant," Anal. Chem., 38, 1090 (1966)
- 30) Field, J.H., J.J. Demeter, A.J. Forney, and D. Bienstock, "Development of Catalysts and Reactor Systems for Methanation," Ind. Eng. Chem. Prod. Resch. Develop., 3, 150 (1964)
- 31) Fisher, G.E., and D.E. Becknell, "Saltzman Method for Determination of Low Concentrations of Oxides of Nitrogen in Automotive Exhaust," Anal. Chem., 44, 863 (1972)
- 32) Forney, A.J., S. Katell, W.L. Crentz, "High-Btu Gas from Coal via Gasification and Catalytic Methanation," Proc. Amer. Power Conf., 32, 428 (1970)
- 33) Fouilloux, P., et al., "Study of the Texture and Structure of Raney Nickel," J. Catal., 25, 212 (1972)
- 34) Freel, J., W.J.M. Pieters, and R.B. Anderson, "The Structure of Raney Nickel. I. Pore Structure," J. Catal., 14, 247 (1969)
- 35) Freel, J., W.J.M. Pieters, and R.B. Anderson, "The Structure of Raney Nickel. II. Electron Microprobe Studies," J. Catal., 16, 281 (1970)
- 36) Freel, J., S.D. Robertson, and R.B. Anderson, "The Structure of Raney Nickel. III. The Chemisorption of Hydrogen and Carbon Monoxide," J. Catal., 18, 243 (1970)
- 37) Gilby, A.C., "A Portable Infrared Spectrometer with Long Path Cell for Ambient Air and Gas Analysis," unpublished communication, Wilks Scientific Corporation, Connecticut (1971)

- 38) Gully, A.J., R.R. Graham, J.E. Halligan, and P.C. Bentsen, "Catalytic Removal of Ammonia and Nitrogen Oxides from Spacecraft Atmospheres," NASA CR-2132, NASA Contract. Rep. (1973)
- 39) Hall, W.K., "On the Surface Composition of Cu-Ni Alloy Catalysts," J. Catal., 6, 314 (1966)
- 40) Havlena, E.J., and K.A. Hutchinson, "Determination of Argon, Oxygen, and Nitrogen by Gas Chromatography," J. Gas Chromatogr., 6, 419 (1968)
- 41) Heftman, E., "Chromatography," Reinhold, New York (1961)
- 42) Heylman, G.W., "Improved Analysis of Argon-Oxygen-Nitrogen Mixtures by Gas Chromatography," J. Gas Chromatogr., 3, 82 (1965)
- 43) Hollis, O.L., "Separation of Gaseous Mixtures Using Porous Polyaromatic Polymer Beads," Anal. Chem., 38, 309 (1966)
- 44) Hollis, O.L., and W.V. Hayes, "Gas Separations on Microporous Polymers," Gas. Chromatogr., Int. Symp. Anal. Instrum. Div., Instrum. Soc. Amer., 6, 57 (1966)
- 45) Howard, J.N., and J.S. Garing, "The Transmission of the Atmosphere in the Infrared--A Review," Infr. Phys., 2, 155 (1962)
- 46) Jamieson, A.M., "A Gas Chromatographic Method for the Determination of the Argon and Oxygen Contents of Air in Bottled Beverages," J. Chromatogr. Sci., 9, 750 (1971)
- 47) Johnson, C.L., "Analysis of Gas Mixtures Containing Oxides of Nitrogen," Anal. Chem., 24, 1572 (1952)
- 48) Joithe, W., A.T. Bell, and S. Lynn, "Removal and Recovery of NO_x from Nitric Acid Plant Tail Gas by Adsorption on Molecular Sieves," Ind. Eng. Chem. Process Des. Develop., 11, 434 (1972)
- 49) Juvet Jr., R.S., and F. Zado, "Inorganic Gas Chromatography," Adv. Chromatogr., 1, 249 (1967)
- 50) Klimisch, R.L., and K.C. Taylor, "Dual Functionality and Synergism in the Catalytic Reduction of Nitric Oxide," General Motors Research Publication GMR-1195 (1972)

- 51) Lamb, A., and E.L. Tollefson, "Catalytic Reduction of Nitric Oxide in Low Concentration High Velocity Gas Streams," presented at 22nd. C.S.Ch.E. Conference, Toronto, (1972)
- 52) Lard, E.W., and R.C. Horn, "Separation and Determination of Argon, Oxygen, and Nitrogen by Gas Chromatography," Anal. Chem., 32, 878 (1960)
- 53) Littlewood, A.B., "Gas Chromatography," p. 464, Academic Press, London (1962)
- 54) Lyman, T. (ed), "Metals Handbook," 1948 Edition, ASM
- 55) Markvart, M., and Vl. Pour, "The Influence of Oxygen on the Catalytic Reduction of Nitric Oxide by Ammonia," J. Catal., 7, 279 (1967)
- 56) Morikawa, K., T. Shirasaki, and M. Okada, "Correlation among Methods of Preparation of Solid Catalysts, Their Structures, and Catalytic Activities," Adv. Catal., 20, 98 (1969)
- 57) Morrison, M.E., and W.H. Corcoran, "Optimum Conditions and Variability in Use of Pulsed Voltage in Gas-Chromatographic Determination of Parts-Per-Million Quantities of Nitrogen Dioxide," Anal. Chem., 39, 255 (1967)
- 58) Nicksic, S.W., and J. Harkins, "Spectrophotometric Determination of Nitric Oxide in Auto Exhaust," Anal. Chem., 34, 985 (1962)
- 59) Nishimura, S., and Y. Urushibara, "Method for the Preparation of Raney Nickel Catalyst with Greater Activity," Bull. Chem. Soc. Jap., 20, 199 (1957)
- 60) Obermiller, E.L., and R.W. Freedman, "Single-Stage Determination of Argon, Oxygen, and Nitrogen in Air," J. Gas Chromatogr., 3, 243 (1965)
- 61) Otto, K., M. Shelef, and J.T. Kummer, "Studies of Surface Reactions of Nitric Oxide by Nitrogen-15 Isotope Labeling. I. The Reaction between Nitric Oxide and Ammonia over Supported Platinum at 200-250°C," J. Phys. Chem., 74, 2690 (1970)
- 62) Otto, K., M. Shelef, and J.T. Kummer, "Studies of Surface Reactions of Nitric Oxide by Isotope Labeling. II. Deuterium Kinetic Isotope Effect in the Ammonia-Nitric Oxide Reaction on a Supported Platinum Catalyst," J. Phys. Chem., 75, 875 (1971)

- 63) Otto, K., and M. Shelef, "Studies of Surface Reactions of Nitric Oxide by Isotope Labeling. IV. The Reaction between Nitric Oxide and Ammonia over Copper Surfaces at 150-200°C," J. Phys. Chem., 76, 37 (1972)
- 64) Owczarek, J.A., "Fundamentals of Gas Dynamics," p.230, International Textbook Co., Scranton, Penn. (1964)
- 65) Pauleau, Y., M. Azzopardi, L. Bonnetain, and J. Besson, "Oxidation of Nickel and Copper by Nitrogen Monoxide," C.R. Acad. Sci., Ser. C., 270, 588 (Fr) (1970)
- 66) Pearce, E.E., and D. Lewis, "X-Ray Diffraction Line Broadening Studies of Raney Copper and Nickel," J. Catal., 26, 318 (1972)
- 67) Perry, R.H. (ed), "The Chemical Engineering Handbook," 4th edition, McGraw-Hill, New York (1965)
- 68) Petrov, B.F., et al., "Influence of the Phase Composition on the Properties of Skeletal Nickel-Manganese Catalysts," Kinet. Katal., 10, 1146 (1968)
- 69) Petrov, F.R., A.B. Fasman, and D.V. Sokol'skii, "Effect of Manganese Compounds on the Properties of the Raney Nickel Catalyst," Russ. J. Phys. Chem., 44, 1736 (1970)
- 70) Pierson, R.H., A.N. Fletcher, and E. St. Clair Ganta, "Catalogue of Infrared Spectra for Qualitative Analysis of Gases," Anal. Chem., 28, 1218 (1950)
- 71) Plank, C.J., and L.C. Drake, "Differences Between Silica and Silica-Alumina Gels. I. Factors Affecting the Porous Structure of these Gels," J. Colloid. Sci., 2, 399 (1947)
- 72) Ranganathan, R., N.N. Bakhshi, and J.F. Mathews, "Effect of Ultrasonic Waves on the Catalytic Activity of Silica Gel," J. Catal., 21, 186 (1971)
- 73) Reynolds, P.W., "Heterogeneous Catalysis. Part II. Hydrogenation by Binary Alloys," J. Chem. Soc. (London), 265 (1950)
- 74) Rimberg, D., "Pressure Drop Across Sharp-End Capillary Tubes," Ind. Eng. Chem. Fundam., 6, 599 (1967)
- 75) Robertson, S.D., and R.B. Anderson, "The Structure of Raney Nickel. IV. X-Ray Diffraction Studies," J. Catal., 23, 286 (1971)

- 76) Robertson, S.D., J. Freel, and R.B. Anderson, "The Nature of Raney Nickel. VI. Transmission and Scanning Electron Microscopy Studies," J. Catal., 24, 130 (1972)
- 77) Rommers, P.J., and J. Visser, "Spectrophotometric Determination of Micro Amounts of Nitrogen as Indophenol," Analyst, 94, 653 (1969)
- 78) Sachtler, W.M.H., and G.J.H. Dorgelo, "The Surface of Copper-Nickel Alloy Films. I. Work Function and Phase Composition," J. Catal., 4, 654 (1965)
- 79) Sachtler, W.M.H., G.J.H. Dorgelo, and R. Jongepier, "Phase Composition and Work Function of Vacuum-Deposited Copper-Nickel Alloy Films," J. Catal., 4, 100 (1965)
- 80) Sachtler, W.M.H., and R. Jongepier, "The Surface Composition of Copper-Nickel Alloy Films. II. Phase Equilibrium and Distribution and their Implications for Work Function, Chemisorption, and Catalysis," J. Catal., 4, 665 (1965)
- 81) Saier, E.L., and A. Pozefsky, "Quantitative Determination of Nitric Oxide and Nitrous Oxide by Infrared Absorption," Anal. Chem., 26, 1079 (1954)
- 82) Sassoulas, R., and Y. Trambouze, "Raney Nickel. III. Structure and Catalytic Activity of Nickel Prepared from Pure Inter-metallic Compounds in the System Ni-Al," Bull. Soc. Chim. Fr., 5, 985 (1964)
- 83) Sinfelt, J.H., "Catalytic Specificity," A.I.Ch.E.J., 19, 673 (1973)
- 84) Sinfelt, J.H., "Supported 'Bimetallic Cluster' Catalysts," J. Catal., 29, 308 (1973)
- 85) Sing, K.S.W., and J.D. Madeley, "The Surface Properties of Silica Gels. I. Importance of pH in the Preparation from Sodium Silicate and Sulphuric Acid," J. Appl. Chem., 3, 549 (1953)
- 86) Sing, K.S.W., and J.D. Madeley, "The Surface Properties of Silica Gels. II. Adsorption of Water Vapor," J. Appl. Chem., 4, 365 (1954)
- 87) Snyder, R.G., and I.C. Hisatsune, "Infrared Spectrum of Dinitrogen Tetroxide," J. Mol. Spectrosc., 1, 139 (1957)

- 88) Stephens, E.R., "Long-Path Infrared Spectroscopy For Air Pollution Research," *Infr. Phys.*, 1, 187 (1961)
- 89) Takasu, Y., and H. Shimizu, "Relation Between Catalytic Activity Pattern and Surface Composition of Cu-Ni Alloy: An Application of Auger Electron Spectroscopy to the Study on Catalysis," *J. Catal.*, 29, 479 (1973)
- 90) Taylor, F.R., "The Elimination of Oxides of Nitrogen From Automobile Exhaust," prepared for the Air Pollution Foundation, San Marino, California (1959)
- 91) Teske, W., "Emissions and Abatement of Oxides of Nitrogen in Nitric Acid Manufacture," *Chem. Eng. (London)*, 221, 263 (1968)
- 92) Van der Plank, P., and W.M.H. Sachtler, "Surface Composition of Equilibrated Copper-Nickel Alloy Films," *J. Catal.*, 7, 300 (1967)
- 93) Van Hardeveld, R., and F. Hartog, "Influence of Metal Particle Size in Nickel-on-Aerosil Catalysts on Surface Site Distribution, Catalytic Activity, and Selectivity," *Adv. Catal.*, 22, 75 (1972)
- 94) Vlach, V., "Elements of Material Science," p. 136, Addison Wesley Publishing Co., Reading, Massachusetts (1964)
- 95) Wilhite, W.F., and O.L. Hollis, "Use of Porous Polymer Beads for Analysis of the Martian Atmosphere," *J. Gas Chromatogr.*, 6, 84 (1968)